COMPRESSION OF A THIN COHESSIONLESS LAYER OVERLAYING A DEEP DEPOSIT

ELENA DROBOTEA

A Thesis

in

THE DEPARTMENT OF BUILDING, CIVIL AND ENVIRONMENTAL ENGINEERING

Presented in Partial Fulfillment of the Requirements

For the Degree of Master in Applied Science

CONCORDIA UNIVERSITY

Montreal, Quebec, Canada

July 2004

Library and Archives Canada

Published Heritage Branch

395 Wellington Street
Ottawa ON K1A 0N4
Canada

Bibliothèque et Archives Canada

Direction du Patrimoine de l'édition

395, rue Wellington
Ottawa ON K1A 0N4
Canada

Your file Votre référence
ISBN: 0-612-94685-1
Our file Notre référence
ISBN: 0-612-94685-1

The author has granted a non-exclusive license allowing the Library and Archives Canada to reproduce, loan, distribute or sell copies of this thesis in microform, paper or electronic formats.

L'auteur a accordé une licence non exclusive permettant à la Bibliothèque et Archives Canada de reproduire, prêter, distribuer ou vendre des copies de cette thèse sous la forme de microfiche/film, de reproduction sur papier ou sur format électronique.

The author retains ownership of the copyright in this thesis. Neither the thesis nor substantial extracts from it may be printed or otherwise reproduced without the author's permission.

L'auteur conserve la propriété du droit d'auteur qui protège cette thèse. Ni la thèse ni des extraits substantiels de celle-ci ne doivent être imprimés ou aturement reproduits sans son autorisation.

In compliance with the Canadian Privacy Act some supporting forms may have been removed from this thesis.

Conformément à la loi canadienne sur la protection de la vie privée, quelques formulaires secondaires ont été enlevés de cette thèse.

While these forms may be included in the document page count, their removal does not represent any loss of content from the thesis.

Bien que ces formulaires aient inclus dans la pagination, il n'y aura aucun contenu manquant.

Canada

ABSTRACT

COMPRESSION OF A THIN LAYER OVERLAYING A DEEP DEPOSIT

ELENA DROBOTEA

In geotechnical and road engineering, it is quite common to encounter ground represented by a layered system consisting of a thin upper subgrade layer overlaying a deep natural soil deposit. Structures built on such type of ground usually experience low bearing capacity and, consequently, large settlement. In order to achieve better results, the subgrade layer is compacted using the conventional techniques. The level of the densification achieved is influenced not only by the compacting effort applied on soil surface, but also by the strength of the underlying soil deposit. In the literature, several reports can be found dealing with the subject matter. The majority of these reports have ignored the contribution of underlying soil on the compression of the upper thin layer.

The objective of this thesis is to develop a numerical model using the finite element technique, to examine the compression of a thin subgrade layer overlying a deep deposit. In this model all the parameters believed to govern the compression of the subgrade layer will be incorporated. The compression of the subgrade layer under various applied loads will be evaluated. The results are presented in the form of charts and tables in order to determine the total settlement of the foundation and the compression of the upper layer. Empirical formula is proposed to predict the compression of the upper subgrade layer for practicing use.

ACKNOWLEDGEMENTS

As with any other research work, the number of individuals who have made it possible far exceeds those whose names grace the title page. At the hazard of leaving someone out, I would like to explicitly thank the following individuals for their contribution.

First and foremost, I want to thank my professor, Dr. A.M. Hanna who supervised the research. His constructive criticism and independent testing of the material have been exceptionally helpful.

To Mohab Sabry, my esteemed friend and colleague, I offer my sincere appreciation for his help with the software PLAXES.

TABLE OF CONTENTS

LIST OF TABLES

LIST OF FIGURES

LIST OF SYMBOLS

Symbol	Representation
H, h_1	Thickness of the upper layer
H_2	Thickness of the lower layer
Φ_1	Internal friction angle of the upper layer
Φ_2	Internal friction angle of the lower layer
E	Elasticity modulus
N	Poisson's ratio
W	Width of the geometry model
B	Width of the applied load
P_{ref}	Reference pressure
E_{50}^{ref}	Plastic straining due to primary deviatoric loading- secant stiffness in standard drained triaxial test
E_{oed}^{ref}	Plastic straining due to primary compression - tangent stiffness for primary odometer loading
E_{ur}^{ref}	Elastic unloading/reloading - unloading/reloading stiffness (default value $E_{ur}^{ref} = 3\ E_{50}^{ref}$(kN/m^2)).
ν_{ur}	Poisson's ratio for unloading-reloading
γ_1	Unit weight of the upper layer
γ_2	Unit weight of the lower layer
γ_{unsat}	Unsaturated unit weight of the soil
γ_{sat}	Saturated unit weight of the soil
M	Stress dependent stiffness according to a power law
C	Cohesion

$\mathbf{R_{inter}}$	Interface strength reduction factor
S	Total settlement
$\mathbf{S_I}$	Settlement of the upper layer
$\mathbf{S_{II}}$	Settlement of the lower layer
$\mathbf{E_S}$	Compression modulus
$\mathbf{I_z}$	Vertical strain influence factor
$\mathbf{C_1}$	Correction factor for depth
$\mathbf{C_2}$	Correction factor for creep
Q	Overburden pressure at the footing level
$\mathbf{q_0}$	Pressure imposed on the soil by the footing
Z	Depth of the profile
$\mathbf{\Delta z}$	Thickness of the sublayer
$\mathbf{z_i}$	Depth to the center of the sublayer
$\mathbf{C_S}$	Compression value
$\mathbf{\Delta}$	Mean square error

CHAPTER 1

INTRODUCTION

1.1 Soil compressibility

The technologies of ground improvement process for strengthening loose or soft soils to support buildings, roadways, and other heavy construction have been successfully employed. Soil improvement by means of compaction is used increasingly for the solution of different types of foundation problems in coarse-grained soil deposits. The level of compaction achieved depends on the soil characteristics.

The theory of consolidation is one of the most important geotechnical regularities describing the stress-strain properties of soils and the mechanism of compression. Practical application of this phenomenon is used in settlement calculation. Soil compressibility, resulting from porosity changes and, consequently, the change of its total volume under the load applied. However, it is necessary to distinguish soil compressibility as the main soil characteristic from soil deformability, which is a typical to all physical agents. Soil compressibility is the ability of a soil's structure (solid particle packing) to change, under the influence of external stresses (compressive load, drying, colloid coagulation, etc.), to a more compact one due to soil porosity reduction. It is necessary to distinguish soil consolidation under applied short-term dynamic load (mechanical) from its densification under the long-term static load (compression, consolidation, etc).

In practice, the grounds of building sites are quite often presented by a two-layered system, where a thin layer is overlaying a deep natural deposit.

1.2 Objectives of the Thesis

This research was conducted for the case of cohesionless soil where the thin subgrade weaker layer is overlaying a strong deep deposit in order to examine how the relationships of the variable upper layer parameters and properties (subgrade layer thickness and the angle of shearing resistance) between fixed properties of the lower strong layer influence the compression of the subgrade level under various applied loads.

The total settlement calculations of the upper layer were made with PLAXIS Version 8 software application - a finite element package [29, 30]. This code is intended for the two dimensional analysis of deformation and stability in geotechnical engineering and includes advanced constitutive models for the simulation of the non-linear, time dependent and anisotropic behaviour of soils as a multi-phase material.

The objectives of the present study are to predict the compression of the subgrade layer depending on three variable parameters of the upper layer: the thickness of the upper layer **H**, the angle of shearing resistance ϕ and the applied load. The properties of the lower layer were kept constant. The results will be presented in the form of design charts and formula to predict the compression of the subgrade layer.

CHAPTER 2

LITERATURE REVIEW

2.1 Background

Settlements (as well as compressions) on cohesionless soil take place immediately under the load applied. Several methods for predicting settlement on cohesionless soils were reported in literature and they were successfully implemented in practice.

A natural soil [26] is a multiphase system of dispersed particles. The determination of the stress strain state in multiphase, dispersive soils is a very important and a difficult problem, and has vast practical significance. There are various hypotheses to solve the problem; one can use elasticity theory for continuous media, the theory of two-phase soils (i.e., completely saturated soils containing free, hydraulically continuous water), the theory of plasticity or the theory of creep in continuous materials. However, the stress-strain state of the soil is affected by the deformability of all the individual phases, which constitute the ground, as well as their interaction. For example, for foundations on loose, completely saturated soils, the settlement is predicted by the filtrational consolidation theory, which is fully in accord with practical requirements.

In multiphase soils the time variation of the stress-strain state depends not only on the rheological properties of the soil "skeleton", but also on the flow of pore fluid due to drainage, the compressibility of air, etc. The term "consolidation" means the time-deformation of a multiphase medium under a constant external load. The process of deformation occurs as a result of both the gradual extrusion of pore fluid and the simultaneous action of rheological processes occurring in the "skeleton". That is why the term "consolidation" is used in a broad sense to describe not only volumetric compression, but also the general deformation of a multiphase soil affected by complex stress states.

Many attempts have been made [25] to develop a physically consistent theory for infiltrated porous materials. For the quasi-static case, i.e., without the inertial effect, Terzaghi [24] and Biot [2, 3, 4] were among the first to present a widely accepted model. Their models are respectively known as the theory of consolidation and the theory of poroelasticity. An important assumption in Terzaghi's one-dimensional theory of consolidation is that the soil skeleton behaves elastically. On the other hand, Buisman [5] recognized that creep deformations in settlement analysis could be important. This has led to extensions of Terzaghi's theory by various investigators. Wave propagation in porous media is an important topic geomechanics [25], for example. Due to the interplay of the solid skeleton with the fluid, the so-called second compressional wave appears. The existence of this wave is reported in literature not only for Biot's theory but also for theoretical approaches based on the Theory of Porous Media - mixture theory extended by the concept of volume fractions. Assuming a geometrically linear description (small displacements and small deformation gradients) and linear constitutive equations (Hook's law), the governing equations are derived, for Biot's theory and the Theory of Porous Media, respectively. In each case, the solid displacements and the pore pressure are the primary unknowns.

One of the most difficult geotechnical problems is to select an appropriate theoretical model reflecting soil deformation under applied load [21]. Variety of a soil's skeleton with its unique mechanical properties, formation conditions and complex diagenesis processes has led to the development of a large number of mathematical models created based on summarising of experimental data. Impossibility of finding the empirical solution in the closed species and the tendency to simplify the problem for technical calculations in a reasonable manner forces the introduction of various assumptions. There are a lot of discussions about the appropriateness of some theories e.g. such as the absence of initial gradient of head pressure, neglecting of structure strength, etc.

2.2 Hypotheses and theories predicting the deformation of the soil

As a result of international discussion of the applicability of existing theories of filtrational consolidation for its practical implementation [21] the bound problem of consolidation theory and the theory of linear elasticity were demonstrated as the most effective.

The development of the bound problem can be divided into two periods [10]. The first period (1950-1960) includes:

1. Elaboration of determinative equations as well as introduction of linear and non-linear dependences in these equations;
2. Obtaining of analytical solutions in closed species.

The second period is related to numerical devices perfection and also to the development of numerical methods. Combined equations of the bound problem with complex load geometry system and complex soil stratification can be solved using numerical methods. The most popular method among investigators attacking the filtrational consolidation problem is the finite-element method [20].

Investigations of Russian scientist V. Florin in the field of consolidation theory [11, 12] also present interesting facts. One of the main directions of his research was the elaboration of modern consolidation theory for water-saturated soils. In 1938-1939 a series of articles were published where Florin first formulated the statement of two-dimensional and three-dimensional problems of two-phase and three-phase soil consolidation within the boundaries of the "bulk forces" model. This model is similar to above-mentioned Biot's model, formulated in 1941-1943. Only around 1970 – 1980 these models could begin to be practically applied with the development of high-capacity computers. In his research Florin, examined in detail initial stresses of soil skeleton under the instant application of any type of distributed load. It was demonstrated, that under conditions of two-dimensional and three-dimensional problems even in the case of saturated medium, the immediate settlement appears and increases with the consolidation process. Thus, the assumption that in the boundaries of two-dimensional and three-dimensional problems, initial applied load is taken mainly by water as it happens in the boundary of the one-dimensional problem was proven false. In 1948 Florin formulated the statement of the consolidation problem, accepting any design model for soil skeleton; it was named "the main calculation model of Florin". In conformity with this model, elaboration of the system of numerical solution of consolidation problems by means of finite-element method taking into account the influence of many factors on the consolidation process (stage-by-stage building erection, variability of the consolidation zone, drainage availability, soil heterogeneity and anisotropy, etc) was conducted. Florin also claimed that it is very important to take into consideration the initial gradient of pressure head, the structure strength and non-linear compression of the soil, creep of the soil skeleton as well as the phenomenon of soil aging. Of principal concern was the problem of evaluation of the domain of applicability of different design models. In particular, the criterion of applicability of elasticity theory solutions to the soils was argued – it is the range of the zone of plastic deformations development.

Basically, most of existing methods for the real prediction of settlement on cohesionless soils under the load applied are represented in the form of empirical formulas to correlate the results of standard penetrations tests or static-cone tests to the settlement of designed footings [16].

In present, the most widely used methods of settlement calculation on sands can be classified into two main categories:

I. Methods based on field measurement.

II. Methods based on the elasticity theory.

Terzaghi and Peck in 1948 [24] were the first to develop an empirical formula to predict settlement of footings based on the results of the standard penetration test. Thus, the field measurements have been introduced in practice. The method considered the subgrade sand as homogeneous and the number of blows N is constant with depth. They also elaborated another formula to correlate predicted settlement with the results of the plate-load test. Later, Alpan in 1964 [1], Meyerhof in 1965 [18] and Peck in 1974 [19] have introduced modified formulas to take into account the overburden pressure effect. The methods based on field tests strongly depend on the accuracy of field measurements.

Several researchers have developed procedures of settlement prediction using elasticity theory. Among them are: DeBeer [9], D'Appolonia [8], Schmertmann [22], and Hanna [14]. The main design parameters utilised in these methods are:

1. Elasticity modulus E
2. Poisson's ratio ν

The above-mentioned parameters can be determined from laboratory tests or they can be correlated with field data. However, methods based on the elasticity theory have some limitations, for instance, Schmertmann method of settlement calculation is limited by the depth below the footing equal to twice the width of the footing.

2.3 Settlement of a cohesionless weak layer overlying a strong dense sand deposit.

As it is quite common to encounter ground represented by a layered system consisting of a thin upper layer overlaying a deep soil deposit, the densification effect is strongly influenced by the dynamic response characteristics of the soil to be compacted, but also by the underlying soil layers. In fact, several methods for predicting the settlement of foundations before compaction was applied, have considered variable mechanical parameters of layer soils. It is very important to determine the interaction between these layers and the energy consumed by each layer [7].

Recent investigation of Hanna on this issue is of great interest. It was emphasized that the stiffness of the lower deep natural deposit constitutes a serious parameter that must be taken into account to achieve the desired level of compaction of the upper thin subgrade layer. Design charts were presented to prove the fact that compactability of a thin layer is dependent on the stiffness of the lower natural deep deposit. Experimental and numerical research [15] showed that compactability of a subgrade thin layer, besides such factors as water content, temperature, size, shape of grain, and grain size distribution depends mainly on:

1. Compressibility of deep underlying layer;
2. The stiffness of the lower deposit and the compaction effort.

In this way, future investigations in this field may be very important for the domain of road engineering. Present study is directed toward predicting the range of compression of the thin subgrade weaker soil layer depending on its parameters as stated in section 1.2 under the different applied loads using the geotechnical software PLAXIS for total settlement calculations.

CHAPTER 3

NUMERICAL MODEL

3.1 Geometry model

The case of a thin layer overlying a deep deposit was simulated using a plane strain model with 15-noded elements. The basic geometric parameters of a finite element model have been chosen as follows:

- The width of the geometry model of the soil, w = 2m;
- The depth of the lower layer, h_2 = 14m;
- The depth of the upper layer h_1 was varied from 0.5 to 10 meters;

The geometry model is shown in Figure 3.1. Seconds were used as the unit of time in order to reflect immediate deformations of the subgrade layer.

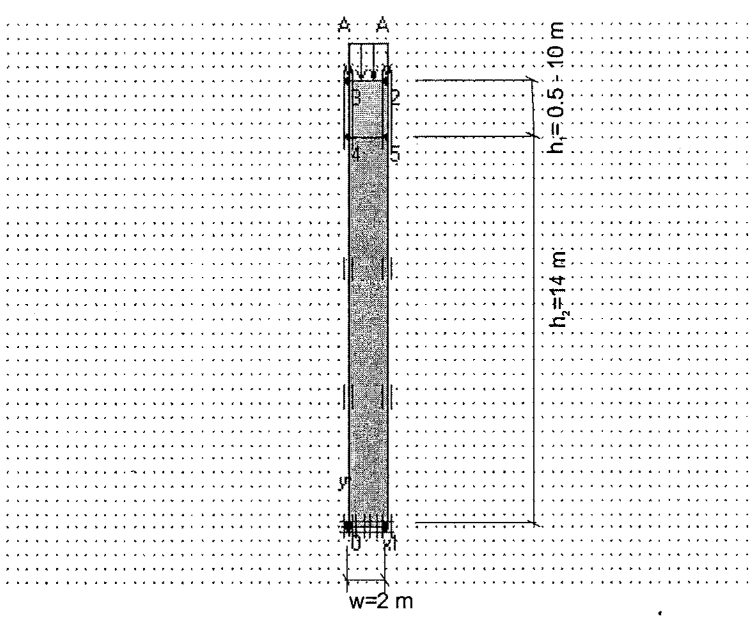

Figure 3.1 Geometry model of the two-layered system

Static analysis was made to examine upper layer soil compression under applied load. Distributed load was taken to simulate the field compaction process as prescribed forces included in PLAXIS code for deformation problems. The compaction effort will be justified along the width of the model.

3.1.1 Boundary conditions

Boundary conditions must be defined to take into account that in reality the soil is a semi-infinite medium, without this option the waves would be reflected on the model boundaries, causing perturbations. Standard fixities boundary conditions option was applied as a convenient input for practical PLAXIS calculation application. It makes impossible to extend stress strain state of the model outside of the chosen width of the model.

3.2 Material model

Hardening soil (HS) model was applied to reflect the behaviour of the two-layered soil model. The hardening plasticity model is an advanced one for simulating different types of soil, both soft and stiff. There are two types of hardening in present model: shear and compression hardening.

Compression hardening was selected to reflect the two-layered soil behaviour. It is used to model irreversible plastic strains due to primary compression in isotropic loading. HS soil model uses the theory of plasticity, includes soil dilatancy and introduces a yield cap. As a basic feature of the HS model is the stress dependency of soil stiffness, it was decided reasonable to use this model for both upper and lower layers to observe the compressibility of the subgrade softer layer. Basic characteristics are listed in tables 3.1 and 3.2. Plastic straining and elastic unloading were taken according to [34, 35]. Reference pressure P_{ref} was taken to be 100kPa.

3.2.1 Elasticity modulus E

The hardening soil model implies using the following basic parameters of soil stiffness as mechanical characteristics, which have been selected according to the Table 8.1 Arbitrary HS parameters for sands [30]:

E_{50}^{ref} - plastic straining due to primary deviatoric loading or so-called secant stiffness in standard drained triaxial test (kN/m^2);

E_{oed}^{ref} – plastic straining due to primary compression or so-called tangent stiffness for primary oedometer loading (kN/m^2);

E_{ur}^{ref} - elastic unloading/reloading, or unloading/reloading stiffness (default value E_{ur}^{ref} = 3 E_{50}^{ref}(kN/m^2)).

The range of these parameters are shown in the Tables 3.1 and 3.2

The Poisson's ratio for unloading-reloading ν_{ur} used in hardening soil model was given in its default value 0.2 [29, 30].

3.3 Properties of the soil layers

3.3.1 Lower deep soil deposit

The properties of the strong lower deep natural cohesionless deposit were taken as constant and are listed in Table 3.1.

3.3.2 Subgrade upper weaker layer

The values of the thickness of the upper layer were taken in the range of 0.5 – 10 meters (10 different values, Table 3.4) for each type of four values of internal angle of friction of the subgrade layer under four different loads: 300; 100; 50 and 40 kN/m^2. It was decided to examine the thickness parameter input to the total settlement and compression values starting from its minimum thickness 0.5 m and then by increasing it to this, oncoming the depth of the lower layer.

Table 3.1 Material properties of the lower soil layer

Parameter	Symbol	Value	Unit
Material model	Model	Hardening soil model	-
Type of material behaviour	Type	Drained	-
Unsaturated unit weight	γ_{unsat}	18	kN/m^3
Saturated unit weight	γ_{sat}	20	kN/m^3
Plastic straining due to primary deviatoric loading	E_{50}^{ref}	40000	kN/m^2
Plastic straining due to primary compression	E_{oed}^{ref}	40000	kN/m^2
Elastic unloading	E_{ur}^{ref}	120000	kN/m^2
Stress dependent stiffness according to a power law	m	0.5	-
Cohesion	c	1	kN/m^2
Friction angle	ϕ_2	45	^{0}
Dilatance angle	ψ	10	^{0}
Poisson's ratio	V_{ur}	0,2	-
Interface strength reduction factor	R_{inter}	1.0(rigid)	-

Table 3.2 Properties of the upper soil layers with different internal friction angle

Symbol	Value for $\phi = 25^0$	Value for $\phi = 30^0$	Value for $\phi = 35^0$	Value for $\phi = 40^0$	Unit
γ_{unsat}	12	14	16	17	kN/m^3
γ_{sat}	14	16	18	19	kN/m^3
E_{50}^{ref}	20000	25000	30000	30000	kN/m^2
E_{oed}^{ref}	20000	25000	30000	30000	kN/m^2
E_{ur}^{ref}	60000	75000	90000	90000	kN/m^2
m	0.5	0.5	0.5	0.5	-
c	2	4	5	3	kN/m^2
ψ	0	0	5	5	0
R_{inter}	0.6	0.6	0.6	0.6	-

3.4 Finite Element mesh

The soil is modeled by the 15- node elements plane-strain.

In accordance with PLAXIS input procedure, initial stresses have been generated after the mesh was created and refined (Figure 3.2).

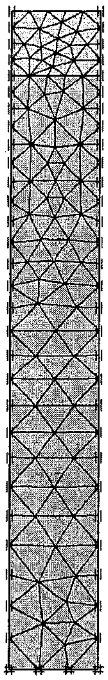

Figure 3.2 Generated mesh of the finite-element model

3.5 Calculation of the total settlement and the compression of the upper layer

As mentioned above, several series of total settlement calculations were made with PLAXIS application. The properties of the lower layer have been kept constant while the values of distributed load (four values), internal friction angle (four values) and the thickness of the upper layer (ten values) were varied. Thus, 160 calculations have been done; they are listed in the Table 3.3.

Table 3.3 Parameters of the serial calculations

Load kN/m²	Series	Serial number	Unit weight of the upper layer, kN/m³ (γ_1)	Internal friction angle of the upper layer, °ϕ_1	Thickness of the upper layer, H (m)
300; 100; 50; 40	1; 5; 9; 13	1;41;81;121	12	25	0,5
		2;42;82;122			0,7
		3;43;83;123			1,0
		4;44;84;124			1,5
		5;45;85;125			2.0
		6;46;86;126			2,5
		7;47;87;127			3,0
		8;48;88;128			5,0
		9;49;89;129			7,0
		10;50;90;130			10,0
	2;6; 10; 14	11;51;91;131	14	30	0,3
		12;52;92;132			0,7
		13;53;93;133			1,0
		14;54;94;134			1,5
		15;55;95;135			2.0
		16;56;96;136			2,5
		17;57;97;137			3,0
		18;58;98;138			5,0
		19;59;99;139			7,0
		20;60;100;140			10,0
	3; 7; 11; 15	21;61;101;141	16	35	0,5
		22;62;102;142			0,7
		23;63; 103;143			1,0
		24;64;104;144			1,5
		25;65;105;145			2.0
		26;66;106;146			2,5
		27;67;107;147			3,0
		28;68;108;148			5,0
		29;69;109;149			7,0
		30;70;110;150			10,0
	4; 8; 12; 16	31;71;111;151	17	40	0,5
		32;72;112;152			0,7
		33;73;113;153			1,0
		34;74;114;154			1,5
		35;75;115;155			2.0
		36;76;116;156			2,5
		37;77;117;157			3,0
		38;78;118;158			5,0
		39;79;119;159			7,0
		40;80;120;160			10,0

The total settlement S is shown in the output of the PLAXIS subprogram and was also derived from "PLAXIS curves" option. For example, for run # 37 of the fourth series of calculations, the output is shown in Figures 3.3 and 3.4, the total settlement of the surface point of the upper layer S (point A) and the displacement of the interface point S_i (point B) between the subgrade and lower layers are shown in the Figure 3.5

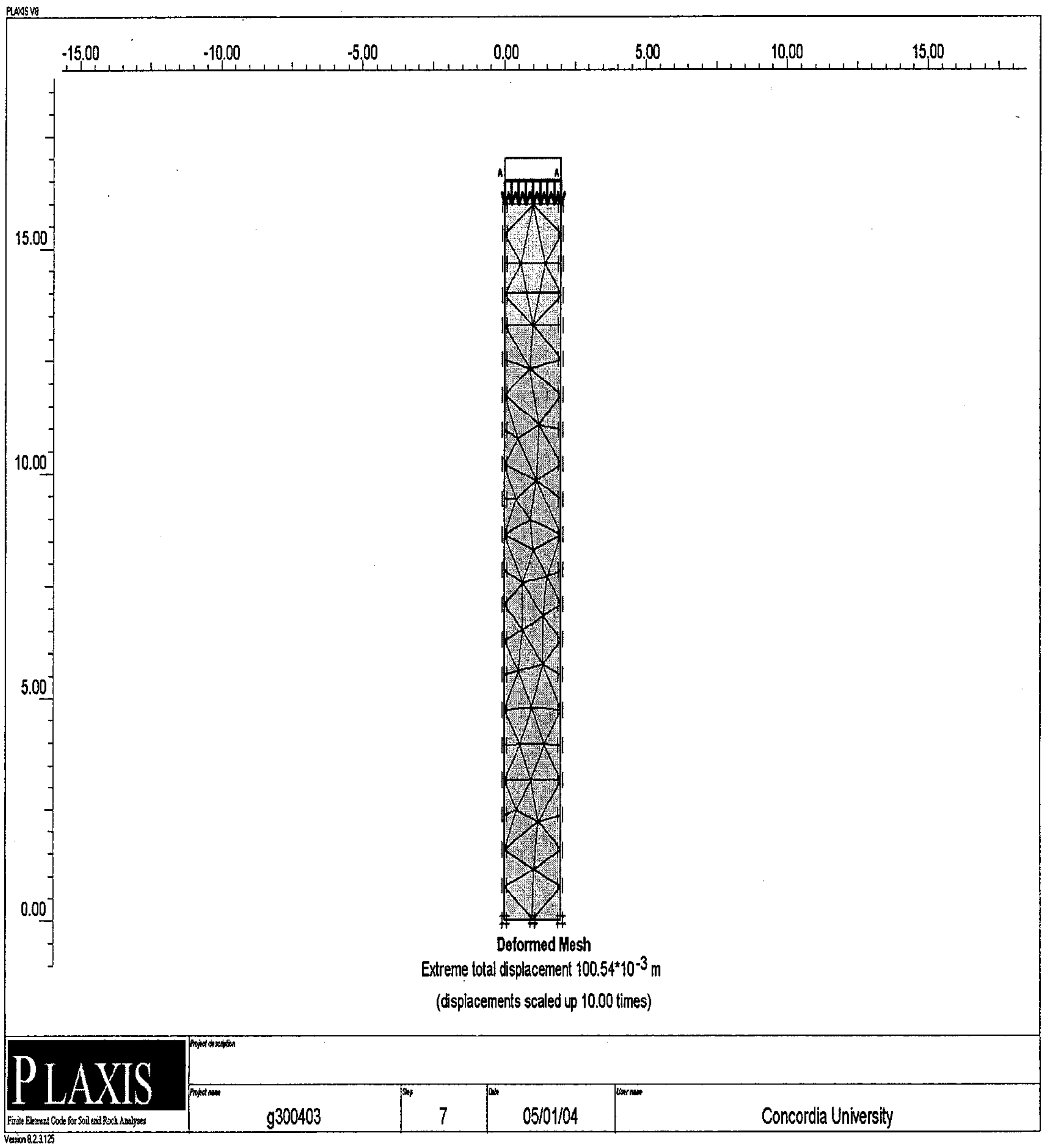

Figure 3.3 Deformed mesh of the finite-element model

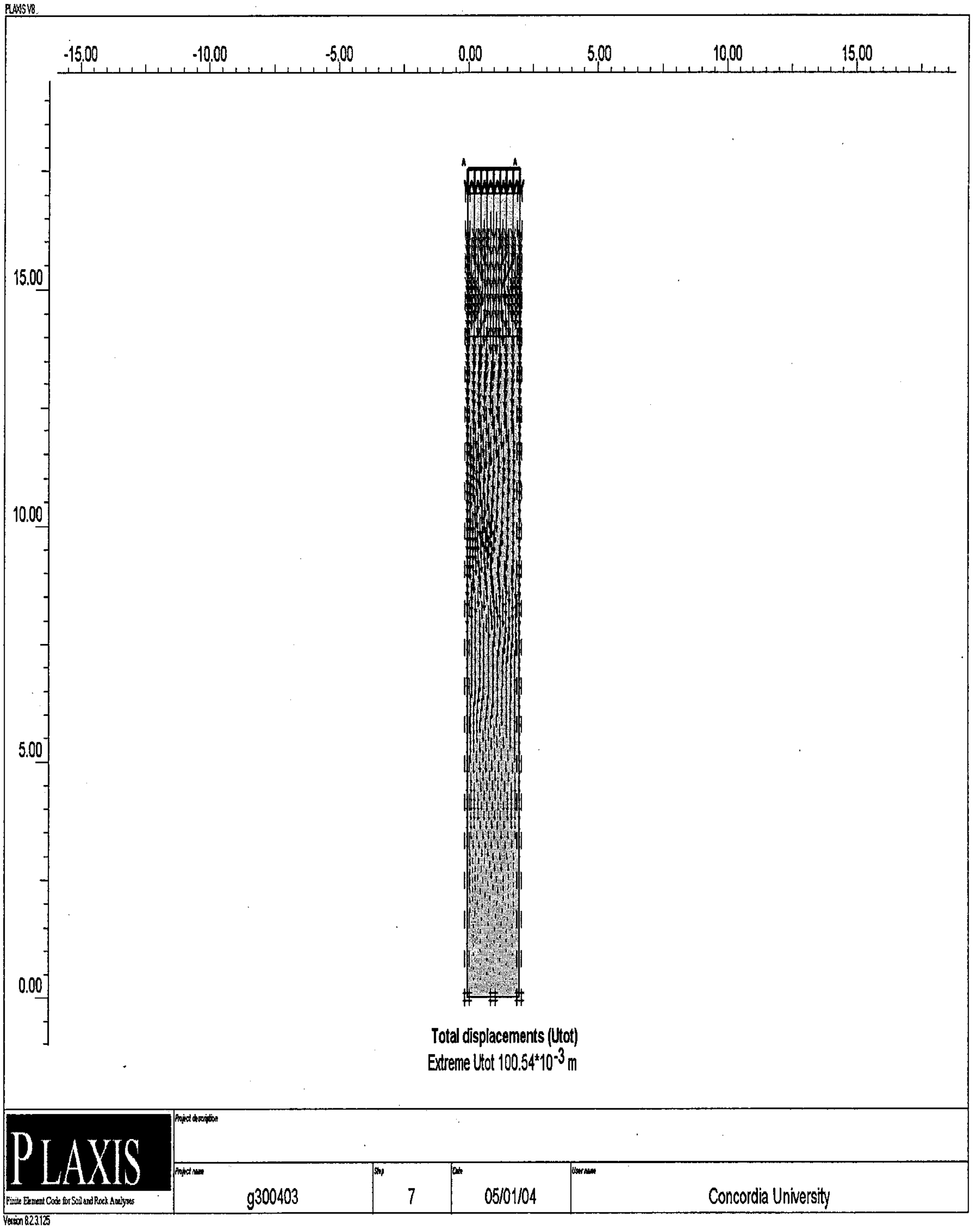

Figure 3.4 Output results

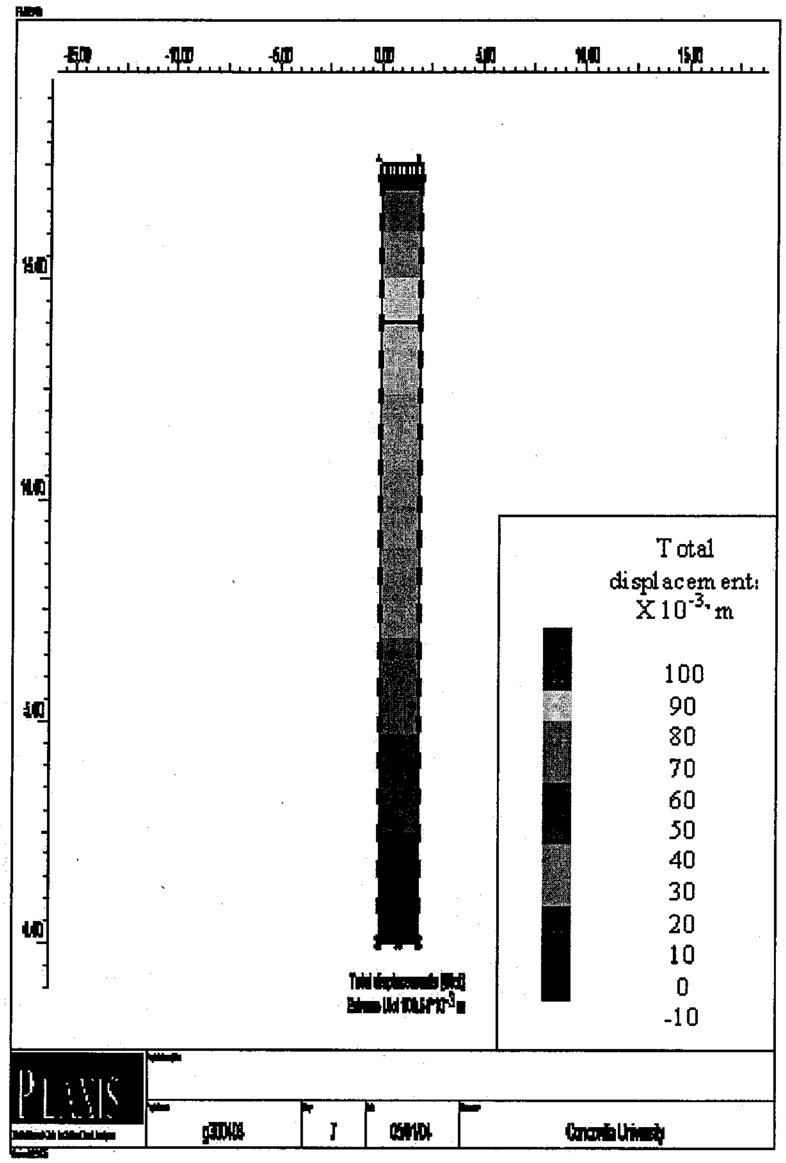

Figure 3.5 Total displacements of the surface points of the upper layer

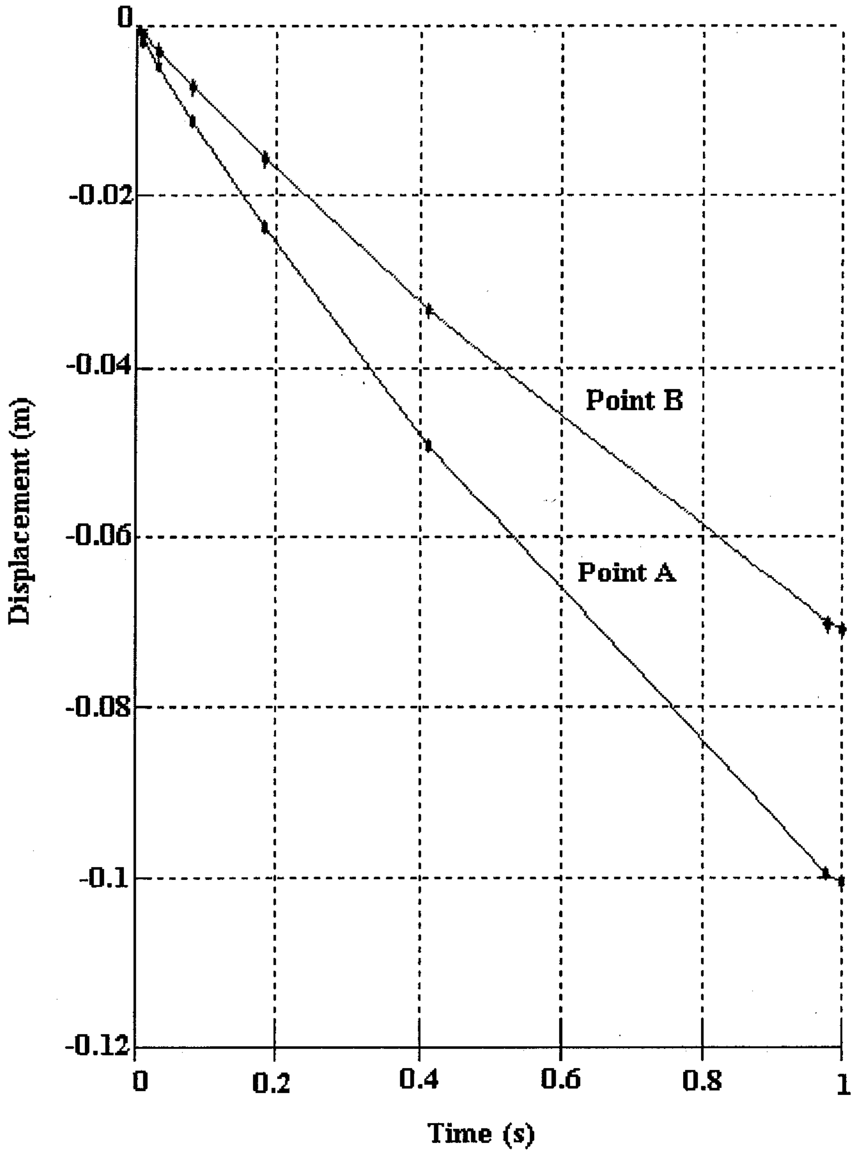

Figure 3.6 Total settlement of the surface (point A) and the displacement of the interface (point B)

All the total settlements, S, of the 160 calculations are listed in the Table 3.4 in column number 7. All total displacements S_i of the interface points between the two layers are listed in column 8. In accordance with the total settlement definition it is evident that compression **Δh** (column number 9) of the subgrade layer is the difference between the total settlement S of the surface point and the total displacement S_i of the interface point of the layers (Figure 3.6).

$$\Delta \mathbf{h} = S - S_i \quad (3.1)$$

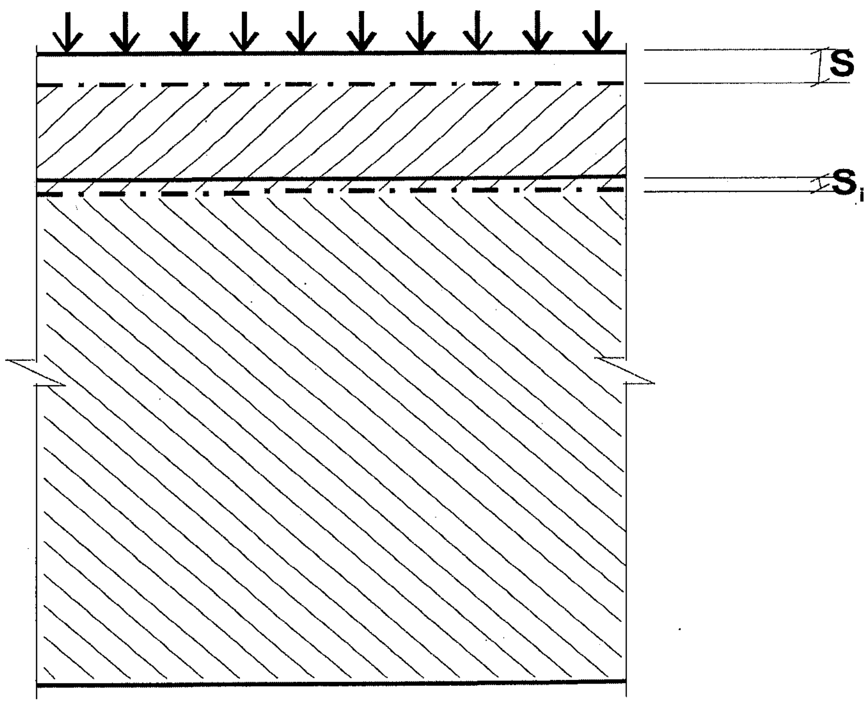

Figure 3.7 Settlement of the two-layered soil under applied load

Table 3.4 Total settlement and compression of the subgrade layer

Load, kN/m²	Series	Serial number	γ_1, kN/m³	ϕ_1, °	h_1, m	Total settlement of the surface point, x 10^{-3}, S, m	Extreme total displacement of the interface point, x 10^{-3}, Si, m	Compression of the upper layer, x 10^{-3}, Δh, m
1	2	3	4	5	6	7	8	9
300	1	1	12	25	0,5	89	80	9
300	1	2	12	25	0,7	91	79	12
300	1	3	12	25	1,0	94	76	18
300	1	4	12	25	1,5	99	75	24
300	1	5	12	25	2	105	73	32
300	1	6	12	25	2,5	111	72	39
300	1	7	12	25	3,0	117	71	46
300	1	8	12	25	5,0	140	67	73
300	1	9	12	25	7,0	160	64	96
300	1	10	12	25	10,0	188	60	128
300	2	11	14	30	0,3	82	75	7
300	2	12	14	30	0,7	88	79	9
300	2	13	14	30	1,0	91	78	13
300	2	14	14	30	1,5	95	76	19
300	2	15	14	30	2	99	74	25
300	2	16	14	30	2,5	103	73	30
300	2	17	14	30	3,0	107	71	36
300	2	18	14	30	5,0	122	66	56
300	2	19	14	30	7,0	137	63	74
300	2	20	14	30	10,0	159	59	100
300	3	21	16	35	0,5	80	75	5
300	3	22	16	35	0,7	82	74	8
300	3	23	16	35	1,0	84	73	11
300	3	24	16	35	1,5	91	75	16
300	3	25	16	35	2	94	74	20
300	3	26	16	35	2,5	97	72	25
300	3	27	16	35	3,0	100	71	29
300	3	28	16	35	5,0	110	65	45
300	3	29	16	35	7,0	122	62	60
300	3	30	16	35	10,0	139	59	70
300	4	31	17	40	0,5	81	75	6
300	4	32	17	40	0,7	82	74	8
300	4	33	17	40	1,0	84	73	11
300	4	34	17	40	1,5	87	72	15
300	4	35	17	40	2	94	73	21
300	4	36	17	40	2,5	97	72	25
300	4	37	17	40	3,0	101	71	30
300	4	38	17	40	5,0	112	66	46
300	4	39	17	40	7,0	122	62	60
300	4	40	17	40	10,0	137	57	70

Load, kN/m^2	Series	Serial number	γ_1, kN/m^3	ϕ_1, °	h_1, m	Total settlement of the surface point, x $^{10-3}$, S, m	Extreme total displacement of the interface point, x $^{10-3}$, Si, m	Compression of the upper layer, x $^{10-3}$, Δh, m
1	2	3	4	5	6	7	8	9
100	5	41	12	25	0,3	35	31	4
		42			0,7	37	31	6
		43			1,0	38	30	8
		44			1,5	41	30	11
		45			2.0	44	29	15
		46			2,5	47	29	18
		47			3,0	49	28	21
		48			5,0	59	26	33
		49			7,0	67	25	42
		50			10,0	78	23	55
	6	51	14	30	0,3	34	31	3
		52			0,7	35	31	4
		53			1,0	36	30	6
		54			1,5	38	30	8
		55			2.0	40	29	11
		56			2,5	41	28	13
		57			3,0	43	27	16
		58			5,0	49	25	24
		59			7,0	55	23	32
		60			10,0	63	22	41
	7	61	16	35	0,3	34	31	3
		62			0,7	34	31	3
		63			1,0	35	30	5
		64			1,5	36	29	7
		65			2.0	38	29	9
		66			2,5	39	28	11
		67			3,0	40	27	13
		68			5,0	44	25	19
		69			7,0	48	23	25
		70			10,0	54	21	33
	8	71	17	40	0,3	34	31	3
		72			0,7	34	30	1
		73			1,0	35	30	5
		74			1,5	37	29	8
		75			2.0	38	29	9
		76			2,5	39	28	11
		77			3,0	41	27	14
		78			5,0	44	25	19
		79			7,0	48	23	25
		80			10,0	54	21	33

Load, kN/m²	Series	Serial number	γ_1, kN/m³	ϕ_1, °	h_1, m	Total settlement of the surface point, x 10^{-3}, S, m	Extreme total displacement of the interface point, x 10^{-3}, Si, m	Compression of the upper layer, x 10^{-3}, Δh, m
1	2	3	4	5	6	7	8	9
50	9	81	12	25	0,3	20	17	3
		82			0,7	20	17	3
		83			1,0	21	17	4
		84			1,5	23	16	7
		85			2.0	25	16	9
		86			2,5	26	15	11
		87			3,0	28	15	13
		88			5,0	33	14	19
		89			7,0	37	13	24
		90			10,0	42	12	30
	10	91	14	30	0,3	19	17	2
		92			0,7	19	16	3
		93			1,0	20	16	4
		94			1,5	21	16	5
		95			2.0	22	16	6
		96			2,5	22	14	8
		97			3,0	23	14	9
		98			5,0	26	13	13
		99			7,0	30	12	18
		100			10,0	34	11	23
	11	101	16	35	0,3	18	17	1
		102			0,7	18	16	2
		103			1,0	19	16	3
		104			1,5	19	15	4
		105			2.0	20	15	5
		106			2,5	21	14	7
		107			3,0	21	14	7
		108			5,0	24	13	11
		109			7,0	26	12	14
		110			10,0	30	11	19
	12	111	17	40	0,3	18	17	1
		112			0,7	18	16	2
		113			1,0	19	16	3
		114			1,5	20	15	5
		115			2.0	20	15	5
		116			2,5	21	14	7
		117			3,0	21	14	7
		118			5,0	24	13	11
		119			7,0	26	12	14
		120			10,0	29	11	18

Load, kN/m²	Series	Serial number	γ_1, kN/m³	ϕ_1, °	h_1, m	Total settlement of the surface point, x 10^{-3}, S, m	Extreme total displacement of the interface point, x 10^{-3}, Si, m	Compression of the upper layer, x 10^{-3}, Δh, m
1	2	3	4	5	6	7	8	9
40	13	121	12	25	0,3	16	14	2
		122			0,7	17	14	3
		123			1,0	17	13	4
		124			1,5	19	13	6
		125			2.0	20	12	8
		126			2,5	21	12	9
		127			3,0	22	12	10
		128			5,0	26	11	15
		129			7,0	30	10	20
		130			10,0	34	9	25
	14	131	14	30	0,3	15	14	1
		132			0,7	16	13	3
		133			1,0	16	13	3
		134			1,5	17	13	4
		135			2.0	18	13	5
		136			2,5	18	11	7
		137			3,0	19	12	7
		138			5,0	22	11	11
		139			7,0	24	10	14
		140			10,0	28	9	19
	15	141	16	35	0,3	15	14	1
		142			0,7	15	14	1
		143			1,0	16	13	3
		144			1,5	16	13	3
		145			2.0	17	13	4
		146			2,5	17	12	5
		147			3,0	18	12	6
		148			5,0	19	10	9
		149			7,0	21	10	11
		150			10,0	23	9	14
	16	151	17	40	0,3	15	14	1
		152			0,7	15	14	1
		153			1,0	16	13	3
		154			1,5	16	13	3
		155			2.0	17	13	4
		156			2,5	17	12	5
		157			3,0	18	12	6
		158			5,0	19	10	9
		159			7,0	21	9	12
		160			10,0	23	9	14

CHAPTER 4

RESULTS AND ANALYSIS

4.1 Contribution of the upper soil layer to the settlement of the layered system

160 series of tests were performed to predict the settlement on the two-layered cohesionless soil system with the weaker upper layer; it is possible to observe the contribution of each parameter (thickness of the upper layer h_1, angle of shearing resistance ϕ_1 and different loading) to the output value of the settlement.

4.1.1 Effect of the load applied

1. The greater is the applied load (column number 1), the greater is the total settlement of the upper layer (column number 7), as well as the total displacement of the interface point (column number 8) between the layers;
2. In case of layers of the same thickness and angle of shearing resistance, the compression (column number 9) increases due to an increase of the applied load.

4.1.2 Effect of the thickness of the subgrade layer

1. The total settlement of the subgrade layer (column number 7) increases due to an increase of the thickness of the upper layer (column number 6).

2. The thicker of the upper layer (column number 6), the lesser is the total displacement of the interface points between the subgrade and the lower deeper layers (column number 8);
3. The thicker of the upper layer (under the same applied load and for the layers with the same angle of shearing resistance), the greater is the compression of the upper layer;

4.1.3 Effect of the angle of shearing resistance

1. The higher the is angle of shearing resistance of the upper layer (under the same applied load and for layers of the same thickness), the lesser is the total settlement of the upper layer and the total displacement of the interface points;
2. The higher is angle of shearing resistance of the upper layer (under the same applied load and for the layers of the same thickness), the lesser is the compression.

4.2 Design charts

In order to illustrate the relationships of the parameters from the Table 3.4 various charts have been constructed. Most of them are shown in the Appendix A. Typical charts reflecting the settlements of the surface and interface points of the layers, the compression of the upper layer and its interaction with the thickness of subgrade layer, its internal friction angle and the load applied are presented in the Figures 4.1. – 4.6.

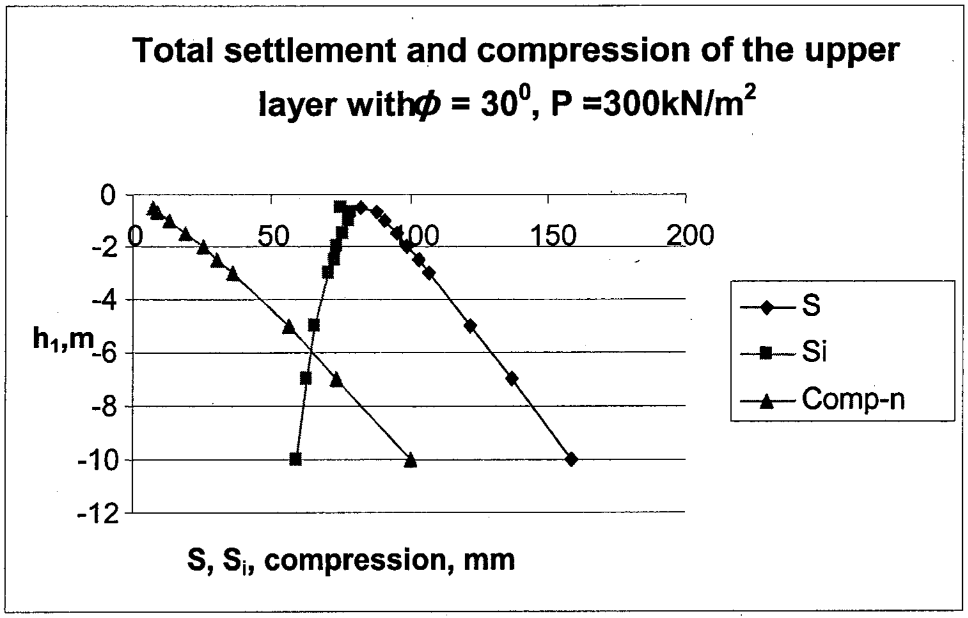

Figure 4.1 Total settlements, total displacements and the values of compression of the subgrade layers

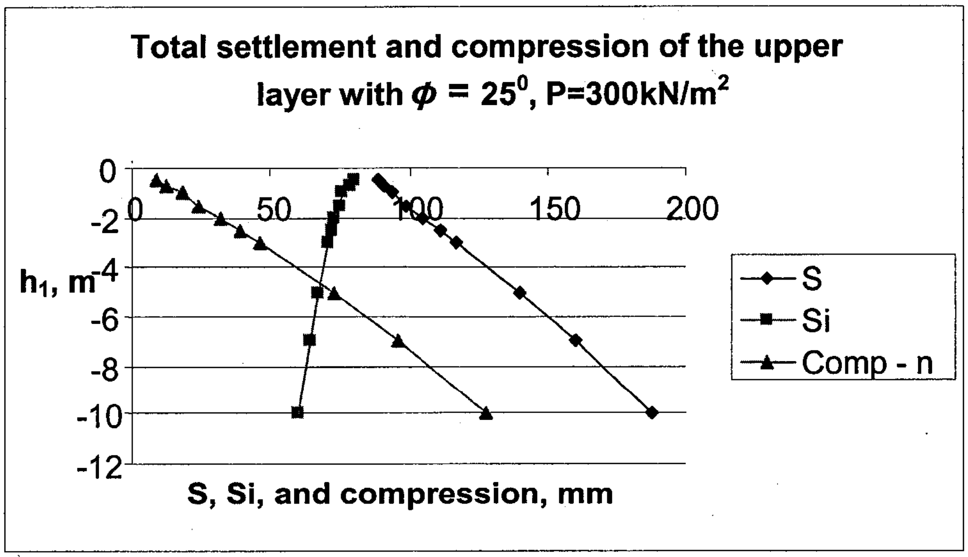

Figure 4.2 Total settlements, total displacements and the values of compression of the subgrade layers

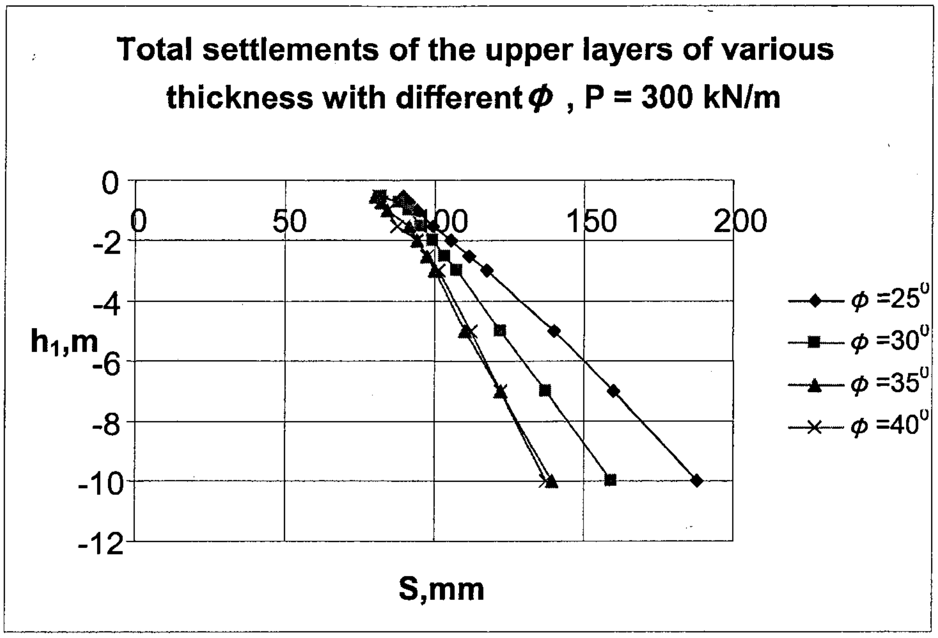

Figure 4.3 Total settlements of the subgrade layers

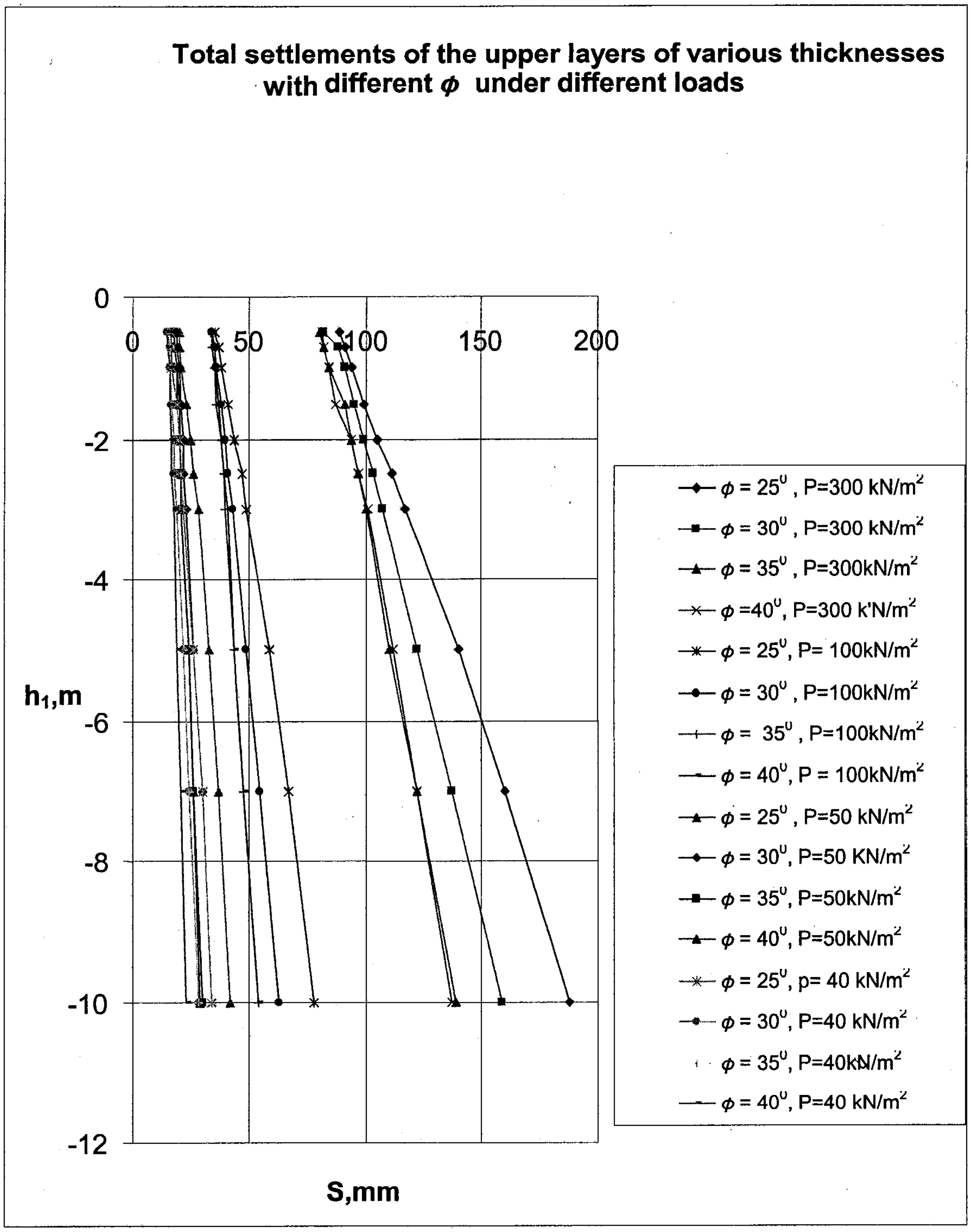

Figure 4.4 Total settlements of two-layered systems

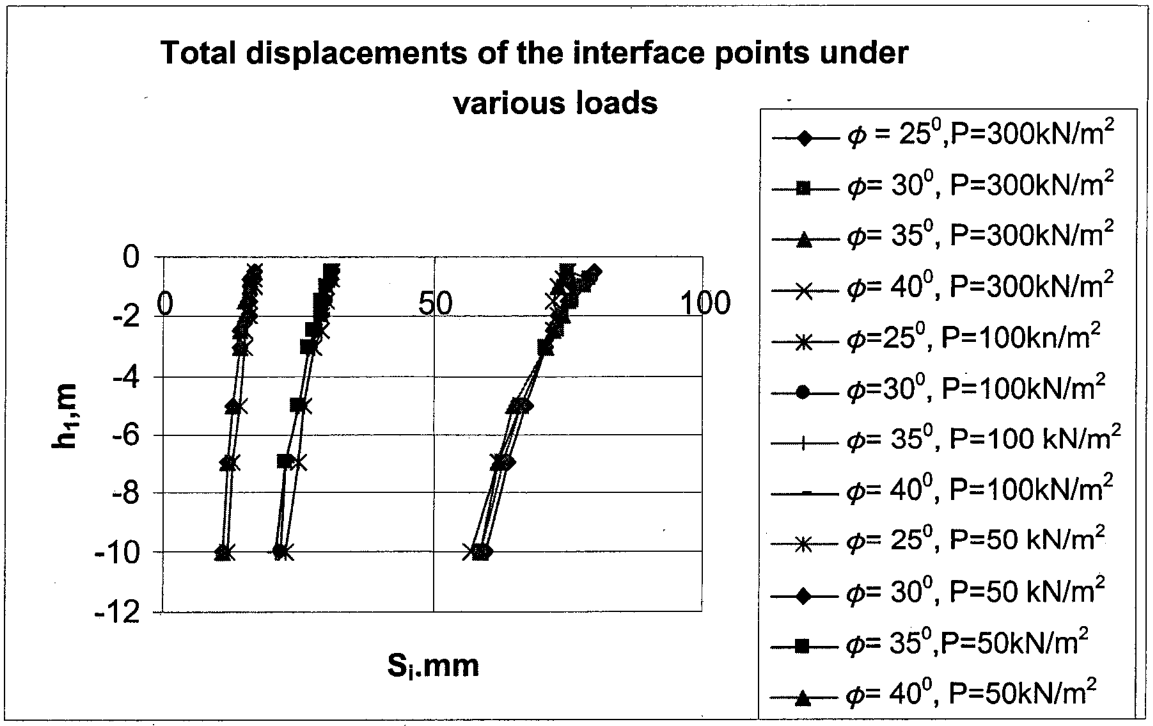

Figure 4.5 Total settlements of subgrade layers of various thicknesses

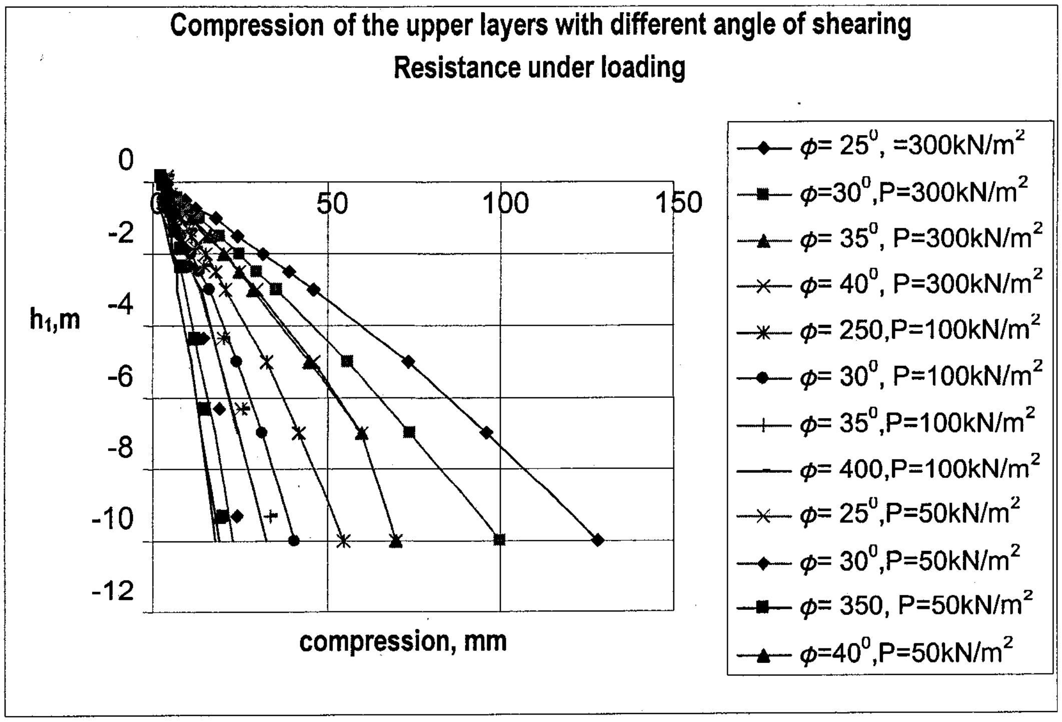

Figure 4.6 Compression values of the subgrade layers

4.3 Comparison between the results produced by the Numerical Model and Schmertmann's method of settlement calculation

It was decided to compare the calculated values of settlement from the Table 3.4 with the existing standard procedure of settlement computation for cohesionless soil. Schmertmann's method of settlement calculation was chosen as the most convenient for available input data parameters. In spite of some limitations of Schmertmann's calculation procedure (homogeneous soil and the depth, limited by the value equal to 2B, where B is the width of the foundation) several series of calculation have been done, while some assumptions were made:

1. The immediate settlement of the two-layered soil system was computed for each layer separately and then they were summed together.

2. As the width of the applied loading was previously chosen 2 meters, and according to Schmertmann's limitation for the depth equal to 2B (for strain vertical influence factor decreases linearly to zero at a depth of 2B), it was decided reasonable to use the series of calculations with the thickness of the subgrade layer h_l in the range of 1 – 3 meters.
3. Compression modulus E_s used for settlement calculation in Schmertmann's method was correlated with the input default parameter of the material soil model in Plaxis series of calculation according to [29] using the following relationship:

$$E_s = \frac{E}{2(1+\nu)} \tag{4.1}$$

Where:

E - is the input value of the secant stiffness in standard drained triaxial test E^{ref}_{50};

ν – is Poisson's ratio, ν_{ur} – for unloading- reloading input values used in hardening soil material model.

The most close results were obtained while computing the settlements under the load $P = 300\ kN/m^2$.

Below are several calculations for different h_l and ϕ_l parameters:

4.3.1 The case where the thickness of the upper layer h_l= 2 m and its $\phi_1 = 25^0$

The load P= 300 kN/m^2
$B_l = 2$ m
$h_l = 2$ m
$\phi_1 = 25^0$; $\phi_2 = 45^0$
$\gamma_1 = 12\ kN/m^3$; $\gamma_2 = 20\ kN/m^3$
$E_{50}{}^{ref}{}_1 = 20000 kN/m^2$; $E_{50}{}^{ref}{}_2 = 40000 kN/m^2$

According to equation (4.1) compression modulus for each layer:

$$E_{s1} = \frac{20000}{2(1+0,2)} = 9091 \text{ kN/m}^2$$

$$E_{sI1} = \frac{40000}{2(1+0,2)} = 18182 \text{ kN/m}^2$$

Maximum value for the vertical strain influence factor was taken 0.6 according to [23].

4.3.1. 1 Settlement of the first layer

Effective depth for settlement calculation was obviously taken 2 meters, equal to the thickness of this subgrade layer. Minimum (0.1), maximum (0.6) and zero values for the vertical strain influence factor I_z were taken according to [23] at the depth:

$z = 0 \rightarrow I_z = 0.1$

$0.5\,B_1 = 0.5 \text{ x } 2 = 1 \text{ m} \rightarrow I_z = 0.6$

$2\,B_1 = 2 \text{ x } 2 = 4 \text{ m} \rightarrow I_z = 0$

Table 4.1 was made according to Schmertmann's method procedure. Values for vertical strain influence factor were determined according the figure 4.7

Table 4.1 Intermediate parameters for settlement of the upper layer calculation for the input data: $h_1 = 2$m, $\gamma_1 = 12$ kN/m^3

Depth m	Δz m	z_i m	E_s kN/m^2	Average I_z	$\frac{I_z}{E_S}\Delta z$ x 10^{-4} m^3/kN
0-1	1	0.5	9091	0.35	$\frac{0.35}{9091}x1 = 0.385$
1-2	1	1.5	9091	0.50	$\frac{0.50}{9091}x1 = 0.550$

$$\sum_{0}^{2B} \Delta Z = 2 \text{ m} \qquad \sum_{0}^{2B} \frac{I_z}{E_S} \Delta Z = 0.935 \times 10^{-4} \text{ m}^3/\text{kN}$$

Correction factors:

for depth:

$$C_1 = 1\text{-}0.5 \left(\frac{q_0}{q - q_0} \right)$$

Where: q - is the overburden pressure at the foundation level;

$(q - q_0)$ - is net increase in foundation pressure

q_0- is the pressure imposed on the soil by the footing.

C_1 was taken equal to 1 for the upper layer as the load applied directly on the surface.

For creep:

$C_2 = 1 + 0.2 \log \left(\frac{t}{0.1} \right)$, where t – is time in years was taken 50 years.

$$C_2 = 1 + 0.2 \log \left(\frac{50}{0.1} \right) = 1.54$$

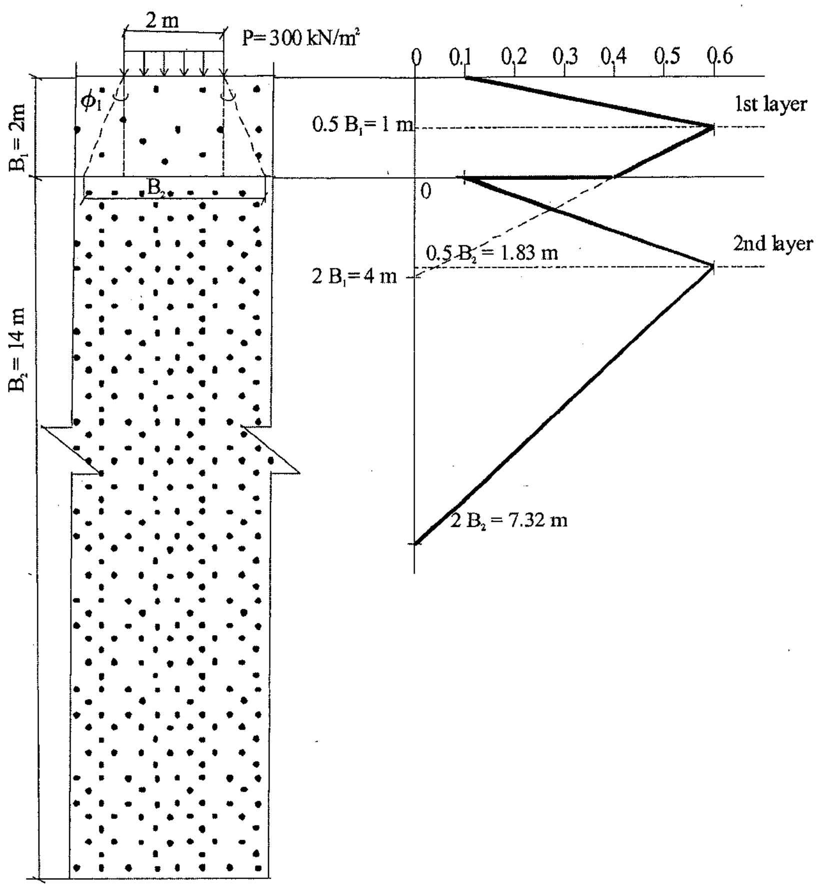

Figure 4.7 General diagram for I_z determination according to Schmertmann, for the case with h_1=2m and ϕ_1= 25^0

Hence, the settlement of the first layer was calculated by using Schmertmann formula:

$$S_I = C_1 \text{ x } C_2\,(q - q_0)\sum_0^{2B}\frac{I_z}{E_S}\Delta Z = 1\text{x}1.54\text{x } 300(\text{kN/m}^2)\text{x } 0.935 \text{ x } 10^{-4}\ (\text{m}^3/\text{kN}) =$$

$= 431.97 \text{ x } 10^{-4}$ (m) = 43.2 mm

4.3.1. 2 Settlement of the second layer

Effective width B_2 of the applied load in the interface was taken in consideration with the added pressure of the upper layer. Thus it was computed (figure 4.7) as:

$B_2 = B_1 + 2h_1 tg\phi_1 = 2 + 2\text{x } 2tg\ 25^0 = 3.66$ m

Minimum (0.1), maximum (0.6) and zero values for the vertical strain influence factor were taken according to [23] at the depth:

$z = 0 \rightarrow I_z = 0.1$

$0.5\ B_2 = 0.5 \times 3.66 = 1.83\ m \rightarrow I_z = 0.6$

$2\ B_2 = 2 \times 3.66 = 7.32\ m \rightarrow I_z = 0$

Table 4.1.1 was made for standard procedure of determining the values for vertical strain influence factor as well as the total settlement of the lower layer I_z was determined for each sublayer according to the figure 4.7.

Table 4.1.1 Intermediate parameters for the lower layer settlement calculation for the input data of the upper layer: $h_1 = 2m$, $\gamma_1 = 12\ kN/m^3$

Depth m	Δz m	z_i m	E_s kN/m^2	Average I_z	$\frac{I_z}{E_S}\Delta z$ x 10^{-4} m^3/kN
0-1	1	0.5	18182	0.24	$\frac{0.24}{18182}x1 = 0.127$
1-1.83	1.83	1.915	18182	0.58	$\frac{0.58}{18182}x1.83 = 0.584$
1.83-3	1.17	2.415	18182	0.53	$\frac{0.53}{18182}x1.17 = 0.341$
3-5	2	5	18182	0.30	$\frac{0.30}{18182}x2 = 0.330$
5-7.32	2.32	6.16	18182	0.13	$\frac{0.13}{18182}x2.32 = 0.166$

$\sum_{0}^{2B} \Delta Z = 7.32$ m $\qquad \sum_{0}^{2B} \frac{I_z}{E_S} \Delta Z = 1.548 \times 10^{-4}$ m^3/kN

$$C_1 = 1\text{-}0.5\left(\frac{q_0}{q-q_0}\right) = 1 - 0.5\ \frac{12x2}{300-12x2} = 0.96$$

$C_2 = 1.54$ (the same as for the upper layer)

Hence, $S_{II} = C_1 \times C_2 (q - q_0) \sum_{0}^{2B} \frac{I_z}{E_S} \Delta Z = 0.96x1.54x\ (300\text{-}\ 12x2)(\text{kN/m}^2) \times 1.548 \times 10^{-4}$ $(\text{m}^3/\text{kN}) = 631.6 \times 10^{-4}$ (m) = 63.2 mm

Total settlement $S_t = S_I + S_{II} = 43.2 + 63.2 = 106.4$ mm.

This calculation corresponds to the Plaxis serial running # 5 from the Table 3.4, where the value of computed settlement is equal to 105 mm.

Thus, the difference is $\frac{106{,}4-105}{106.4}$ x 100% = 1.3%.

4.3.2 The case where the thickness of the upper layer $h_1 = 2$ m and $\phi_1 = 30^0$

The load P= 300 kN/m^2
B = 2 m
$h_1 = 2$ m
$\phi_1 = 30^0$; $\phi_2 = 45^0$
$\gamma_1 = 14$ kN/m^3; $\gamma_2 = 20$ kN/m^3
$E_{50}{}^{ref}{}_1 = 25000$kN/m^2; $E_{50}{}^{ref}{}_2 = 40000$kN/m^2

4.3.2. 1 Settlement of the first layer

According to equation (4.1) compression modulus for the first layer:

$$E_{s1} = \frac{25000}{2(1+0{,}2)} = 11364 \text{ kN/m}^2$$

Geometrical parameters for sub layers of thee upper layer are going to be the same as in previous calculation, because of the same width of the applied load.

Corrections factors will be the same:

$C_1=1$

$C_2 = 1.54$

The settlement of the first layer is calculated by using the table 4.2, completed in accordance with the diagram from the figure 4.8:

$$S_I = C_1 \text{ x } C_2 (q - q_0) \sum_0^{2B} \frac{I_z}{E_S} \Delta Z = 1\text{x}1.54\text{x } 300(\text{kN/m}^2)\text{x } 0.748 \text{ x } 10^{-4} \text{ (m}^3\text{/kN)} =$$

$$= 345.6 \text{ x } 10^{-4} \text{ (m)} = 34.6 \text{ mm}$$

Table 4.2 Intermediate parameters for settlement of the upper layer calculation for the input data: $h_1 = 2m$, $\gamma_1 = 14$ kN/m^3

Depth m	Δz m	z_i m	E_s kN/m^2	Average I_z	$\frac{I_z}{E_S}\Delta z$ x 10^{-4} m^3/kN
0-1	1	0.5	11364	0.35	$\frac{0.35}{11364} x1 = 0.308$
1-2	1	1.5	11364	0.50	$\frac{0.50}{11364} x1 = 0.440$

$\sum_0^{2B} \Delta Z = 2$ m

$\sum_0^{2B} \frac{I_z}{E_S} \Delta Z = 0.748 \text{ x } 10^{-4}$ m^3/kN

4.3.2. 2 Settlement of the second layer

Effective width B_2 of the applied load in the interface was taken in consideration with the added pressure of the upper layer. Thus it was computed (figure 4.8) as:

$B_2 = B_1 + 2h_1 tg\phi_1 = 2 + 2\text{x } 2tg\ 30^0 = 4.31 \approx 4$ m

Minimum (0.1), maximum (0.6) and zero values for the vertical strain influence factor were taken according to [23] at the depth:

$z = 0 \rightarrow I_z = 0.1$

$0.5\ B_2 = 0.5 \times 4 = 2\ m \rightarrow I_z = 0.6$

$2\ B_2 = 2 \times 4 = 8\ m \rightarrow I_z = 0$

Table 4.2.1 was made for standard procedure of determining the values for vertical strain influence factor as well as the total settlement of the lower layer. I_z was determined for each sublayer according to the figure 4.8.

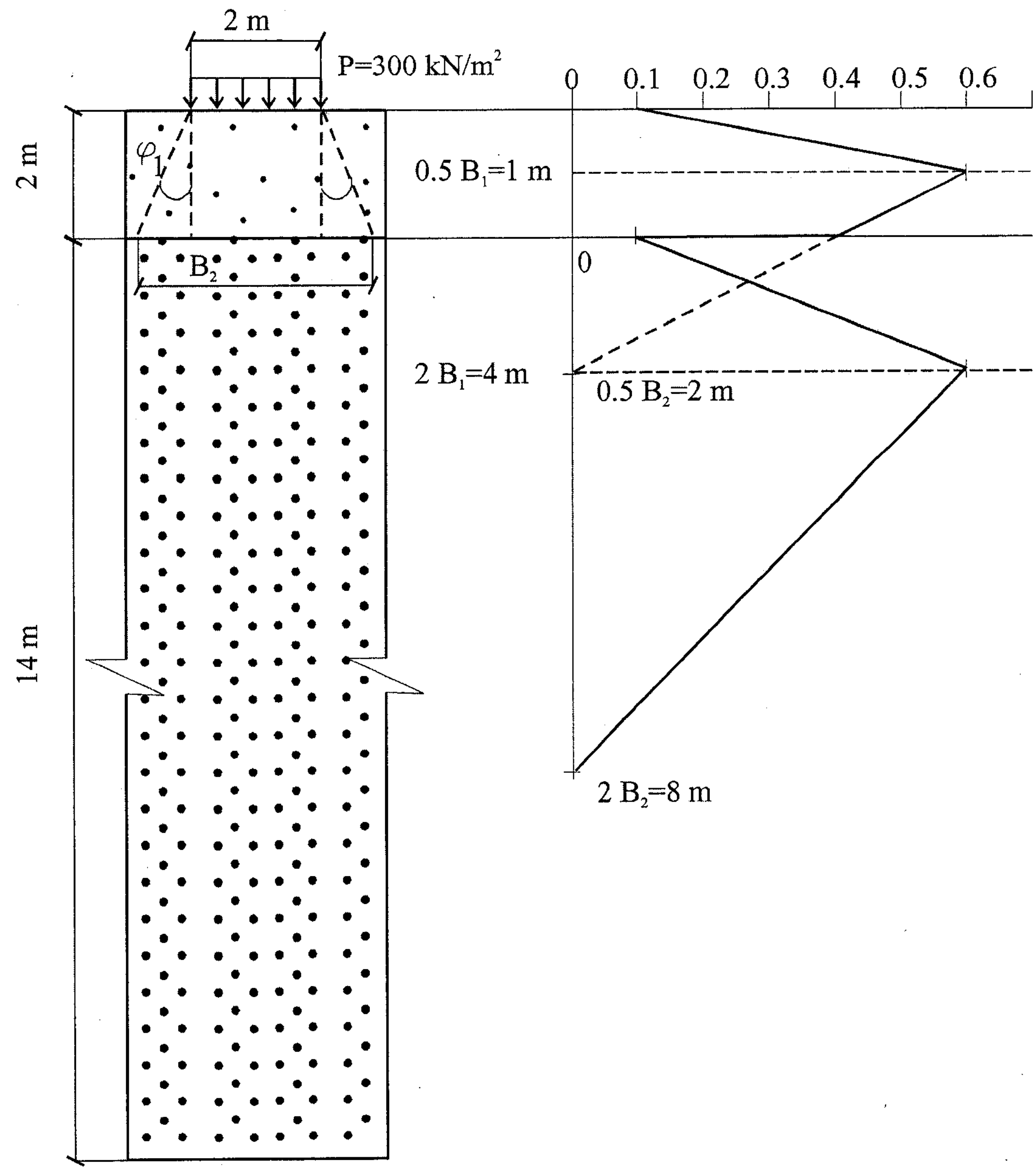

Figure 4.8 General diagram for I_z determination according to Schmertmann, for the case with h_1=2m and ϕ_1= 30^0

Table 4.2.1 Intermediate parameters for the lower layer settlement calculation for the input data of the upper layer: $h_1 = 2m$, $\gamma_1 = 14\ kN/m^3$

Depth M	Δz m	z_i m	E_s kN/m²	Average I_z	$\frac{I_z}{E_S}\Delta z$ x 10^{-4} m³/kN
0-2	2	1	18182	0.35	$\frac{0.35}{18182}x2 = 0.385$
2-4	2	3	18182	0.50	$\frac{0.50}{18182}x2 = 0.550$
4-6	2	5	18182	0.30	$\frac{0.30}{18182}x2 = 0.330$
6-8	2	7	18182	0.10	$\frac{0.10}{18182}x2 = 0.110$

$\sum_{0}^{2B}\Delta Z = 8$ m $\qquad \sum_{0}^{2B}\frac{I_z}{E_S}\Delta Z = 1.375 \times 10^{-4}$ m³/kN

$$C_1 = 1\text{-}0.5\left(\frac{q_0}{q-q_0}\right) = 1\text{-}\ 0.5\ \frac{14x2}{300-14x2} = 0.95$$

$C_2 = 1.54$ (the same as for the upper layer)

Hence, $S_{II} = C_1 \times C_2\,(q - q_0)\sum_{0}^{2B}\frac{I_z}{E_S}\Delta Z = 0.95x1.54x\ (300\text{-}\ 14x2)(kN/m^2) \times 1.375 \times 10^{-4}$

$(m^3/kN) = 547.16 \times 10^{-4}\ (m) = 54.7$ mm

Total settlement $S_t = S_I + S_{II} = 34.6 + 54.7 = 89.3$ mm.

This calculation corresponds to the Plaxis serial running # 15 from the Table 3.4, where the value of computed settlement is equal to 99 mm.

Thus, the difference is $\frac{99-89.3}{99}$ x 100% = 9%.

4.3.3 The case where the thickness of the upper layer $h_1 = 2$ m and $\phi_1 = 35^0$

The load P= 300 kN/m^2
B = 2 m
$h_1 = 2$ m
$\phi_1 = 35^0$; $\phi_2 = 45^0$
$\gamma_1 = 16$ kN/m^3; $\gamma_2 = 20$ kN/m^3
$E_{50}{}^{ref}{}_1 = 30000$kN/m^2; $E_{50}{}^{ref}{}_2 = 40000$kN/m^2

4.3.3. 1 Settlement of the first layer

According to equation (4.1) compression modulus for the first layer:

$$E_{s1} = \frac{30000}{2(1+0,2)} = 13636 \text{ kN/m}^2$$

Geometrical parameters for sub layers of thee upper layer are going to be the same as in the cases 4.3.1. 1 and 4.3.2.1, because of the same width of the applied load. Corrections factors will be the same:

C_1=1; C_2 = 1.54

The settlement of the first layer is calculated by using the table 4.3, completed in accordance with the diagram from the figure 4.9:

$$S_I = C_1 \text{ x } C_2 (q - q_0) \sum_0^{2B} \frac{I_z}{E_S} \Delta Z = 1\text{x}1.54\text{x } 300(\text{kN/m}^2)\text{x } 0.624 \text{ x } 10^{-4} \text{ (m}^3\text{/kN)} =$$

$$= 288.3 \text{ x } 10^{-4} \text{ (m)} = 28.8 \text{ mm}$$

Table 4.3 Intermediate parameters for settlement of the upper layer calculation for the input data: $h_1 = 2m$, $\gamma_1 = 16\ kN/m^3$

Depth M	Δz m	z_i m	E_s kN/m^2	Average I_z	$\frac{I_z}{E_S}\Delta z$ x 10^{-4} m^3/kN
0-1	1	0.5	13636	0.35	$\frac{0.35}{13636} x1 = 0.257$
1-2	1	1.5	13636	0.50	$\frac{0.50}{13636} x1 = 0.367$

$\sum_{0}^{2B} \Delta Z = 2$ m

$\sum_{0}^{2B} \frac{I_z}{E_S} \Delta Z = 0.624 \text{ x } 10^{-4}\ m^3/kN$

4.3.3. 2 Settlement of the second layer

Effective width B_2 of the applied load in the interface was taken in consideration with the added pressure of the upper layer. Thus it was computed (figure 4.9) as:

$B_2 = B_1 + 2h_1 tg\phi_1 = 2 + 2\text{x } 2tg\ 35^0 = 4.45$ m

Minimum (0.1), maximum (0.6) and zero values for the vertical strain influence factor were taken according to [23] at the depth:

$z = 0 \rightarrow I_z = 0.1$

$0.5\ B_2 = 0.5 \text{ x } 4.45 = 2.225 \text{ m} \rightarrow I_z = 0.6$

$2\ B_2 = 2 \text{ x } 4.45 = 8.9 \text{ m} \rightarrow I_z = 0$

Table 4.3.1 was made for standard procedure of determining the values for vertical strain influence factor as well as the total settlement of the lower layer. I_z was determined for each sublayer according to the figure 4.9.

Table 4.3.1 Intermediate parameters for the lower layer settlement calculation for the input data of the upper layer: $h_1 = 2$m, $\gamma_1 = 16$ kN/m^3

Depth m	Δz m	z_i m	E_s kN/m^2	Average I_z	$\frac{I_z}{E_S}\Delta z$ x 10^{-4} m^3/kN
0-2.25	2.25	1.125	18182	0.32	$\frac{0.32}{18182}x2.25 = 0.396$
2.25-4	1.75	3.125	18182	0.53	$\frac{0.53}{18182}x1.75 = 0.510$
4-6	2	5	18182	0.35	$\frac{0.35}{18182}x2 = 0.385$
6-8.9	2.9	7.45	18182	0.12	$\frac{0.12}{18182}x2.9 = 0.191$

$\sum_{0}^{2B}\Delta Z = 8.9$ m

$\sum_{0}^{2B}\frac{I_z}{E_S}\Delta Z = 1.482 \times 10^{-4}$ m^3/kN

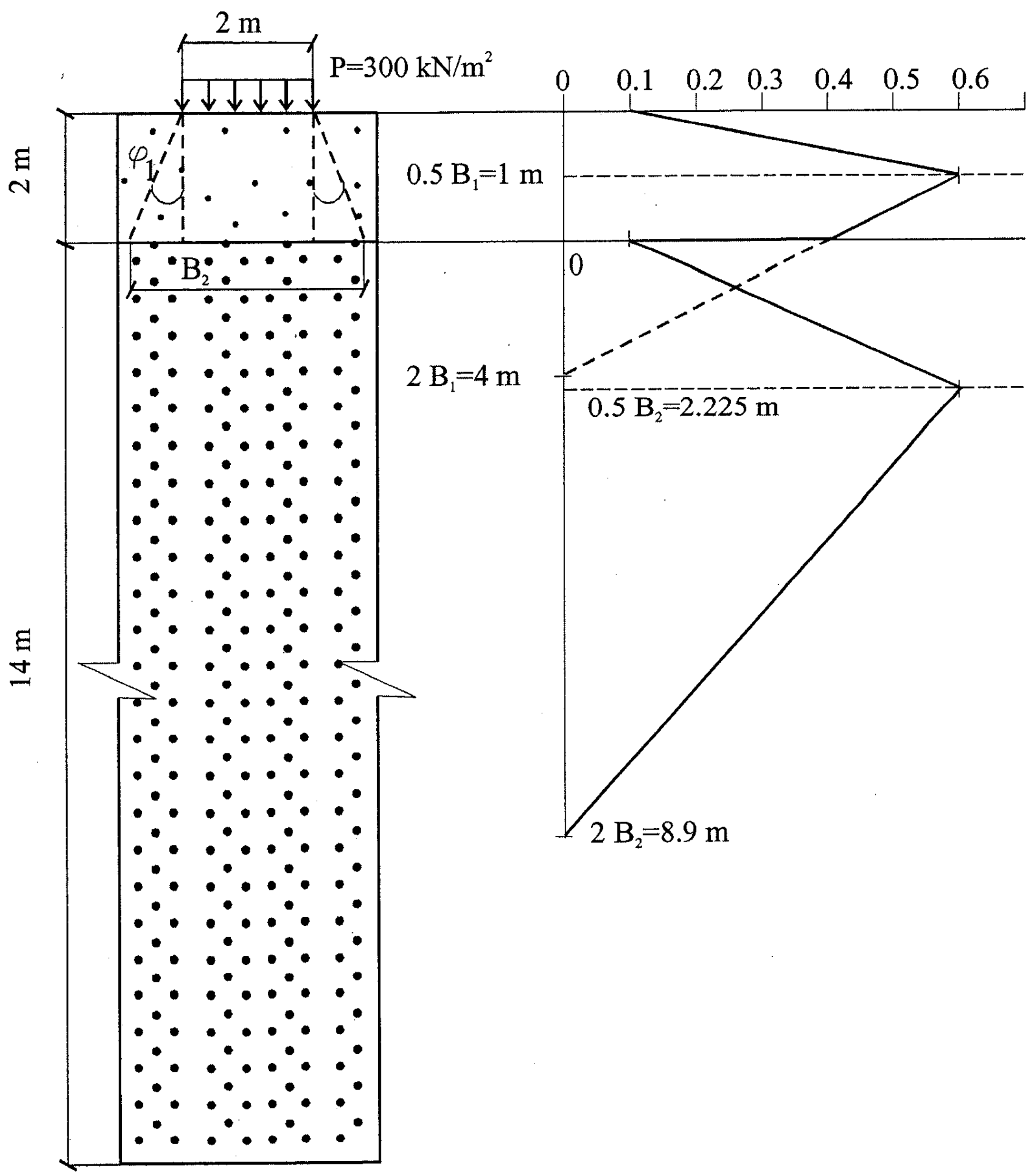

Figure 4.9 General diagram for I_z determination according to Schmertmann, for the case with h_1=2m and ϕ_1= 35^0

$$C_1 = 1\text{-}0.5\left(\frac{q_{\ 0}}{q - q_0}\right) = 1\text{-}\ 0.5\ \frac{16x2}{300 - 16x2} = 0.94$$

C_2 = 1.54 (the same as for the upper layer)

Hence, $S_{II} = C_1 \times C_2 (q - q_0) \sum_{0}^{2B} \frac{I_z}{E_S} \Delta Z = 0.94 \times 1.54 \times (300 - 16 \times 2)(kN/m^2) \times 1.482 \times 10^{-4}$ $(m^3/kN) = 574.9 \times 10^{-4}$ (m) = 57.5 mm

Total settlement $S_t = S_I + S_{II} = 28.8 + 57.5 = 86.3$ mm.

This calculation corresponds to the Plaxis serial running # 25 from the Table 3.4, where the value of computed settlement is equal to 94 mm.

Thus, the difference is $\frac{94 - 86.3}{94} \times 100\% = 8\%$.

4.3.4 The case where the thickness of the upper layer $h_1 = 2$ m and $\phi_1 = 40^0$

The load P= 300 kN/m^2
B = 2 m
$h_1 = 2$ m
$\phi_1 = 40^0$; $\phi_2 = 45^0$
$\gamma_1 = 17$ kN/m^3; $\gamma_2 = 20$ kN/m^3
$E_{50}^{ref}{}_1 = 30000 kN/m^2$; $E_{50}^{ref}{}_2 = 40000 kN/m^2$

4.3.4. 1 Settlement of the first layer

Compression modulus E_{s1} for the first layer will be of the same value as in the case 4.3.3. 1. and equal to $E_{s1} = 13636$ kN/m^2. Geometrical parameters for sub layers of the upper layer and correction factors C_1, C_2 are going to be the same as in the 4.3.3 calculation. Hence, the settlement of the first layer will also be the same as the settlement of the first layer in the 4.3.3. 1' calculation.

$S_I = 28.8$ mm

4.3.4. 2 Settlement of the second layer

Effective width B_2 of the applied load in the interface was taken in consideration with the added pressure of the upper layer. Thus it was computed (figure 4.10) as:

$$B_2 = B_1 + 2h_1 tg\phi_1 = 2 + 2x\ 2tg\ 40^0 = 4.9\ m$$

Minimum (0.1), maximum (0.6) and zero values for the vertical strain influence factor were taken according to [23] at the depth:

$$z = 0 \rightarrow I_z = 0.1$$

$$0.5\ B_2 = 0.5\ x\ 4.9 = 2.45\ m \rightarrow I_z = 0.6$$

$$2\ B_2 = 2\ x\ 4.9 = 9.8\ m \rightarrow I_z = 0$$

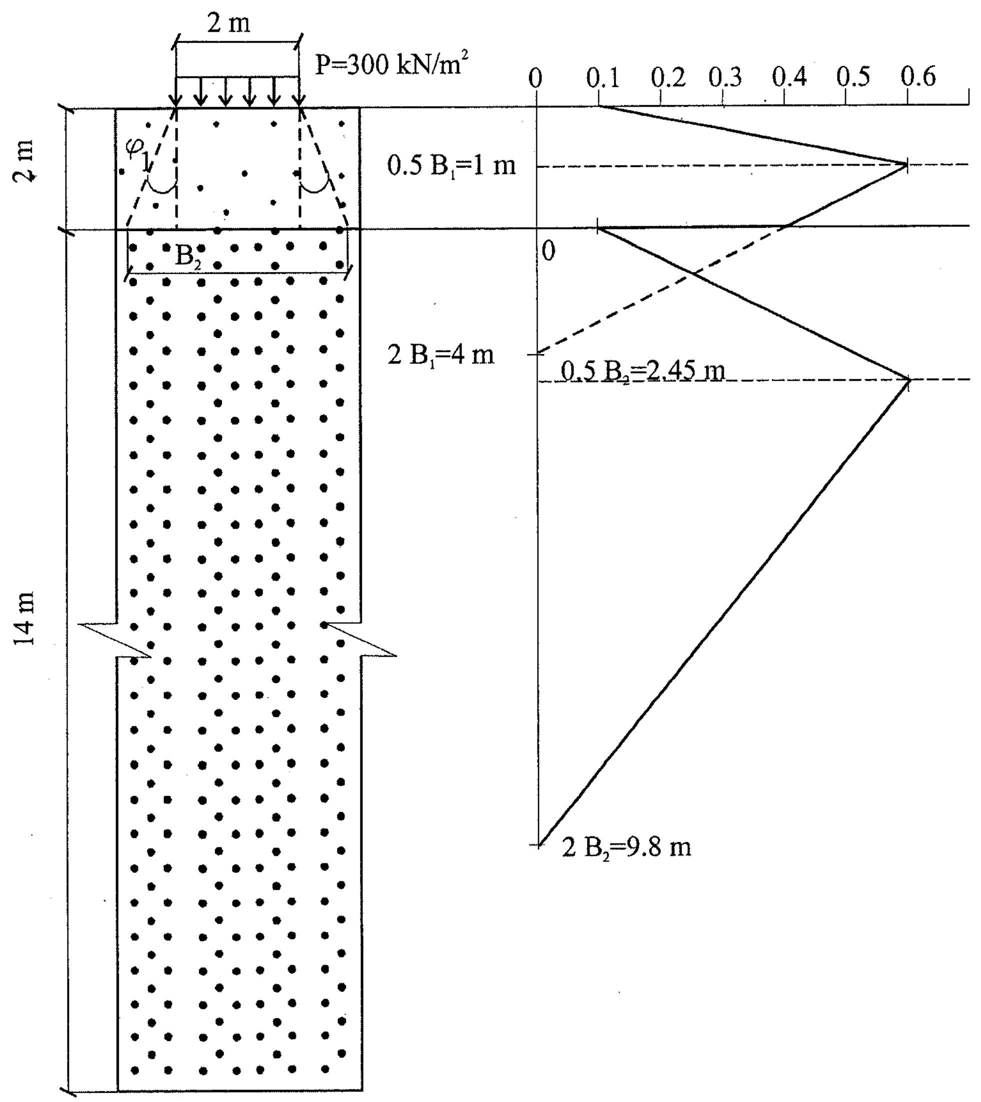

Figure 4.10 General diagram for I_z determination according to Schmertmann, for the case with h_1=2m and ϕ_1= 40^0

Table 4.4 was made for standard procedure of determining the values for vertical strain influence factor as well as the total settlement of the lower layer. I_z was determined for each sublayer according to the figure 4.10.

Table 4.4 Intermediate parameters for the lower layer settlement calculation for the input data of the upper layer: h_1 = 2m, γ_1 = 17 kN/m^3

Depth m	Δz m	z_i m	E_s kN/m^2	Average I_z	$\frac{I_z}{E_S}\Delta z$ x 10^{-4} m^3/kN
0-2.45	2.45	1.225	18182	0.35	$\frac{0.31}{18182}x2.45 = 0.472$
2.45-5	2.55	3.725	18182	0.475	$\frac{0.475}{18182}x2.55 = 0.666$
5-7	2	6	18182	0.31	$\frac{0.31}{18182}x2 = 0.341$
7-9.8	2.8	8.4	18182	0.11	$\frac{0.11}{18182}x2.8 = 0.169$

$$\sum_0^{2B} \Delta Z = 9.8 \text{ m} \qquad \sum_0^{2B} \frac{I_z}{E_S}\Delta Z = 1.648 \text{ x } 10^{-4} \text{ m}^3/\text{kN}$$

Correction factors:

$$C_1 = 1\text{-}0.5\left(\frac{q_0}{q - q_0}\right) = 1\text{-}\ 0.5\ \frac{17x2}{300 - 17x2} = 0.94$$

$C_2 = 1.54$

Hence,

$$S_{II} = C_1 \times C_2 \,(q - q_0) \sum_{0}^{2B} \frac{I_z}{E_S} \Delta Z = 0.94\text{x}1.54\text{x}\ (300\text{- }17\text{x}2)(\text{kN/m}^2) \text{ x } 1.648 \text{ x } 10^{-4}\ (\text{m}^3/\text{kN})$$

$= 634.6 \text{ x } 10^{-4}$ (m) = 63.5 mm

Total settlement $S_t = S_I + S_{II} = 28.8 + 63.5 = 92.3$ mm.

This calculation corresponds to the Plaxis serial running # 35 from the Table 3.4, where the value of computed settlement is equal to 94 mm.

Thus, the difference is $\frac{94 - 92.3}{94}$ x 100% = 1.8%.

4.3.5 The case where the thickness of the upper layer h_1= 3 m and $\phi_1 = 25^0$

The load P= 300 kN/m^2
$B_1 = 2$ m
$h_1 = 3$ m
$\phi_1 = 25^0$; $\phi_2 = 45^0$
$\gamma_1 = 12$ kN/m^3 ; $\gamma_2 = 20$ kN/m^3
$E_{50}{}^{ref}{}_1 = 20000$kN/m^2; $E_{50}{}^{ref}{}_2 = 40000$kN/m^2

4.3.5. 1 Settlement of the first layer

$$E_{s1} = \frac{20000}{2(1+0,2)} = 9091 \text{ kN/m}^2$$

Effective depth for settlement calculation was obviously taken 3 meters, equal to the thickness of this subgrade layer. Minimum (0.1), maximum (0.6) and zero values for the vertical strain influence factor were taken according to [23] at the same depths as for the calculations 4.3.1 – 4.3.4.

Table 4.5 was made according to Schmertmann's method procedure. Values for vertical strain influence factor were determined according the figure 4.11

Table 4.5 Intermediate parameters for settlement of the upper layer calculation for the input data: $h_1 = 3m$, $\gamma_1 = 12\ kN/m^3$

Depth m	Δz m	z_i m	E_s kN/m^2	Average I_z	$\frac{I_z}{E_S}\Delta z$ x 10^{-4} m^3/kN
0-1	1	0.5	9091	0.35	$\frac{0.35}{9091} x1 = 0.385$
1-3	2	2	9091	0.40	$\frac{0.40}{9091} x2 = 0.880$

$\sum_{0}^{2B} \Delta Z = 3$ m

$\sum_{0}^{2B} \frac{I_z}{E_S} \Delta Z = 1.265 \times 10^{-4}\ m^3/kN$

Correction factors:

$C_1 = 1$

$C_2 = 1 + 0.2 \log\left(\frac{50}{0.1}\right) = 1.54$

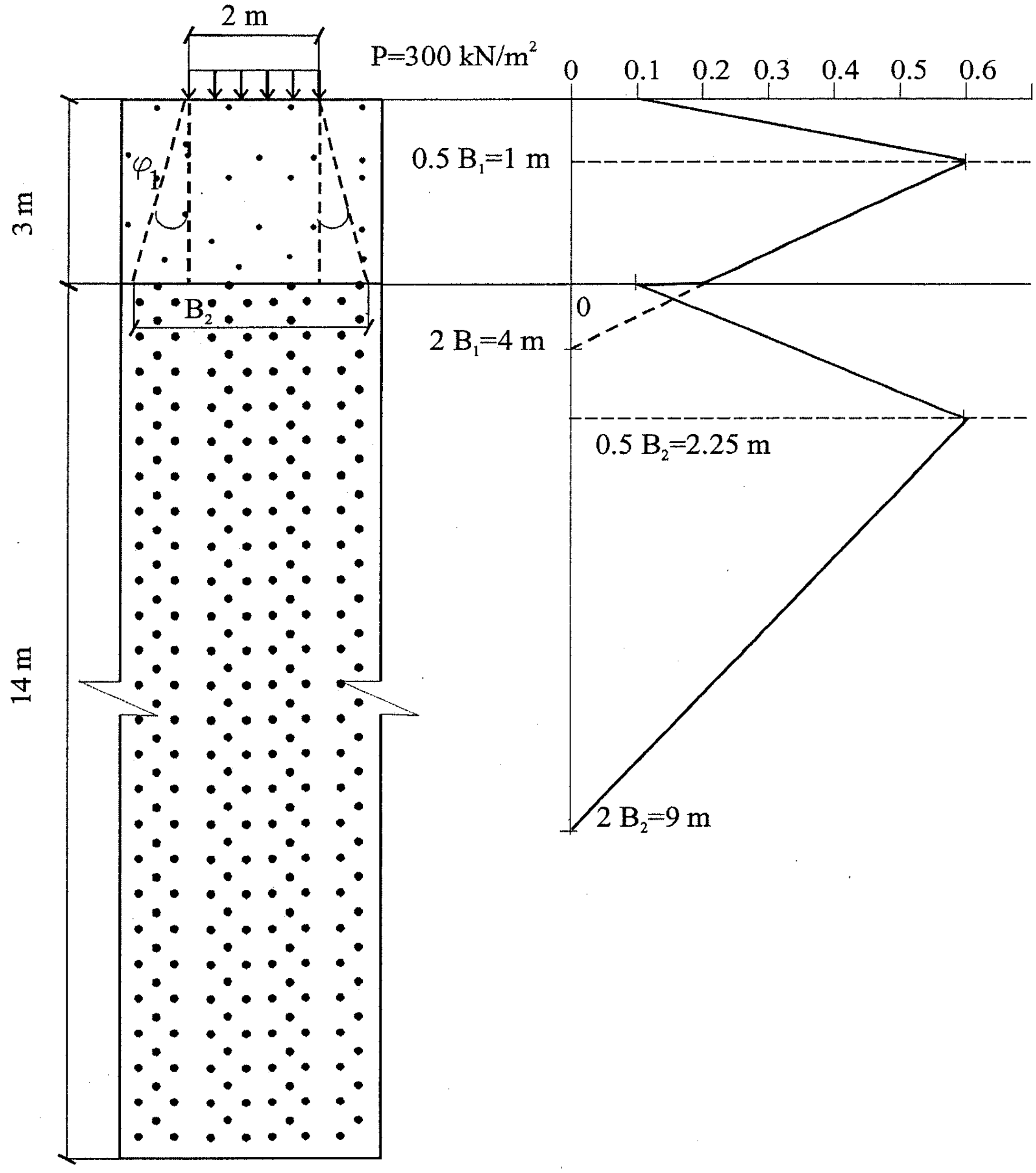

Figure 4.11 General diagram for I_z determination according to Schmertmann, for the case with h_1=3m and ϕ_1= 35^0

Hence, the settlement of the first layer:

$$S_I = C_1 \times C_2\,(q - q_0) \sum_0^{2B} \frac{I_z}{E_S} \Delta Z = 1 \times 1.54 \times 300(\text{kN/m}^2) \times 1.265 \times 10^{-4}\ (\text{m}^3/\text{kN}) =$$

$$= 584.4 \times 10^{-4}\ (\text{m}) = 58.4\ \text{mm}$$

4.3.5. 2 Settlement of the second layer:

$$E_{sII} = \frac{40000}{2(1+0{,}2)} = 18182\ \text{kN/m}^2$$

Effective width B_2 of the applied load in the interface was taken in consideration with the added pressure of the upper layer. Thus it was computed (figure 4.11) as:

$$B_2 = B_1 + 2h_1 tg\phi_1 = 2 + 2 \times 3tg\, 25^0 = 4.5\ \text{m}$$

Minimum (0.1), maximum (0.6) and zero values for the vertical strain influence factor were taken according to [23] at the depth:

$z = 0 \rightarrow I_z = 0.1$

$0.5\, B_2 = 0.5 \times 4.5 = 2.25\ \text{m} \rightarrow I_z = 0.6$

$2\, B_2 = 2 \times 4.5 = 9\ \text{m} \rightarrow I_z = 0$

Table 4.5.1 was made for standard procedure of determining the values for vertical strain influence factor as well as the total settlement of the lower layer I_z was determined for each sublayer according to the figure 4.11.

$$C_1 = 1\text{-}0.5\left(\frac{q_{\ 0}}{q - q_0}\right) = 1\text{-}\ 0.5\ \frac{12x3}{300 - 12x3} = 0.93$$

$C_2 = 1.54$ (the same as for the upper layer)

Table 4.5.1 Intermediate parameters for the lower layer settlement calculation for the input data of the upper layer: h_1 = 3m, γ_1 = 12 kN/m^3

Depth m	Δz m	z_i m	E_s kN/m^2	Average I_z	$\frac{I_z}{E_S}\Delta z$ x 10^{-4} m^3/kN
0-2.25	2.25	1.125	18182	0.35	$\frac{0.35}{18182}x2.25 = 0.433$
2.25-4	1.75	3.125	18182	0.52	$\frac{0.52}{18182}x1.75 = 0.500$
4-6	2	5	18182	0.34	$\frac{0.34}{18182}x2 = 0.374$
6-7	1	6.5	18182	0.16	$\frac{0.16}{18182}x1 = 0.088$
7-9	2	8	18182	0.12	$\frac{0.12}{18182}x2 = 0.132$

$\sum_0^{2B}\Delta Z = 9$ m $\qquad \sum_0^{2B}\frac{I_z}{E_S}\Delta Z = 1.527 \times 10^{-4}$ m^3/kN

Hence, $S_{II} = C_1 \times C_2\,(q - q_0)\sum_0^{2B}\frac{I_z}{E_S}\Delta Z = 0.93 \times 1.54 \times (300 - 12 \times 3)(\text{kN/m}^2) \times 1.527 \times 10^{-4}$

$(\text{m}^3/\text{kN}) = 577.4 \times 10^{-4}\ (\text{m}) = 57.7$ mm

Total settlement $S_t = S_I + S_{II} = 58.4 + 57.7 = 116.1$ mm.

This calculation corresponds to the Plaxis serial running # 7 from the Table 3.4, where the value of computed settlement is equal to 117 mm.

Thus, the difference is $\frac{117-116.1}{117}$ x 100% = 0.8%.

4.3.6 The case where the thickness of the upper layer h_1= 3 m and $\phi_1 = 30^0$

The load P= 300 kN/m^2
$B_1 = 2$ m
$h_1 = 3$ m
$\phi_1 = 30^0$; $\phi_2 = 45^0$
$\gamma_1 = 14$ kN/m^3 ; $\gamma_2 = 20$ kN/m^3
$E_{50}{}^{ref}{}_1 = 25000$kN/m^2; $E_{50}{}^{ref}{}_2 = 40000$kN/m^2

4.3.6. 1 Settlement of the first layer

According to equation (4.1) compression modulus for the first layer:

$$E_{s1} = \frac{25000}{2(1+0{,}2)} = 11364 \text{ kN/m}^2$$

Geometrical parameters for sub layers of the upper layer are going to be the same as in the 4.3.5.1 calculation.

Table 4.6 Intermediate parameters for settlement of the upper layer calculation for the input data: h_1 = 3m, γ_1 = 14 kN/m^3

Depth m	Δz m	z_i m	E_s kN/m^2	Average I_z	$\frac{I_z}{E_S}\Delta z$ x 10^{-4} m^3/kN
0-1	1	0.5	11364	0.35	$\frac{0.35}{11364}x1 = 0.308$
1-3	2	2	11364	0.40	$\frac{0.40}{11364}x2 = 0.704$

$$\sum_0^{2B} \Delta Z = 3 \text{ m} \qquad \sum_0^{2B} \frac{I_z}{E_S}\Delta Z = 1.012 \text{ x } 10^{-4} \text{ m}^3/\text{kN}$$

Corrections factors will be the same:

C_1=1; C_2 = 1.54

So, the settlement of the first layer will be according to the table 4.6, completed in accordance with the diagram from the picture 4.12.

$$S_I = C_1 \text{ x } C_2 (q - q_0) \sum_0^{2B} \frac{I_z}{E_S} \Delta Z = 1\text{x}1.54\text{x } 300(\text{kN/m}^2)\text{x } 1.012 \text{ x } 10^{-4} \text{ (m}^3\text{/kN)} =$$

$$= 467{,}5\text{x}10^{-4}\text{m} = 46.8\text{mm}$$

4.3.6. 2 Settlement of the second layer

Effective width B_2 of the applied load in the interface was taken in consideration with the added pressure of the upper layer. Thus it was computed (figure 4.12) as:

$$B_2 = B_1 + 2h_1 tg\phi_1 = 2 + 2\text{x } 3tg\, 30^0 \approx 5 \text{ m}$$

Minimum (0.1), maximum (0.6) and zero values for the vertical strain influence factor were taken according to [23] at the depth:

$z = 0 \rightarrow I_z = 0.1$
$0.5\, B_2 = 0.5 \text{ x } 5 = 2.5 \text{ m} \rightarrow I_z = 0.6$
$2\, B_2 = 2 \text{ x } 5 = 10 \text{ m} \rightarrow I_z = 0$

Table 4.6 was made for standard procedure of determining the values for vertical strain influence factor as well as the total settlement of the lower layer. I_z was determined for each sublayer according to the figure 4.12.

Table 4.6.1 Intermediate parameters for the lower layer settlement calculation for the input data of the upper layer: $h_1 = 3m$, $\gamma_1 = 14\ kN/m^3$

Depth M	Δz m	z_i m	E_s kN/m^2	Average I_z	$\frac{I_z}{E_S}\Delta z$ x 10^{-4} m^3/kN
0-2.5	2.5	1.25	18182	0.35	$\frac{0.35}{18182}x2.5 = 0.481$
2.5-5	2.5	3.75	18182	0.50	$\frac{0.50}{18182}x2.5 = 0.687$
5-6	1	5.5	18182	0.36	$\frac{0.36}{18182}x1 = 0.198$
6-8	2	7	18182	0.24	$\frac{0.24}{18182}x2 = 0.264$
8-10	2	9	18182	0.18	$\frac{0.11}{18182}x2 = 0.198$

$\sum_{0}^{2B} \Delta Z = 10\ m$ $\qquad$ $\sum_{0}^{2B} \frac{I_z}{E_S}\Delta Z = 1.827 \times 10^{-4}\ m^3/kN$

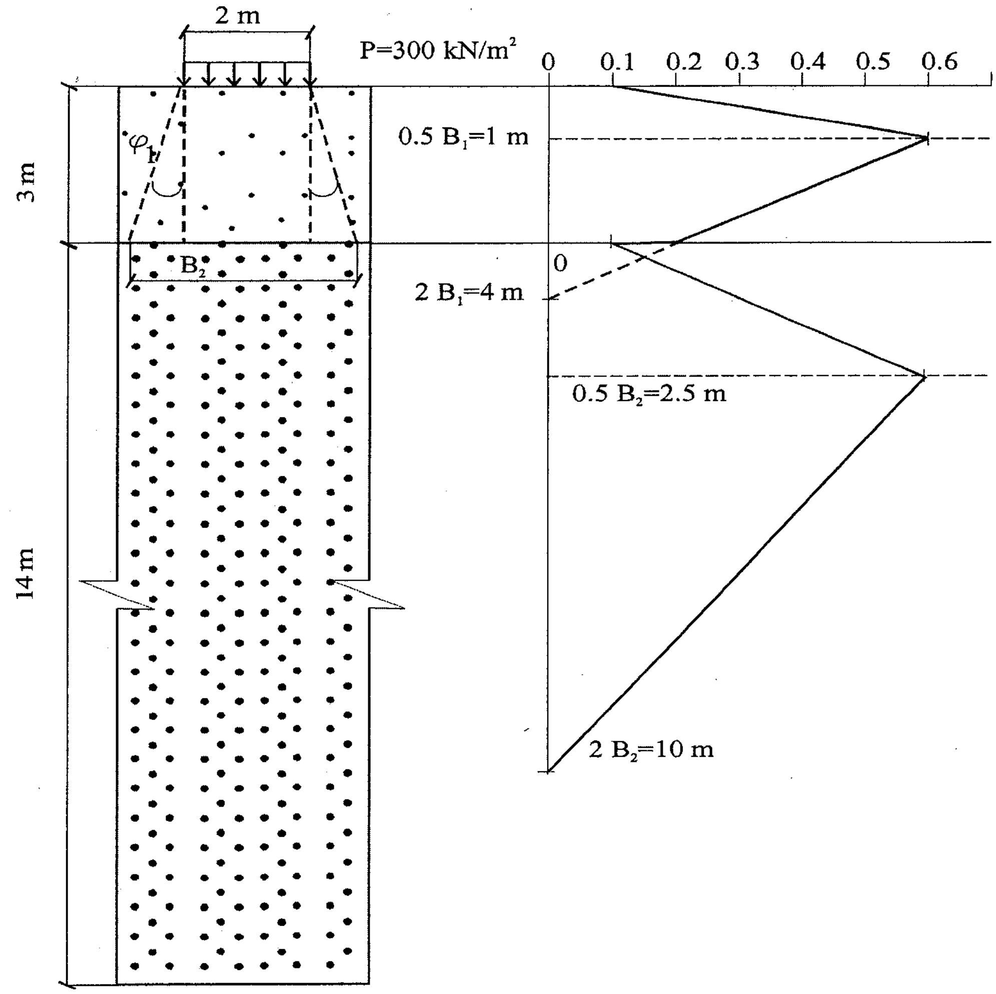

Figure 4.12 General diagram for I_z determination according to Schmertmann, for the case with h_1=3m and ϕ_1= 30^0

$$C_1 = 1\text{-}0.5\left(\frac{q_{\ 0}}{q-q_0}\right) = 1\text{-}\ 0.5\ \frac{14x3}{300-14x3} = 0.92; \quad C_2 = 1.54$$

$$S_{II} = C_1 \text{ x } C_2\,(q - q_0)\sum_0^{2B}\frac{I_z}{E_S}\Delta Z = 0.92\text{x}1.54\text{x }(300\text{- }14\text{x}3)(\text{kN/m}^2) \text{ x } 1.827 \text{ x } 10^{-4}\ (\text{m}^3/\text{kN})$$

= 667.8 x 10^{-4} (m) = 66.8 mm

Total settlement $S_t = S_I + S_{II}$ = 46.8 + 66.8 = 113.6 mm.

This calculation corresponds to the Plaxis serial running # 17 from the Table 3.4, where the value of computed settlement is equal to 107 mm.

Thus, the difference is $\frac{113{,}6-107}{113{,}6}$ x 100% = 6 %.

4.3.7 The case where the thickness of the upper layer h_l= 3 m and $\phi_1 = 35^0$

The load P= 300 kN/m^2
$B_l = 2$ m
$h_l = 3$ m
$\phi_1 = 35^0$; $\phi_2 = 45^0$
$\gamma_1 = 16$ kN/m^3; $\gamma_2 = 20$ kN/m^3
$E_{50}{}^{ref}{}_1 = 30000$kN/m^2; $E_{50}{}^{ref}{}_2 = 40000$kN/m^2

4.3.7. 1 Settlement of the first layer

According to equation (4.1) compression modulus for the first layer:

$$E_{s1} = \frac{30000}{2(1+0{,}2)} = 13636 \text{ kN/m}^2$$

Geometrical parameters for sub layers of the upper layer are going to be the same as in 4.3.5.1 and 4.3.6.1 calculations.

Corrections factors will be the same:

C_l=1; C_2= 1.54

The settlement of the first layer is calculated by using the table 4.7, completed in accordance with the diagram from the figure 4.13:

Table 4.7 Intermediate parameters for settlement of the upper layer calculation for the input data: h_l = 3m, γ_l = 14 kN/m^3

Depth m	Δz m	z_i m	E_s kN/m^2	Average I_z	$\frac{I_z}{E_S}\Delta z$ x 10^{-4} m^3/kN
0-1	1	0.5	13636	0.35	$\frac{0.35}{13636}x1 = 0.257$
1-3	2	2	13636	0.40	$\frac{0.40}{13636}x2 = 0.587$

$$\sum_{0}^{2B} \Delta Z = 3 \text{ m} \qquad \sum_{0}^{2B} \frac{I_z}{E_S} \Delta Z = 0.844 \text{ x } 10^{-4} \text{ m}^3/\text{kN}$$

$$S_I = C_1 \text{ x } C_2 (q - q_0) \sum_{0}^{2B} \frac{I_z}{E_S} \Delta Z = 1\text{x}1.54\text{x } 300(\text{kN/m}^2)\text{x } 0.844 \text{ x } 10^{-4} (\text{m}^3/\text{kN}) =$$

$$= 389.9 \text{ x } 10^{-4} \text{ (m)} \approx 39 \text{ mm}$$

4.3.7. 2 Settlement of the second layer

Effective width B_2 of the applied load in the interface was taken in consideration with the added pressure of the upper layer. Thus it was computed (figure 4.13) as:

$$B_2 = B_1 + 2h_1 tg\phi_1 = 2 + 2\text{x } 3tg\ 35^0 = 5.7 \text{ m}$$

Minimum (0.1), maximum (0.6) and zero values for the vertical strain influence factor were taken according to [23] at the depth:

$z = 0 \rightarrow I_z = 0.1$
$0.5\ B_2 = 0.5 \text{ x } 5.7 = 2.85 \text{ m} \rightarrow I_z = 0.6$
$2\ B_2 = 2 \text{ x } 5.7 = 11.4 \text{ m} \rightarrow I_z = 0$

Table 4.7.1 was made for standard procedure of determining the values for vertical strain influence factor as well as the total settlement of the lower layer. I_z was determined for each sublayer according to the figure 4.13.

Table 4.7.1 Intermediate parameters for the lower layer settlement calculation for the input data of the upper layer: h_1 = 3m, γ_1 = 16 kN/m^3

Depth m	Δz m	z_i m	E_s kN/m^2	Average I_z	$\frac{I_z}{E_S}\Delta z$ x 10^{-4} m^3/kN
0-2.85	2.85	1.425	18182	0.32	$\frac{0.32}{18182}x2.85 = 0.501$
2.85-5	2.15	3.925	18182	0.51	$\frac{0.51}{18182}x2.15 = 0.603$
5-7	2	6	18182	0.36	$\frac{0.36}{18182}x2 = 0.396$
7-9	2	8	18182	0.23	$\frac{0.23}{18182}x2 = 0.253$
9- 11.4	2.4	10.2	18182	0.17	$\frac{0.17}{18182}x2.4 = 0.224$

$$\sum_{0}^{2B}\Delta Z = 11.4\ \text{m}$$

$$\sum_{0}^{2B}\frac{I_z}{E_S}\Delta Z = 1.977 \times 10^{-4}\ \text{m}^3/\text{kN}$$

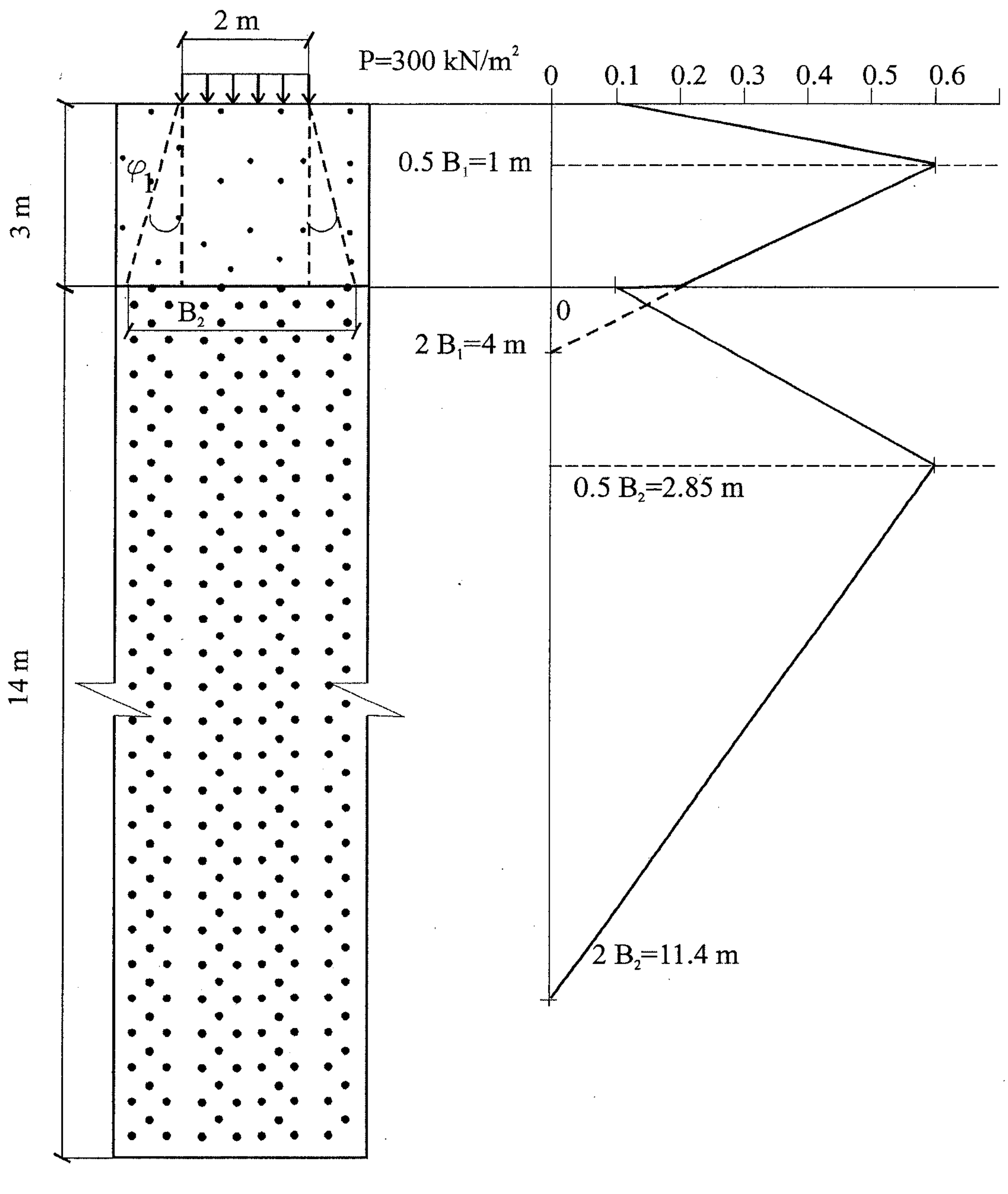

Figure 4.13 General diagram for I_z determination according to Schmertmann, for the case with h_1=3m and ϕ_1= 35^0

$$C_1 = 1\text{-}0.5\left(\frac{q_0}{q-q_0}\right) = 1\text{-}\ 0.5\ \frac{16x3}{300-16x3} = 0.90$$

C_2 = 1.54 (the same as for the upper layer)

Hence, $S_{II} = C_1 \times C_2 (q - q_0) \sum_{0}^{2B} \frac{I_z}{E_S} \Delta Z$ = 0.90x1.54x (300- 16x3)(kN/m^2) x 1.977 x 10^{-4} (m^3/kN) = 690.5 x 10^{-4} (m) = 69.1 mm

Total settlement $S_t = S_I + S_{II}$ = 39 + 69.1 = 108.1 mm.

This calculation corresponds to the Plaxis serial running # 27 from the Table 3.4, where the value of computed settlement is equal to 100 mm.

Thus, the difference is $\frac{108.1-100}{108.1}$ x 100% = 7%.

4.3.8 The case where the thickness of the upper layer h_1= 3 m and $\phi_1 = 40^0$

The load P= 300 kN/m^2
B = 2 m
h_1 = 3 m
$\phi_1 = 40^0$; $\phi_2 = 45^0$
γ_1 = 17 kN/m^3; γ_2 = 20 kN/m^3
$E_{50}{}^{ref}{}_1$ = 30000kN/m^2; $E_{50}{}^{ref}{}_2$ = 40000kN/m^2

4.3.8. 1 Settlement of the first layer

Compression modulus E_{s1} for the first layer will be of the same value as in the 4.3.3. A calculation and equal to E_{s1} = 13636 kN/m^2. Geometrical parameters for sub layers of the upper layer and correction factors C_1, C_2 are going to be the same as in the 4.3.7 calculation. Hence, the settlement of the first layer will also be the same as the settlement of the first layer in the 4.3.7 calculation.

S_I = 39 mm

4.3.8. 2 Settlement of the second layer

Effective width B_2 of the applied load in the interface was taken in consideration with the added pressure of the upper layer. Thus it was computed (figure 4.14) as:

$B_2 = B_1 + 2h_1 tg\phi_1$ = 2 + 2x 3xtg 40^0 = 6.4 m

Minimum (0.1), maximum (0.6) and zero values for the vertical strain influence factor were taken according to [23] at the depth:

$z = 0 \rightarrow I_z = 0.1$

$0.5\ B_2 = 0.5 \times 6.4 = 3.2\ m \rightarrow I_z = 0.6$

$2\ B_2 = 2 \times 6.4 = 12.8\ m \rightarrow I_z = 0$

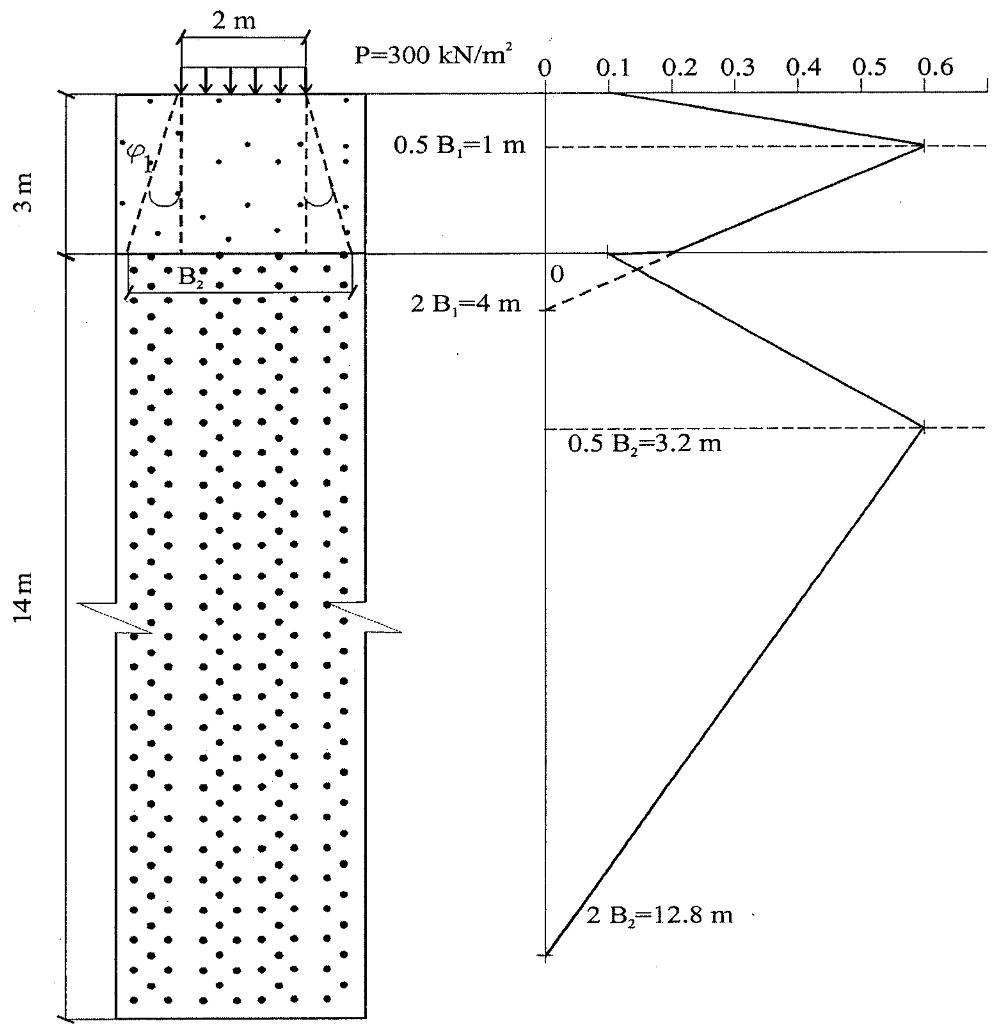

Figure 4.14 General diagram for I_z determination according to Schmertmann, for the case with h_1=3m and ϕ_1= 40^0

Table 4.8 was made for standard procedure of determining the values for vertical strain influence factor as well as the total settlement of the lower layer. I_z was determined for each sublayer according to the figure 4.14.

Table 4.8 Intermediate parameters for the lower layer settlement calculation for the input data of the upper layer: $h_1 = 3$m, $\gamma_1 = 17$ kN/m^3

Depth m	Δz m	z_i m	E_s kN/m^2	Average I_z	$\frac{I_z}{E_S}\Delta z$ x 10^{-4} m^3/kN
0-2	2	1	18182	0.24	$\frac{0.24}{18182}x2 = 0.264$
2-3.2	1.2	2.6	18182	0.48	$\frac{0.48}{18182}x1.2 = 0.317$
3.2-6	2.8	4.6	18182	0.51	$\frac{0.51}{18182}x2.8 = 0.785$
6-8	2	7	18182	0.35	$\frac{0.35}{18182}x2 = 0.385$
8-10	2	9	18182	0.22	$\frac{0.22}{18182}x2 = 0.242$
10-12.8	2.8	11.4	18182	0.08	$\frac{0.08}{18182}x2.8 = 0.123$

$\sum_{0}^{2B} \Delta Z = 12.8$ m

$\sum_{0}^{2B} \frac{I_z}{E_S} \Delta Z = 2.116 \text{ x } 10^{-4}$ m^3/kN

Correction factors:

$$C_1 = 1\text{-}0.5\left(\frac{q_0}{q - q_0}\right) = 1\text{-}\ 0.5\ \frac{17x3}{300 - 17x3} = 0.90; \quad C_2 = 1.54$$

Hence,

$$S_{II} = C_1 \text{ x } C_2 \,(q - q_0) \sum_{0}^{2B} \frac{I_z}{E_S} \Delta Z = 0.90\text{x}1.54\text{x } (300\text{- } 17\text{x}3)(\text{kN/m}^2) \text{ x } 2.116 \text{ x } 10^{-4} \,(\text{m}^3/\text{kN})$$

$= 730.3 \text{ x } 10^{-4}\text{ (m)} \approx 73\text{ mm}$

Total settlement $S_t = S_I + S_{II} = 39 + 73 = 112$ mm.

This calculation corresponds to the Plaxis serial running # 37 from the Table 3.4, where the value of computed settlement is equal to 101 mm.

Thus, the difference is $\dfrac{112-101}{112}$ x 100% = 10%.

4.3.9 The case where the thickness of the upper layer h_1= 2.5 m and $\phi_1 = 25^0$

The load P= 300 kN/m^2
$B_1 = 2$ m
$h_1 = 2.5$ m
$\phi_1 = 25^0$; $\phi_2 = 45^0$
$\gamma_1 = 12$ kN/m^3 ; $\gamma_2 = 20$ kN/m^3
$E_{50}{}^{ref}{}_1 = 20000$kN/m^2; $E_{50}{}^{ref}{}_2 = 40000$kN/m^2

4.3.9. 1 Settlement of the first layer

$$E_{s1} = \frac{20000}{2(1+0,2)} = 9091 \text{ kN/m}^2$$

Effective depth for settlement calculation was obviously taken 2.5 meters, equal to the thickness of this subgrade layer. Minimum (0.1), maximum (0.6) and zero values for the vertical strain influence factor were taken according to [23] at the same depths as for the subgrade layer for all previous calculations.

Table 4.9 was made in order to determinate the intermediate values for settlement of the upper layer calculation and vertical strain influence factor derived from the figure 4.15.

Table 4.9 Intermediate parameters for settlement of the upper layer calculation for the input data: $h_1 = 2.5$ m, $\gamma_1 = 12$ kN/m^3

Depth m	Δz m	z_i m	E_s kN/m^2	Average I_z	$\frac{I_z}{E_S}\Delta z$ x 10^{-4} m^3/kN
0-1	1	0.5	9091	0.35	$\frac{0.35}{9091} x1 = 0.385$
1-2.5	1.5	1.75	9091	0.44	$\frac{0.44}{9091} x1.5 = 0.726$

$\sum_{0}^{2B} \Delta Z = 2.5$ m

$\sum_{0}^{2B} \frac{I_z}{E_S} \Delta Z = 1.111 \text{ x } 10^{-4}$ m^3/kN

Correction factors:

$C_1 = 1$

$$C_2 = 1 + 0.2 \log\left(\frac{50}{0.1}\right) = 1.54$$

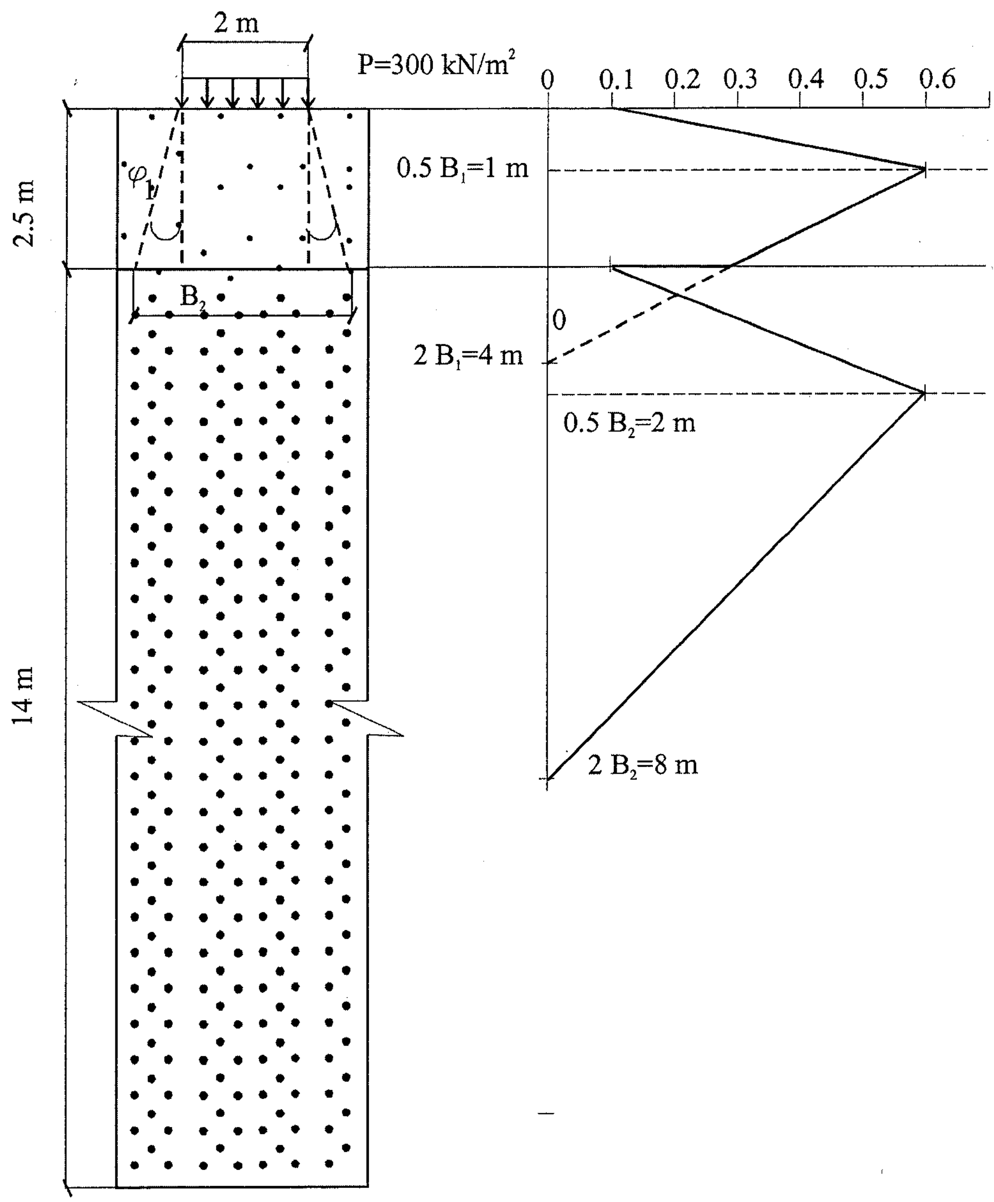

Figure 4.15 General diagram for I_z determination according to Schmertmann, for the case with h_1=2.5 m and ϕ_1= 25^0

Hence, the settlement of the first layer:

$$S_I = C_1 \times C_2 (q - q_0) \sum_{0}^{2B} \frac{I_z}{E_S} \Delta Z = 1 \text{x} 1.54 \text{x } 300 (\text{kN/m}^2) \text{x } 1.111 \text{ x } 10^{-4} (\text{m}^3/\text{kN}) =$$

$= 513.3 \text{ x } 10^{-4}$ (m) = 51.3 mm

4.3.9. 2 Settlement of the second layer

$$E_{sI1} = \frac{40000}{2(1+0,2)} = 18182 \text{ kN/m}^2$$

Effective width B_2 of the applied load in the interface was taken in consideration with the added pressure of the upper layer. Thus it was computed (figure 4.15) as:

$$B_2 = B_1 + 2h_1 tg\phi_1 = 2 + 2x\ 2.5tg\ 25^0 = 4 \text{ m}$$

Minimum (0.1), maximum (0.6) and zero values for the vertical strain influence factor were taken according to [23] at the depth:

$$z = 0 \rightarrow I_z = 0.1$$

$$0.5\ B_2 = 0.5 \text{ x } 4 = 2 \text{ m} \rightarrow I_z = 0.6$$

$$2\ B_2 = 2 \text{ x } 4 = 8 \text{ m} \rightarrow I_z = 0$$

Table 4.9.1 was made for standard procedure of determining the values for vertical strain influence factor as well as the total settlement of the lower layer I_z was determined for each sublayer according to the figure 4.15.

$$C_1 = 1\text{-}0.5\left(\frac{q_0}{q - q_0}\right) = 1\text{-}\ 0.5\ \frac{12x2.5}{300 - 12x2.5} = 0.94$$

$C_2 = 1.54$ (the same as for the upper layer)

Table 4.9.1 Intermediate parameters for the lower layer settlement calculation for the input data of the upper layer: $h_1 = 2.5$ m, $\gamma_1 = 12$ kN/m^3

Depth m	Δz m	z_i m	E_s kN/m^2	Average I_z	$\frac{I_z}{E_S}\Delta z$ x 10^{-4} m^3/kN
0-2	2	1	18182	0.34	$\frac{0.34}{18182}x2 = 0.374$
2-4	2	3	18182	0.49	$\frac{0.49}{18182}x2 = 0.539$
4-6	2	5	18182	0.29	$\frac{0.29}{18182}x2=0.319$
6-8	2	7	18182	0.09	$\frac{0.09}{18182}x2 = 0.099$

$\sum_{0}^{2B}\Delta Z = 8$ m $\qquad\qquad \sum_{0}^{2B}\frac{I_z}{E_S}\Delta Z = 1.231 \times 10^{-4}$ m^3/kN

Hence,

$S_{II} = C_1 \times C_2 (q - q_0)\sum_{0}^{2B}\frac{I_z}{E_S}\Delta Z = 0.94 \times 1.54 \times (300 - 12 \times 2.5)$(kN/m^2) x 1.231 x 10^{-4} (m^3/kN) = 481.1 x 10^{-4} (m) = 48.1 mm

Total settlement $S_t = S_I + S_{II} = 51.3 + 48.1 = 99.4$ mm.

This calculation corresponds to the Plaxis serial running # 6 from the Table 3.4, where the value of computed settlement is equal to 111 mm.

Thus, the difference is $\frac{111 - 99.4}{111}$ x 100% = 10%.

4.3.10 The case where the thickness of the upper layer h_1= 2.5 m and $\phi_1 = 30^0$

The load P= 300 kN/m^2
$B_1 = 2$ m
$h_1 = 2.5$ m
$\phi_1 = 30^0$; $\phi_2 = 45^0$
$\gamma_1 = 14$ kN/m^3 ; $\gamma_2 = 20$ kN/m^3
$E_{50}{}^{ref}{}_1 = 25000$kN/m^2; $E_{50}{}^{ref}{}_2 = 40000$kN/m^2

4.3.10. 1 Settlement of the first layer

According to equation (4.1) compression modulus for the first layer:

$$E_{s1} = \frac{25000}{2(1+0,2)} = 11364 \text{ kN/m}^2$$

Geometrical parameters for sub layers of the upper layer are going to be the same as in the 4.3.9.1 calculation.

Table 4.10 Intermediate parameters for settlement of the upper layer calculation for the input data: h_1 = 2.5 m, γ_1 = 14 kN/m^3

Depth M	Δz m	z_i m	E_s kN/m^2	Average I_z	$\frac{I_z}{E_S}\Delta z$ x 10^{-4} m^3/kN
0-1	1	0.5	11364	0.35	$\frac{0.35}{11364}x1 = 0.308$
1-2.5	1.5	1.75	11364	0.44	$\frac{0.44}{11364}x1.5 = 0.581$

$\sum_0^{2B} \Delta Z = 2.5$ m

$\sum_0^{2B} \frac{I_z}{E_S}\Delta Z = 0.889$ x 10^{-4} m^3/kN

Corrections factors will be the same:

C_1=1; C_2= 1.54

So, the settlement of the first layer will be according to the table 4.10, completed in accordance with the diagram from the picture 4.16.

$$S_I = C_1 \text{ x } C_2 (q - q_0) \sum_0^{2B} \frac{I_z}{E_S} \Delta Z = 1\text{x}1.54\text{x } 300(\text{kN/m}^2)\text{x } 0.889 \text{ x } 10^{-4} \text{ (m}^3\text{/kN)} =$$

$$= 410{,}7\text{x}10^{-4}\text{m} = 41.1\text{mm}$$

4.3.10. 2 Settlement of the second layer

Effective width B_2 of the applied load in the interface was taken in consideration with the added pressure of the upper layer. Thus it was computed (figure 4.16) as:

$$B_2 = B_1 + 2h_1 tg\phi_1 = 2 + 2\text{x } 2.5tg\ 30^0 \approx 4.5 \text{ m}$$

Minimum (0.1), maximum (0.6) and zero values for the vertical strain influence factor were taken according to [23] at the depth:

$z = 0 \rightarrow I_z = 0.1$

$0.5\ B_2 = 0.5 \text{ x } 4.5 = 2.25 \text{ m} \rightarrow I_z = 0.6$

$2\ B_2 = 2 \text{ x } 4.5 = 9 \text{ m} \rightarrow I_z = 0$

Table 4.10.1 was made for standard procedure of determining the values for vertical strain influence factor as well as the total settlement of the lower layer. I_z was determined for each sublayer according to the figure 4.16.

Table 4.10.1 Intermediate parameters for the lower layer settlement calculation for the input data of the upper layer: $h_1 = 2.5$ m, $\gamma_1 = 14$ kN/m^3

Depth m	Δz m	z_i m	E_s kN/m^2	Average I_z	$\frac{I_z}{E_S}\Delta z$ x 10^{-4} m^3/kN
0-2.25	2.25	1.125	18182	0.33	$\frac{0.33}{18182}x2.25 = 0.408$
2.25-4	1.75	3.125	18182	0.53	$\frac{0.53}{18182}x1.75 = 0.510$
4-6	2	5	18182	0.35	$\frac{0.35}{18182}x2 = 0.385$
6-8	2	7	18182	0.17	$\frac{0.17}{18182}x2 = 0.187$
8-9	1	8.5	18182	0.04	$\frac{0.04}{18182}x1 = 0.022$

$\sum_{0}^{2B} \Delta Z = 9$ m

$\sum_{0}^{2B} \frac{I_z}{E_S}\Delta Z = 1.512 \times 10^{-4}$ m^3/kN

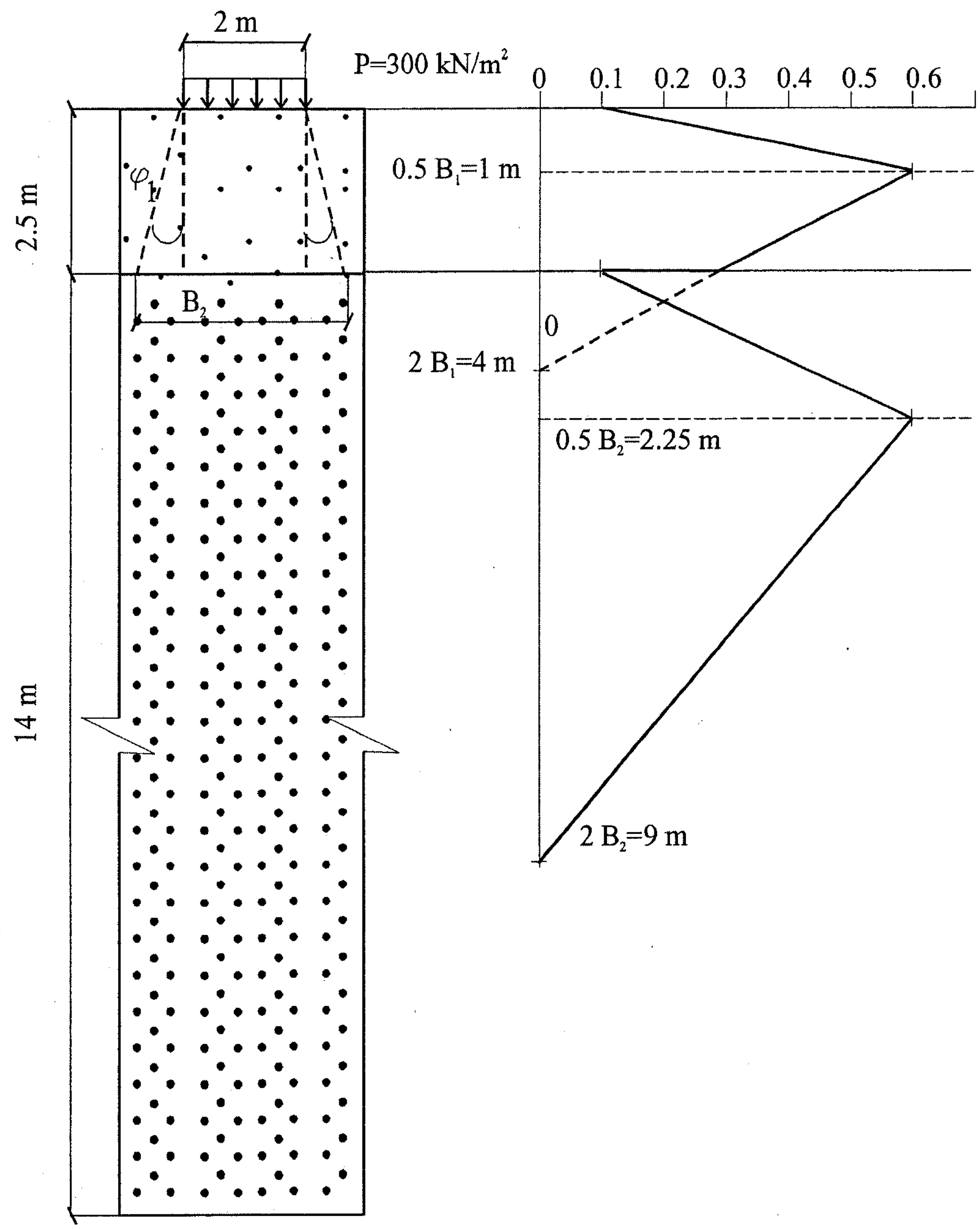

Figure 4.16 General diagram for I_z determination according to Schmertmann, for the case with h_1=2.5 m and ϕ_1= 30^0

$$C_1 = 1\text{-}0.5\left(\frac{q_{\ 0}}{q-q_0}\right) = 1\text{-}\ 0.5\ \frac{14x2.5}{300-14x2.5} = 0.93;$$

$C_2 = 1.54$

S_{II} = C_1 x C_2 (q − q_0)$\sum_0^{2B}\frac{I_z}{E_S}\Delta Z$ = 0.93x1.54x (300-14x2.5)(kN/m^2) x 1.512 x 10^{-4} (m^3/kN) = 573.8 x 10^{-4} (m) = 57.4 mm

Total settlement $S_t = S_I + S_{II} = 41.1 + 57.4 = 98.5$ mm.

This calculation corresponds to the Plaxis serial running # 16 from the Table 3.4, where the value of computed settlement is equal to 103 mm.

Thus, the difference is $\frac{103-98.5}{103}$ x 100% = 4 %.

4.3.11 The case where the thickness of the upper layer h_1= 2.5 m and $\phi_1 = 35^0$

The load P= 300 kN/m^2

$B_1 = 2$ m

$h_1 = 2.5$ m

$\phi_1 = 35^0$; $\phi_2 = 45^0$

$\gamma_1 = 16$ kN/m^3; $\gamma_2 = 20$ kN/m^3

$E_{50}{}^{ref}{}_1 = 30000$kN/m^2; $E_{50}{}^{ref}{}_2 = 40000$kN/m^2

4.3.11. 1 Settlement of the first layer:

According to equation (4.1) compression modulus for the first layer:

$$E_{s1} = \frac{30000}{2(1+0,2)} = 13636 \text{ kN/m}^2$$

Geometrical parameters for sub layers of the upper layer are going to be the same as in 4.3.9.1 and 4.3.10.1 calculations.

Corrections factors will be the same:

C_1=1;

C_2 = 1.54

The settlement of the first layer is calculated by using the table 4.11, completed in accordance with the diagram from the figure 4.17:

$$S_I = C_1 \times C_2 (q - q_0) \sum_0^{2B} \frac{I_z}{E_S} \Delta Z = 1 \text{x} 1.54 \text{x } 300 (\text{kN/m}^2) \text{x } 0.741 \text{ x } 10^{-4} (\text{m}^3/\text{kN}) =$$

$$= 342.3 \text{ x } 10^{-4} (\text{m}) = 34.2 \text{ mm}$$

Table 4.11 Intermediate parameters for settlement of the upper layer calculation for the input data: $h_1 = 2.5$ m, $\gamma_1 = 16$ kN/m^3

Depth m	Δz m	z_i m	E_s kN/m^2	Average I_z	$\frac{I_z}{E_S}\Delta z$ x 10^{-4} m^3/kN
0-1	1	0.5	13636	0.35	$\frac{0.35}{13636} x1 = 0.257$
1-2.5	1.5	1.75	13636	0.44	$\frac{0.44}{13636} x1.5 = 0.484$

$$\sum_0^{2B} \Delta Z = 2.5 \text{ m} \qquad \sum_0^{2B} \frac{I_z}{E_S} \Delta Z = 0.741 \text{ x } 10^{-4} \text{ m}^3/\text{kN}$$

4.3.11. 2 Settlement of the second layer

Effective width B_2 of the applied load in the interface was taken in consideration with the added pressure of the upper layer. Thus it was computed (figure 4.16) as:

$B_2 = B_1 + 2h_1 tg\phi_1 = 2 + 2\text{x } 2.5 tg\ 35^0 \approx 5$ m

Minimum (0.1), maximum (0.6) and zero values for the vertical strain influence factor were taken according to [23] at the depth:

$z = 0 \rightarrow I_z = 0.1$

$0.5\ B_2 = 0.5 \text{ x } 5 = 2.5 \text{ m} \rightarrow I_z = 0.6$

$2\ B_2 = 2 \text{ x } 5 = 10 \text{ m} \rightarrow I_z = 0$

Table 4.11.1 was made for standard procedure of determining the values for vertical strain influence factor as well as the total settlement of the lower layer. I_z was determined for each sublayer according to the figure 4.17.

Table 4.11.1 Intermediate parameters for the lower layer settlement calculation for the input data of the upper layer: $h_1 = 2.5$ m, $\gamma_1 = 16$ kN/m^3

Depth m	Δz m	z_i m	E_s kN/m^2	Average I_z	$\frac{I_z}{E_S}\Delta z$ x 10^{-4} m^3/kN
0-2.5	2.5	1.25	18182	0.34	$\frac{0.34}{18182}x2.5 = 0.467$
2.5-5	2.5	3.75	18182	0.49	$\frac{0.49}{18182}x2.5 = 0.674$
5-7	2	6	18182	0.33	$\frac{0.33}{18182}x2 = 0.363$
7-10	3	8.5	18182	0.13	$\frac{0.13}{18182}x3 = 0.214$

$\sum_{0}^{2B} \Delta Z = 10$ m $\qquad$ $\sum_{0}^{2B} \frac{I_z}{E_S}\Delta Z = 1.718 \text{ x } 10^{-4}$ m^3/kN

$$C_1 = 1\text{-}0.5\left(\frac{q_0}{q - q_0}\right) = 1\text{-}\ 0.5\ \frac{16x2.5}{300 - 16x2.5} = 0.92$$

$C_2 = 1.54$ (the same as for the upper layer)

Hence,

$S_{II} = C_1 \text{ x } C_2 \,(q - q_0)\sum_{0}^{2B}\frac{I_z}{E_S}\Delta Z$ = 0.92x1.54x (300- 16x2.5) (kN/m^2) x 1.718 x 10^{-4}

(m^3/kN) = 632.9 x 10^{-4} (m) = 63.3 mm

Total settlement $S_t = S_I + S_{II}$ = 34.2 + 63.3 = 97.5 mm.

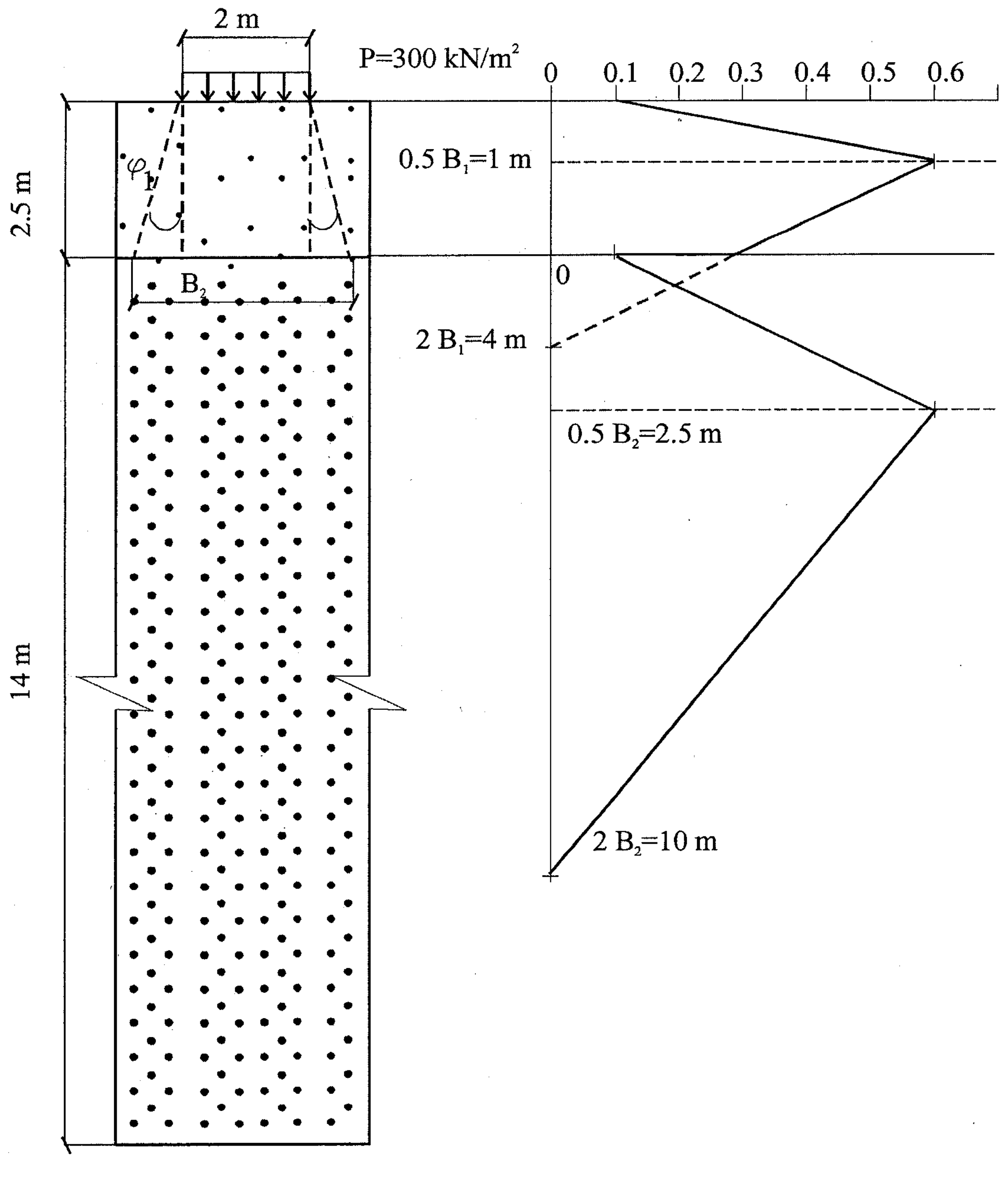

Figure 4.17 General diagram for I_z determination according to Schmertmann, for the case with h_1=2.5 m and ϕ_1= 35^0

This calculation corresponds to the Plaxis serial running # 26 from the Table 3.4, where the value of computed settlement is equal to 97 mm.

Thus, the difference is $\frac{97.5-97}{97.5}$ x 100% ≈ 0.5%.

4.3.12 The case where the thickness of the upper layer h_1= 2.5 m and $\phi_1 = 40^0$

The load P= 300 kN/m^2
$B_1 = 2$ m
$h_1 = 2.5$ m
$\phi_1 = 40^0$; $\phi_2 = 45^0$
$\gamma_1 = 17$ kN/m^3; $\gamma_2 = 20$ kN/m^3
$E_{50}{}^{ref}{}_1 = 30000$kN/m^2; $E_{50}{}^{ref}{}_2 = 40000$kN/m^2

4.3.12. 1 Settlement of the first layer

Compression modulus E_{s1} for the first layer will be of the same value as in the case 4.3.11.1 and equal to E_{s1} = 13636 kN/m^2. Geometrical parameters for sub layers of the upper layer and correction factors C_1, C_2 are also going to be the same as in the previous calculation. Consequently, the settlement of the first layer will also be the same as the settlement of the first layer from the above mentioned calculation.

$S_I = 34.2$ mm

4.3.12. 2 Settlement of the second layer

Effective width B_2 of the applied load in the interface was taken in consideration with the added pressure of the upper layer. Thus it was computed (figure 4.18) as:

$B_2 = B_1 + 2h_1 tg\phi_1 = 2 + 2x\ 2.5xtg\ 40^0 = 5.6$ m

Minimum (0.1), maximum (0.6) and zero values for the vertical strain influence factor were taken according to [23] at the depth:

$z = 0 \rightarrow I_z = 0.1$

$0.5\ B_2 = 0.5 \times 5.6 = 2.8$ m $\rightarrow I_z = 0.6$

$2\ B_2 = 2 \times 5.6 = 11.2$ m $\rightarrow I_z = 0$

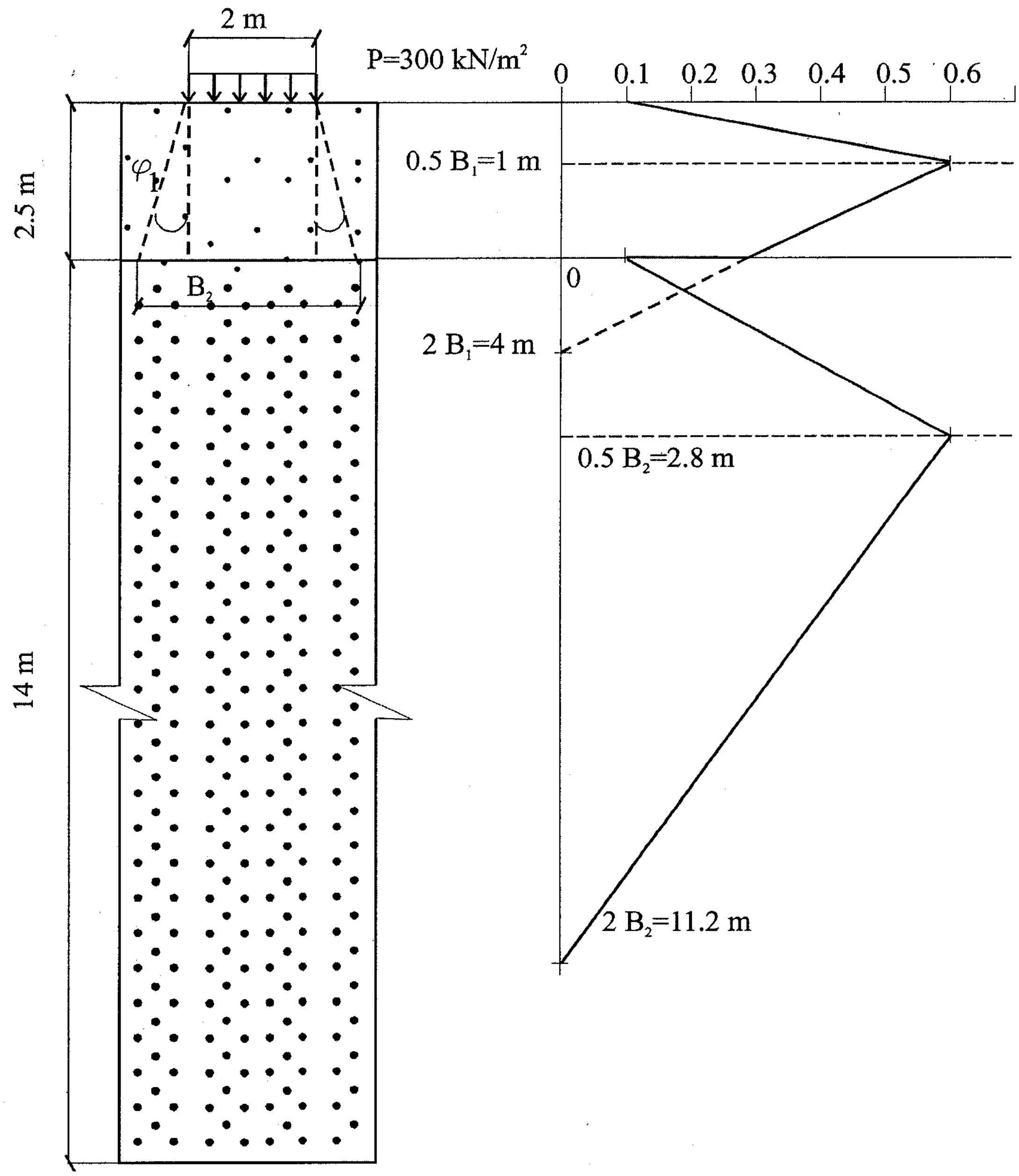

Figure 4.18 General diagram for I_z determination according to Schmertmann, for the case with h_1=2.5 m and ϕ_1= 40^0

Table 4.12 was made for standard procedure of determining the values for vertical strain influence factor as well as the total settlement of the lower layer. I_z was determined for each sublayer according to the figure 4.18.

Table 4.12 Intermediate parameters for the lower layer settlement calculation for the input data of the upper layer: $h_1 = 2.5$ m, $\gamma_1 = 17$ kN/m^3

Depth m	Δz m	z_i m	E_s kN/m^2	Average I_z	$\frac{I_z}{E_S}\Delta z$ x 10^{-4} m^3/kN
0-1	1	0.5	18182	0.16	$\frac{0.16}{18182}x1 = 0.088$
1-2.8	1.8	1.9	18182	0.46	$\frac{0.46}{18182}x1.8 = 0.455$
2.8-5	2.2	3.9	18182	0.53	$\frac{0.53}{18182}x2.2 = 0.641$
5-7	2	6	18182	0.41	$\frac{0.41}{18182}x2 = 0.451$
7-9	2	8	18182	0.18	$\frac{0.18}{18182}x2 = 0.198$
9-11.2	2.2	10.1	18182	0.07	$\frac{0.07}{18182}x2.2 = 0.085$

$\sum_{0}^{2B}\Delta Z = 11.2$ m $\qquad\qquad \sum_{0}^{2B}\frac{I_z}{E_S}\Delta Z = 1.918 \times 10^{-4}$ m^3/kN

Correction factors:

$$C_1 = 1\text{-}0.5\left(\frac{q_0}{q - q_0}\right) = 1\text{-}\ 0.5\ \frac{17x2.5}{300 - 17x2.5} = 0.92; \quad C_2 = 1.54$$

Hence, $S_{II} = C_1 \times C_2 (q - q_0)\sum_{0}^{2B}\frac{I_z}{E_S}\Delta Z = 0.92x1.54x\ (300\text{-}\ 17x2.5)(\text{kN/m}^2) \times 1.918 \times 10^{-4}$

(m^3/kN) = 699.7 x 10^{-4} (m) ≈ 70 mm

Total settlement $S_t = S_I + S_{II} = 34.2 + 70 = 104.2$ mm.

This calculation corresponds to the Plaxis serial running # 36 from the Table 3.4, where the value of computed settlement is equal to 97 mm.

Thus, the difference is $\frac{104.2 - 97}{104.2}$ x 100% = 7%.

Therefore, comparing the settlement values derived from traditional Schmertmann's method and corresponding values computed using Plaxis code, it is possible to conclude that under the great loads these values of settlement are very close. The fact that it is possible to implement the method of level-to-level summering of settlements of different cohesionless soil layers (with different properties) as applied to Schmertmann's method is also of very importance. Table 4.13 reflects the difference between the settlement values computed by Plaxis code and those, computed by Schmertmann's method.

Table 4.13 Difference between the settlement values calculated by PLAXIS geotechnical software and by Schmertmann's method

No	Plaxis software		Corresponding result calculated by Schmertmann's method mm	Difference %
	#	Result Mm		
1	5	105	106.4	1.3
2	15	99	89.3	9
3	25	94	86.3	8
4	35	94	92.3	1.8
5	7	117	116.1	0.8
6	17	107	113.6	6
7	27	100	108.1	7
8	37	101	112	10
9	6	111	99.4	10
10	16	103	98.5	4
11	26	97	97.5	0.5
12	36	97	104.2	7

Average difference according the Table 4.13 is:

$$\Delta = \frac{1}{12}\sum_{1}^{12}\Delta_i = 5.4\ \%$$

4.4 The development of the empirical formula

A snap formula to show the dependence between the compression C_S, applied load **P**, thickness of the upper layer **H** and internal friction angle ϕ, reflecting the results in Table 3.4, has been derived according to least-squares method.

Taking into account the approximately linear dependence of C_S on **H** and making an assumption that there is also direct relation between **P** and C_S but inverse negative relationship between C_S and ϕ, the empirical equation can be written as:

$$C_S = y_0 + y_1 H\phi^{-1} + y_2 PH\,\phi^{-1} \tag{4.1}$$

The coefficients have been defined by the system of equations:

$$\begin{aligned} & y_0 + m\,(H\phi^{-1})\,y_1 + m(PH\,\phi^{-1})\,y_2 = m\,(c_s) \\ & m\,(H\phi^{-1})\,y_0 + m\,(H^2\phi^{-2})\,y_1 + m(PH^2\phi^{-2})\,y_2 = m\,(c_s\,H\phi^{-1}) \\ & m\,(PH\phi^{-1})\,y_0 + m\,(PH^2\phi^{-2})\,y_1 + m(P^2H^2\phi^{-2})\,y_2 = m\,(c_sPH_\phi{}^{-1}) \end{aligned} \tag{4.2}$$

Where simple average coefficients m(x) have been calculated according to least-squares method procedure using the results of PLAXIS calculations written in Table 3.4, by generalized formula:

$$m(x) = \frac{1}{160}\sum_c x \tag{4.3}$$

for example:

$$m\,(H\phi^{-1}) = m\,(\frac{1}{\varphi})m\,(H) = \frac{1}{4}\sum_\phi \frac{1}{\varphi}\frac{1}{10}\sum_H H$$

$$m\,(PH\phi^{-1}) = \frac{1}{4}\sum_P P\frac{1}{4}\sum_\varphi \frac{1}{\varphi}\;\frac{1}{10}\sum_H H$$

$$m\,(H^2\phi^{-2}) = \frac{1}{4}\sum_\varphi \frac{1}{\varphi^2}\;\frac{1}{10}\sum_H H^2$$

$$\mathrm{m}\,(\mathrm{PH}^2\phi^{-2}) = \frac{1}{4}\sum_P P \frac{1}{4}\sum_\varphi \frac{1}{\varphi^2}\ \frac{1}{10}\sum_H H^2$$

$$\mathrm{m}\,(\mathrm{P}^2\mathrm{H}^2\phi^{-2}) = \frac{1}{4}\sum_P P^2 \frac{1}{4}\sum_\varphi \frac{1}{\varphi^2}\ \frac{1}{10}\sum_H H^2 \qquad (4.4)$$

$$m(c) = \frac{1}{160}\sum_c c$$

$$\mathrm{m}(\mathrm{cH}\phi^{-1}) = \frac{1}{160}\sum_c cH\varphi^{-1}$$

$$\mathrm{m}(\mathrm{cPH}\phi^{-1}) = \frac{1}{160}\sum_c cPH\varphi^{-1}$$

The mean square deviation of (4.1) is:

$$\Delta = \sum(y_0 + y_1 H\phi^{-1} + y_2 PH\phi^{-1} - c^2) = \Delta(y_0, y_1, y_2) \qquad (4.5)$$

Differentiating equation (4.5) by required variables the following system of equations has been derived:

$$\frac{\partial\Delta}{\partial y_0} = 2\sum_c \ (y_0 + y_1\,H\,\phi^{-1} + y_2 PH\,\phi^{-1} - c_S) = 0$$

$$\frac{\partial\Delta}{\partial y1} = 2\sum_c \ (y_0 + y_1 H\phi^{-1} + y_2 PH\phi^{-1} - c_S)\,H\,\phi^{-1} = 0 \qquad (4.6)$$

$$\frac{\partial\Delta}{\partial y2} = 2\sum_c \ (y_0 + y_1\,H\,\phi^{-1} + y_2 PH\,\phi^{-1} - c_S)\,PH\,\phi^{-1} = 0$$

Coefficients (4.4) have been calculated by using corresponding data from the Table 3.4, so the systems of equations (4.2) with the aid of the system (4.6) were transformed into the below final system of equations:

$$\begin{cases} y_0 + 0{,}117y_1 + 13{,}01y_2 = 16{,}9 \\ 0{,}11y_0 + 0{,}o2y_1 + 2{,}41y_2 = 3{,}1 \\ 13{,}01y_0 + 2{,}41y_1 + 512{,}7y_2 = 594{,}9 \end{cases} \qquad (4.7)$$

It has been calculated using Gaussian transformation matrix method:

$$M = \begin{pmatrix} 0.........0{,}11....13{,}01....16{,}9 \\ 0{,}11....0{,}02.....2{,}41.....1{,}25 \\ 13{,}01...2{,}41...512{,}7...594{,}9 \end{pmatrix} \rightarrow \begin{pmatrix} 1....0{,}11.....13{,}01......16{,}9 \\ 0....0{,}008...0{,}98.........1{,}25 \\ 0....0{,}98.....343{,}44.....375{,}03 \end{pmatrix} \rightarrow$$

$$\rightarrow \begin{pmatrix} 0.....0{,}11....13{,}01....16{,}9 \\ 0.......1.......122{,}5.....156{,}25 \\ 0........0......223{,}4.....221{,}9 \end{pmatrix} \rightarrow \begin{pmatrix} 1....0{,}11.....13{,}01......16{,}9 \\ 0.......1........122{,}5....156{,}25 \\ 0.......0...........1..........0{,}99 \end{pmatrix} \rightarrow$$

$$\rightarrow \begin{pmatrix} 0.....0{,}11....0.....4{,}02 \\ 0........1......0.....35{,}0 \\ 0........0......1.....0{,}99 \end{pmatrix} \rightarrow \begin{pmatrix} 1.....0.....0.....0{,}17 \\ 0....1......0.....35{,}0 \\ 0.....0.....1......0{,}99 \end{pmatrix}$$

Thus, the only solutions of equation (4.7) are the following coefficients:
$y_0 = 0.17$; $y_1 = 35$; $y_2 = 0.99 \approx 1$. The final empirical formula connecting relationship between the Table 3.4 results is:

$$\mathbf{C_s \approx 0.17 + 35\, H\, \phi^{-1} + P\, H\, \phi^{-1}} \qquad (4.8)$$

The mean square error of this final empirical equation will be:

$$\delta = \sqrt{\frac{1}{160}\sum_{c}(0{,}17 + 35H\varphi + 0{,}99PH\varphi. - c)^2} \approx 3.5 \qquad (4.9)$$

All compression values calculated by derived empirical formula (4.8) are listed in the Table 4.15 in the 9th column.

Table 4.14 Compression of the subgrade layer resulting from PLAXIS calculation program and calculated by empirical formula (4.8)

Load, kN/m^2	Serial number	γ_1 kN/m^3	ϕ_1 ^{0}	H m	S $\times 10^{-3}$ m	S_i $\times 10^{-3}$ m	Compression of the upper layer Δh $\times 10^{-3}$ m	Compression of upper layer, calculated by empirical formula $C_S \times 10^{-3}$ m
1	2	3	4	5	6	7	8	9
300	1	12	25	0,5	89	80	9	7
	2			0,7	91	79	12	10
	3			1,0	94	76	18	14
	4			1,5	99	75	24	21
	5			2.0	105	73	32	27
	6			2,5	111	72	39	34
	7			3,0	117	71	46	41
	8			5,0	140	67	73	67
	9			7,0	160	64	96	94
	10			10,0	188	60	128	134
	11	14	30	0,5	82	75	7	6
	12			0,7	88	79	9	8
	13			1,0	91	78	13	12
	14			1,5	95	76	19	17
	15			2.0	99	74	25	23
	16			2,5	103	73	30	28
	17			3,0	107	71	36	34
	18			5,0	122	66	56	56
	19			7,0	137	63	74	78
	20			10,0	159	59	100	112
	21	16	35	0,5	80	75	5	5
	22			0,7	82	74	8	7
	23			1,0	84	73	11	10
	24			1,5	91	75	16	15
	25			2.0	94	74	20	19
	26			2,5	97	72	25	24
	27			3,0	100	71	29	29
	28			5,0	110	65	45	48
	29			7,0	122	62	60	67
	30			10,0	139	59	70	96
	31	17	40	0,5	81	75	6	4
	32			0,7	82	74	8	6
	33			1,0	84	73	11	9
	34			1,5	87	72	15	13
	35			2.0	94	73	21	17
	36			2,5	97	72	25	21
	37			3,0	101	71	30	26
	38			5,0	112	66	46	42
	39			7,0	122	62	60	59
	40			10,0	137	57	70	84

1	2	3	4	5	6	7	8	9
100	41	12	25	0,5	35	31	**4**	**3**
	42			0,7	37	31	**6**	**4**
	43			1,0	38	30	**8**	**6**
	44			1,5	41	30	**11**	**8**
	45			2.0	44	29	**15**	**11**
	46			2,5	47	29	**18**	**14**
	47			3,0	49	28	**21**	**16**
	48			5,0	59	26	**33**	**27**
	49			7,0	67	25	**42**	**38**
	50			10,0	78	23	**55**	**54**
	51	14	30	0,5	34	31	**3**	**2,5**
	52			0,7	35	31	**4**	**3**
	53			1,0	36	30	**6**	**5**
	54			1,5	38	30	**8**	**7**
	55			2.0	40	29	**11**	**9**
	56			2,5	41	28	**13**	**11**
	57			3,0	43	27	**16**	**14**
	58			5,0	49	25	**24**	**23**
	59			7,0	55	23	**32**	**32**
	60			10,0	63	22	**41**	**45**
	61	16	35	0,5	34	31	**3**	**2**
	62			0,7	34	31	**3**	**3**
	63			1,0	35	30	**5**	**4**
	64			1,5	36	29	**7**	**6**
	65			2.0	38	29	**9**	**8**
	66			2,5	39	28	**11**	**10**
	67			3,0	40	27	**13**	**12**
	68			5,0	44	25	**19**	**20**
	69			7,0	48	23	**25**	**27**
	70			10,0	54	21	**33**	**39**
	71	17	40	0,5	34	31	**3**	**2**
	72			0,7	34	30	**1**	**3**
	73			1,0	35	30	**5**	**4**
	74			1,5	37	29	**8**	**5**
	75			2.0	38	29	**9**	**7**
	76			2,5	39	28	**11**	**9**
	77			3,0	41	27	**14**	**10**
	78			5,0	44	25	**19**	**17**
	79			7,0	48	23	**25**	**24**
	80			10,0	54	21	**33**	**34**

1	2	3	4	5	6	7	8	9
50	81	12	25	0,5	20	17	**3**	**2**
	82			0,7	20	17	**3**	**3**
	83			1,0	21	17	**4**	**4**
	84			1,5	23	16	**7**	**5**
	85			2.0	25	16	**9**	**7**
	86			2,5	26	15	**11**	**9**
	87			3,0	28	15	**13**	**11**
	88			5,0	33	14	**19**	**17**
	89			7,0	37	13	**24**	**24**
	90			10,0	42	12	**30**	**34**
	91	14	30	0,5	19	17	**2**	**1,5**
	92			0,7	19	16	**3**	**2**
	93			1,0	20	16	**4**	**3**
	94			1,5	21	16	**5**	**4**
	95			2.0	22	16	**6**	**6**
	96			2,5	22	14	**8**	**7**
	97			3,0	23	14	**9**	**9**
	98			5,0	26	13	**13**	**14**
	99			7,0	30	12	**18**	**20**
	100			10,0	34	11	**23**	**28**
	101	16	35	0,5	18	17	**1**	**1**
	102			0,7	18	16	**2**	**2**
	103			1,0	19	16	**3**	**3**
	104			1,5	19	15	**4**	**4**
	105			2.0	20	15	**5**	**5**
	106			2,5	21	14	**7**	**6**
	107			3,0	21	14	**7**	**7**
	108			5,0	24	13	**11**	**12**
	109			7,0	26	12	**14**	**17**
	110			10,0	30	11	**19**	**24**
	111	17	40	0,5	18	17	**1**	**1**
	112			0,7	18	16	**2**	**2**
	113			1,0	19	16	**3**	**2**
	114			1,5	20	15	**5**	**3**
	115			2.0	20	15	**5**	**4**
	116			2,5	21	14	**7**	**5,5**
	117			3,0	21	14	**7**	**6,5**
	118			5,0	24	13	**11**	**11**
	119			7,0	26	12	**14**	**15**
	120			10,0	29	11	**18**	**21**

1	2	3	4	5	6	7	8	9
40	121	12	25	0,5	16	14	**2**	**2**
	122			0,7	17	14	**3**	**2**
	123			1,0	17	13	**4**	**3**
	124			1,5	19	13	**6**	**5**
	125			2.0	20	12	**8**	**6**
	126			2,5	21	12	**9**	**8**
	127			3,0	22	12	**10**	**9**
	128			5,0	26	11	**15**	**15**
	129			7,0	30	10	**20**	**21**
	130			10,0	34	9	**25**	**30**
	131	14	30	0,5	15	14	**1**	**1**
	132			0,7	16	13	**3**	**2**
	133			1,0	16	13	**3**	**3**
	134			1,5	17	13	**4**	**4**
	135			2.0	18	13	**5**	**5**
	136			2,5	18	11	**7**	**6,5**
	137			3,0	19	12	**7**	**8**
	138			5,0	22	11	**11**	**13**
	139			7,0	24	10	**14**	**18**
	140			10,0	28	9	**19**	**25**
	141	16	35	0,5	15	14	**1**	**1**
	142			0,7	15	14	**1**	**1,5**
	143			1,0	16	13	**3**	**2**
	144			1,5	16	13	**3**	**3**
	145			2.0	17	13	**4**	**4**
	146			2,5	17	12	**5**	**5,5**
	147			3,0	18	12	**6**	**6**
	148			5,0	19	10	**9**	**11**
	149			7,0	21	10	**11**	**15**
	150			10,0	23	9	**14**	**21**
	151	17	40	0,5	15	14	**1**	**1**
	152			0,7	15	14	**1**	**1**
	153			1,0	16	13	**3**	**2**
	154			1,5	16	13	**3**	**3**
	155			2.0	17	13	**4**	**4**
	156			2,5	17	12	**5**	**5**
	157			3,0	18	12	**6**	**6**
	158			5,0	19	10	**9**	**10**
	159			7,0	21	9	**12**	**13**
	160			10,0	23	9	**14**	**19**

CHAPTER 5

CONCLUSIONS

Numerical model was developed to simulate the case of a thin layer overlying a deep deposit. The objective of the study is to determine the compression of the upper thin layer and accordingly its contribution to the total settlement of the layered system. The following represents the conclusion:

1. The proposed numerical model is capable of providing accurate predictions of the compression of the upper thin layer. PLAXES code appears to be very useful tool to predict these values, rapidly.
2. The proposed empirical formula (4.8) may be used in practice for rapid evaluation of the desirable values of compression as well as of the settlement of the upper thin layer. It may also used in ground improvement projects, especially in surface compaction projects to predict the level of compaction that can be achieved in the subgrade thin layer, depending on its thickness, the mechanical properties of the soils and the applied load.
3. The compressibility of the upper thin layer depends on the stiffness of the lower natural deposit and the load applied. In addition to that, the correlation between the mechanical properties of the layers is an important issue that must be taken into account. Indeed, the values of compression and the settlement of the upper layer reduce as its angle of shearing resistance becomes contiguous to those of the lower stronger layer.

4. Schmertmann's method of settlement calculation for homogeneous cohesionless soils was modified for the case of settlement of a thin layer overlying a deep deposit.
5. Future research in this domain should be conducted to combine to include field or laboratory series of experiments in order to elaborate a precision procedure of evaluation of ground improvement projects.

REFERENCES

1. Alpan, I. Estimating settlement of foundation on sand. Civil Engineering and Public works Review, Vol. 5 No 700, 1964

2. Biot, M. A. 1941. General theory of three-dimensional consolidation. J. Appl. Phys. 12, 155–164.

3. Biot, M. A. 1955. Theory of elasticity and consolidation for a porous anisotropic solid. J. Applied Phys. 26, 182–185.

4. Biot, M. A. 1956a. Theory of propagation of elastic waves in a fluid-saturated porous solid. Part I: low frequency range. J. Acoust. Soc. Am. 28, 168–178.

5. Buisman, A. S. K. 1936. Results of Long Duration Settlement Tests. Proceedings 1st International Conference on Soil Mechanics and Foundation engineering, 1, pp. 103-106.

6. Canadian Foundation Engineering Manual, CFEM, 1992. Third Edition. Canadian Geotechnical Society.

7. Chahbandar R.. 1993. Settlement of strip footings on a strong cohesionless layer overlaying a weak deposit. A thesis in the Department of Civil Engineering, Concordia University, Montreal.

8. D'Appolonia, D.J., D'Appolonia, E. D. and Brissette, R.F. 1970. Settlement of Spread Footing on Sand. Journal of Soil Mechanics and Foundation Division. ASCE, March 1970, pp. 754-761.

9. De Beer, E. 1965. "Bearing Capacity and Settlement of shallow foundations on sand". Bearing Capacity and Settlement of Foundation, Duke University, pp. 15-33.

10. Fadeev A. B. 1987 Finite-element method application in geomechanics, Moscow, Nedra. 224.

11. Florin V. A. 1951 Theory of soil consolidation, Moscow, Stroiizdat.

12. Florin V. A. 1953 Soil medium consolidation and filtration at the variable densification with taking into account the adhesive water influence, Moscow, Academy of science news No. 11.

13. Hanna. A. M. 1982. Bearing Capacity of Foundations on a week sand layer overlaying a strong deposit. Canadian Geotechnical Journal, vol. 19, pp. 392-396.

14. Hanna, A. M., Abd. El-Rahman, M. and Chahbandar, R. 1993. Settlement of Strip Foundation on Homogeneous Sand. Proceedings of AL-AZHAR Engineering Third Conference, Dec. 1993.

15. Hanna A. M. 2003 Laboratory compaction of a subgrade layer overlaying a deep soil deposit, Ground Improvement 7, No.1, 1-8.

16. Jorden, E. 1977. Settlement in Sand. Methods of calculating and Factors Affecting. Ground Engineering, vol. 10, No 1, pp.30-37.

17. Kolymbas D. and Fellin W. 2000 Compaction of soils, granulates and Powders, A. A. Balkema/Rotterdam/Brookfield. 3 , IX.

18. Meyerhof, G.G. 1965. Shallow Foundation. Journal of the Soil Mechanics. Foundation Division, ASCE, vol. 91, No 5, p. 2.

19. Peck, R. B., Hanson, W. E. and Thornburn, T. H. 1974. Foundation Engineering. John Wiley and Sons, 312.

20. Sandhu R. S. and Wilson E. L. 1968 Finite-Element Analyses of Seepage in Elastic Media. J. of Soil Mech. and Found. Div. ASCE, 95, 641-651.

21. Schiffman R. L. and Chean A. T. F. 1969 An Analysis of Consolidation Theories. J. Of Soil Mech. and Found. Div. ASCE, 95, 285-312.

22. Schmertmann, J.H. 1970. Static Cone to Compute Static Settlement over Sand. Journal of the Soil Mechanics. Foundation Division, ASCE, vol. 96 No SM3, May, 1970.

23. Schmertmann, J.H. 1985. Measure and use of the in-situ lateral stress. In the Practice of Foundation Engineering, Edited by R.J. Krizek, C.H. Dowding, and F. Somogyi. Department of Civil Engineering, Technological Institute, Northwestern University, Evanston, 189 - 213.

24. Terzaghi K. 1943. Theoretical soil mechanics, New-York (Wiley).

25. Tsitovich N.A. 1979. Soil mechanics, Moscow, Higher school, 26-37

26. Zaretsky Yu. K.1972. Theory of soil consolidation, edited by N.A. Tsytovich, Moscow, Nauka, vii, 5-37.

27. Probability theory and mathematical statistics hand-book, 1985, Moscow, Nauka, edited under the general editorship of physics and mathematics literature.

28. Russian Foundation Design Guide, edited by Dolmatov. 1985, Moscow, Stroiizdat, 222-226.

29. PLAXIS Version 8, Material Model Manual, The Hardening Soil Model, 5-1 - 5-5. www. PLAXIS.com

30. PLAXIS Version 8, Material Model Manual, Applications of advanced soil models, 8-1 - 8-7. www. PLAXIS.com

Appendix A
Charts plotted in accordance with the Table 3.4

Chart No 1

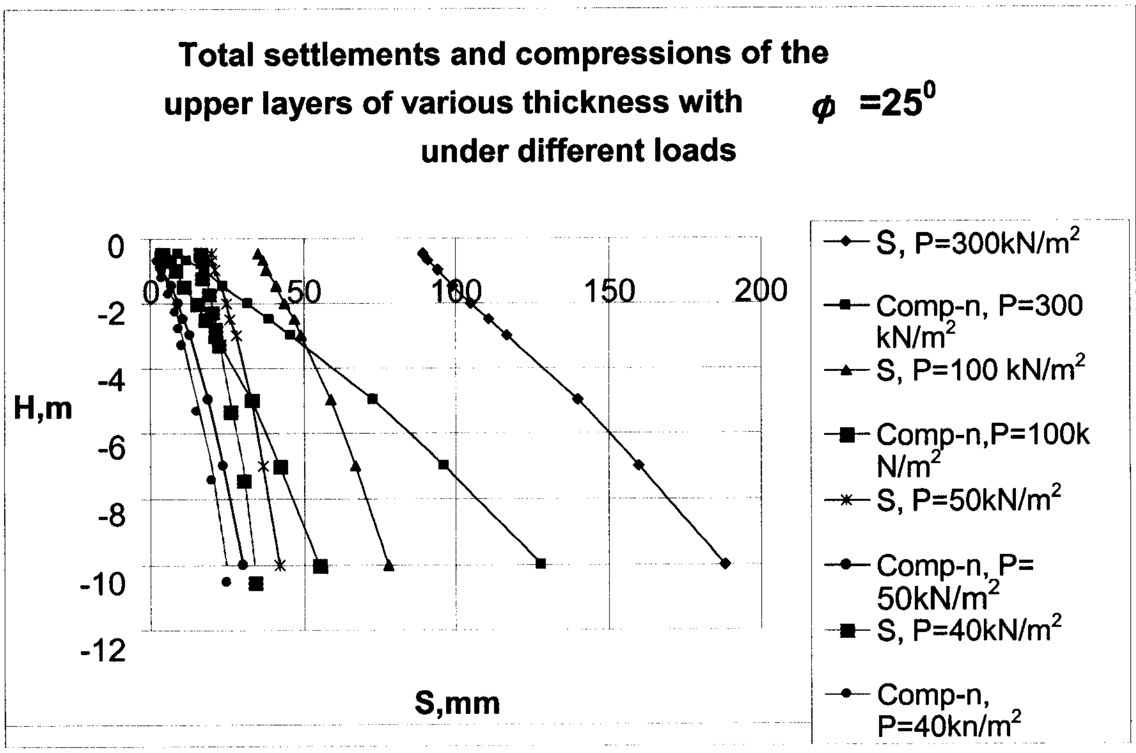

Chart No 2

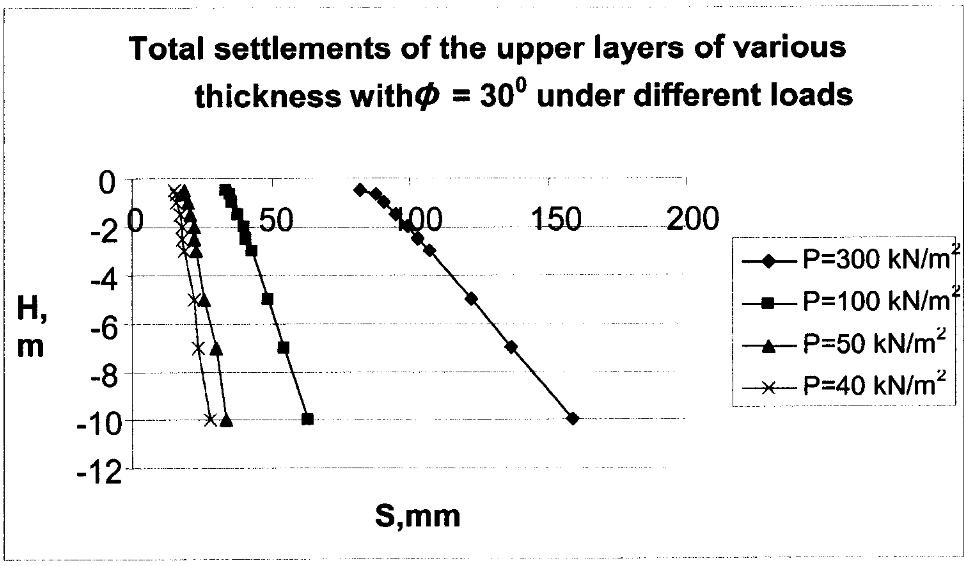

Chart No 3

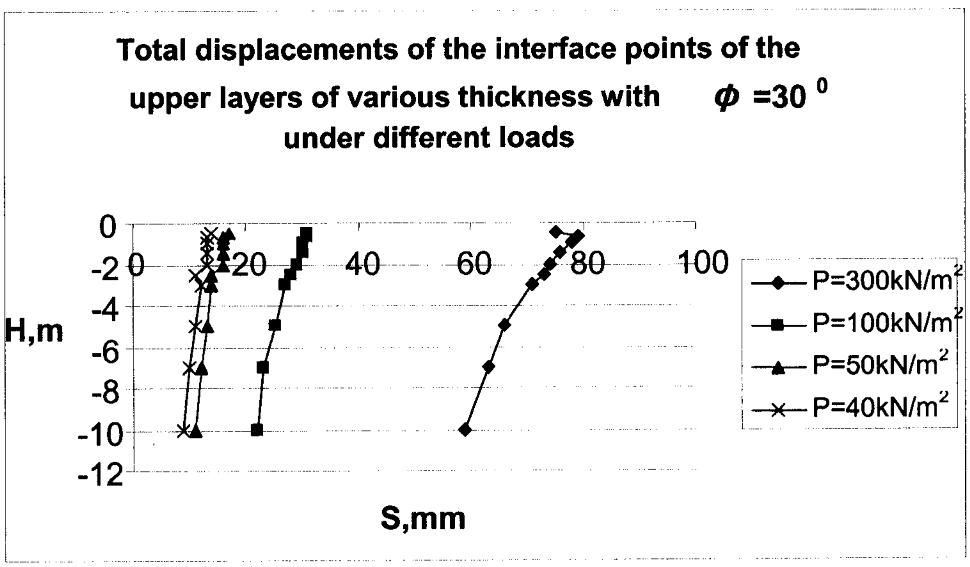

Chart No 4

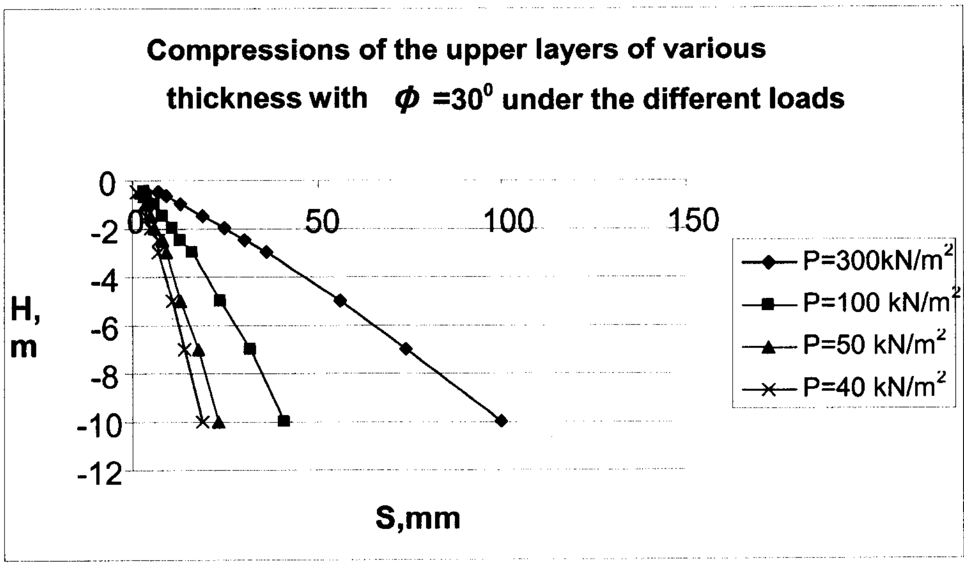

Chart No 5

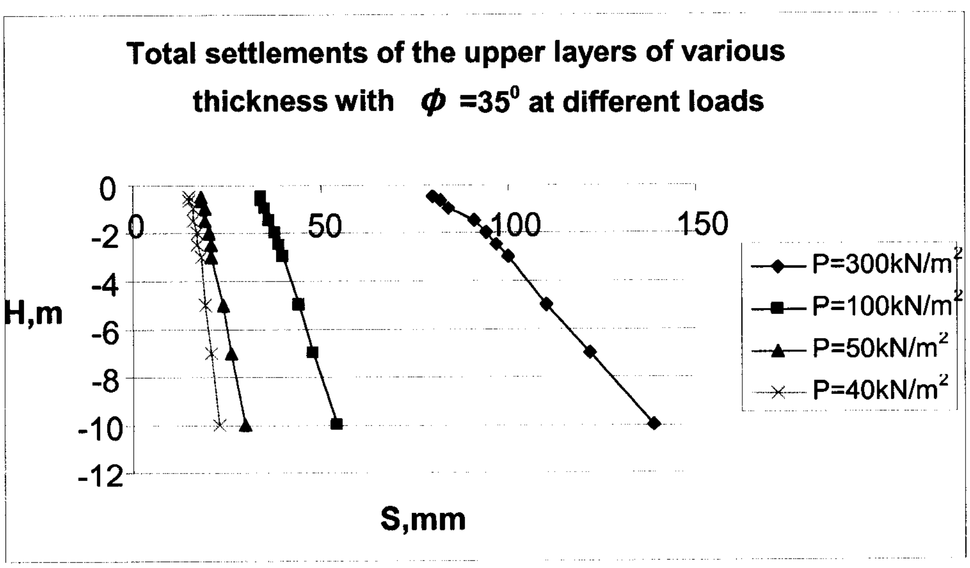

Chart No 6

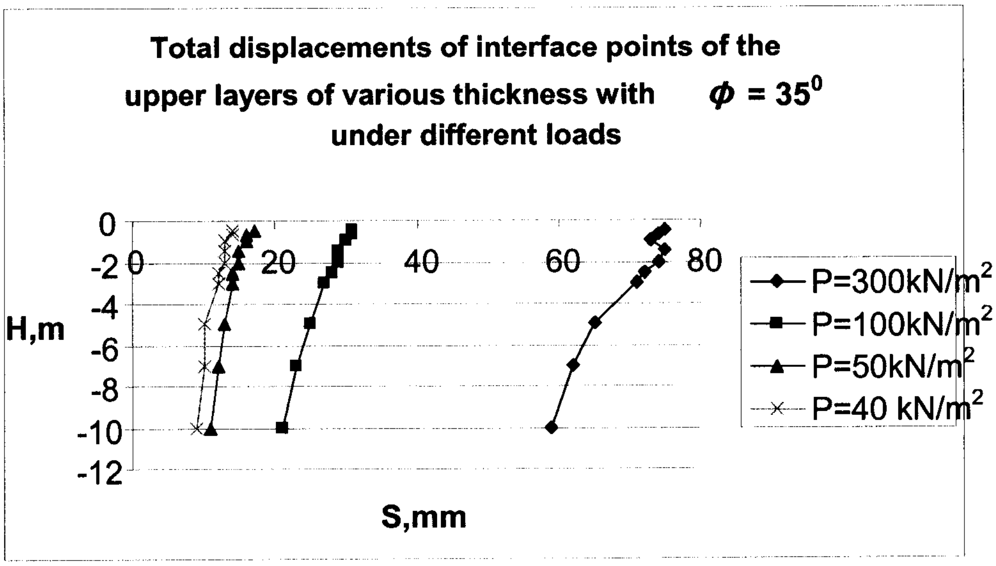
Total displacements of interface points of the upper layers of various thickness with ϕ = 35^0 under different loads
0
-2
-4
-6
-8
-10
-12
0
20
40
60
80
H,m
S,mm
P=300kN/m^2
P=100kN/m^2
P=50kN/m^2
P=40 kN/m^2

Chart No 7

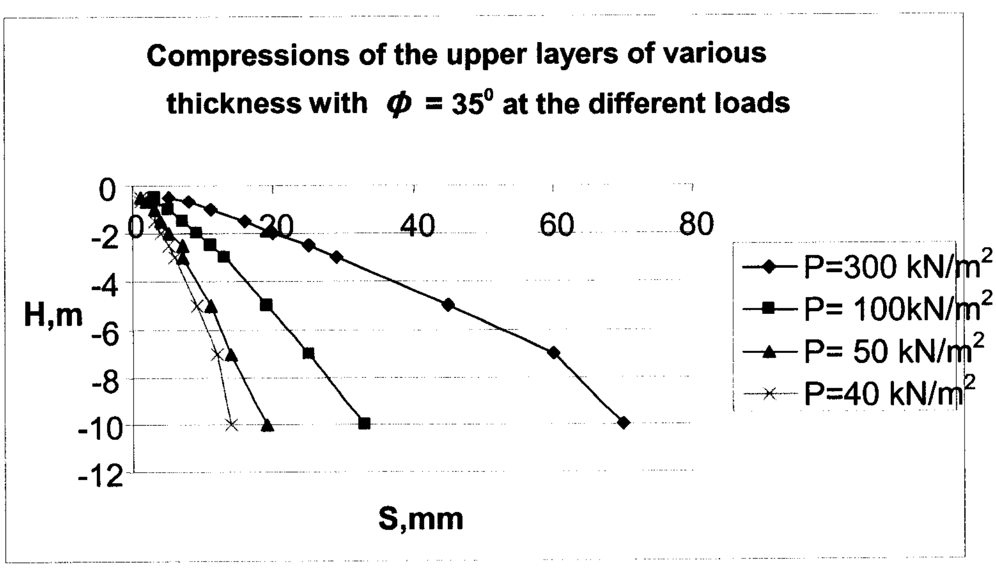
Compressions of the upper layers of various thickness with ϕ = 35^0 at the different loads
0
-2
-4
-6
-8
-10
-12
0
20
40
60
80
H,m
S,mm
P=300 kN/m^2
P= 100kN/m^2
P= 50 kN/m^2
P=40 kN/m^2

Chart No 8

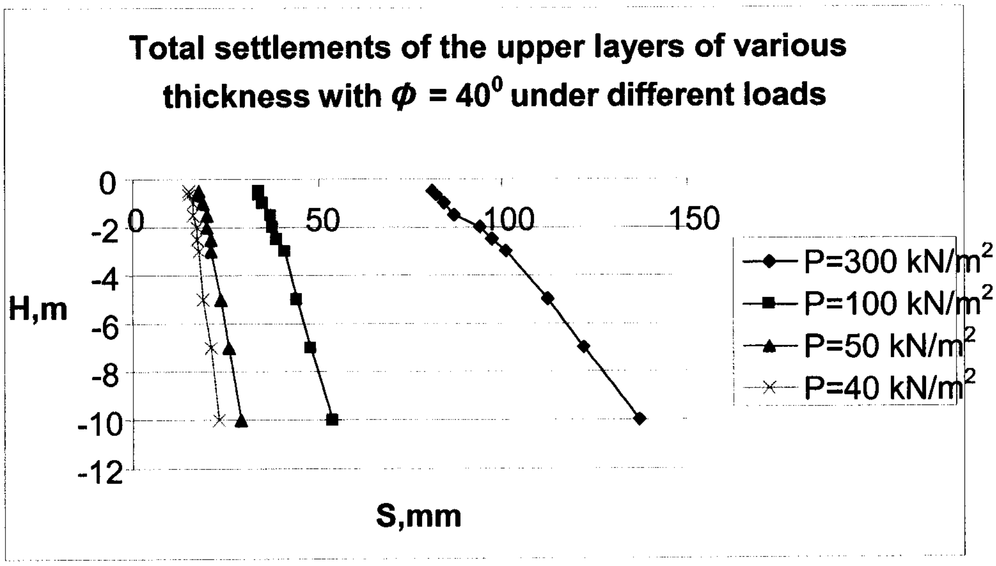

Chart No 9

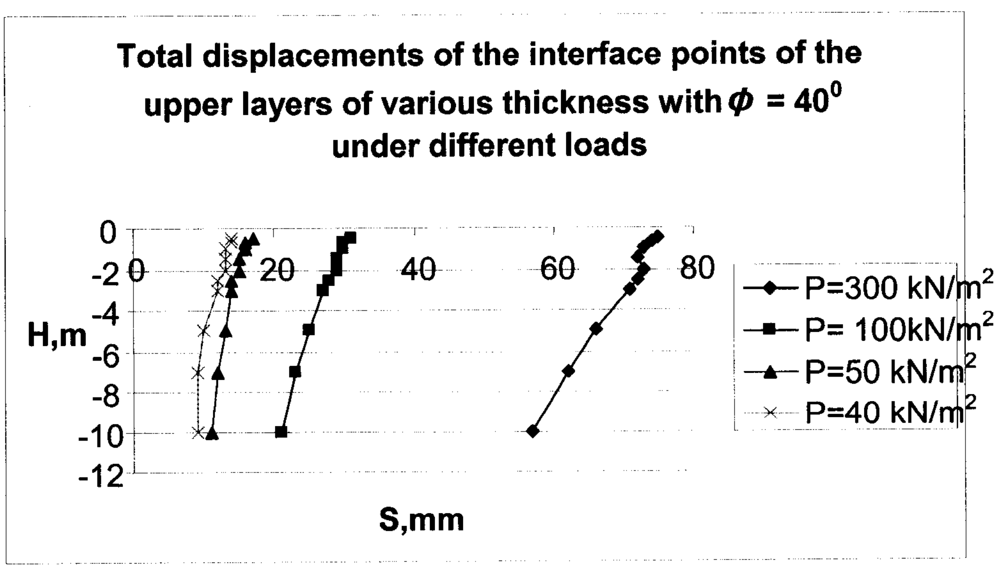

Chart No 10

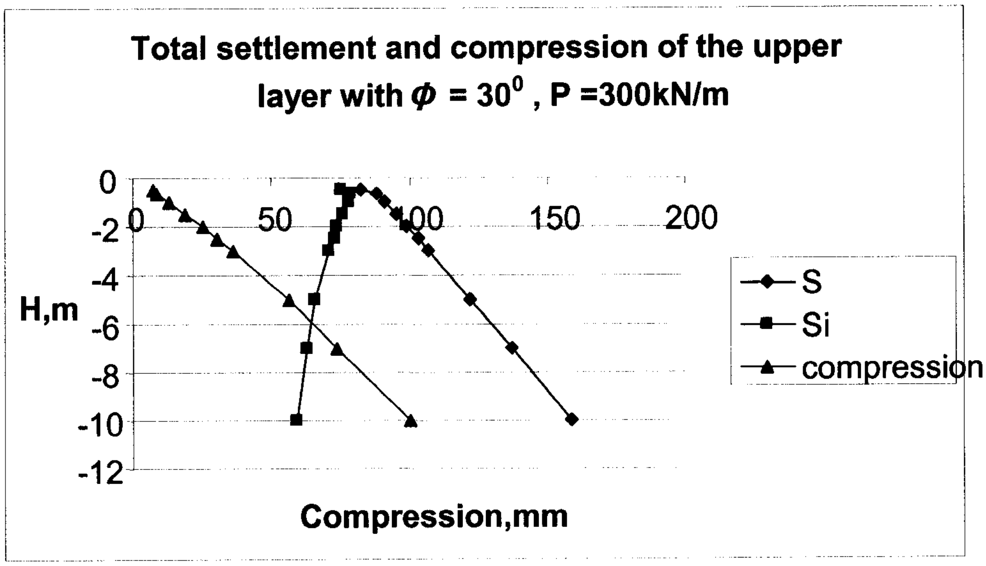

Chart No 11

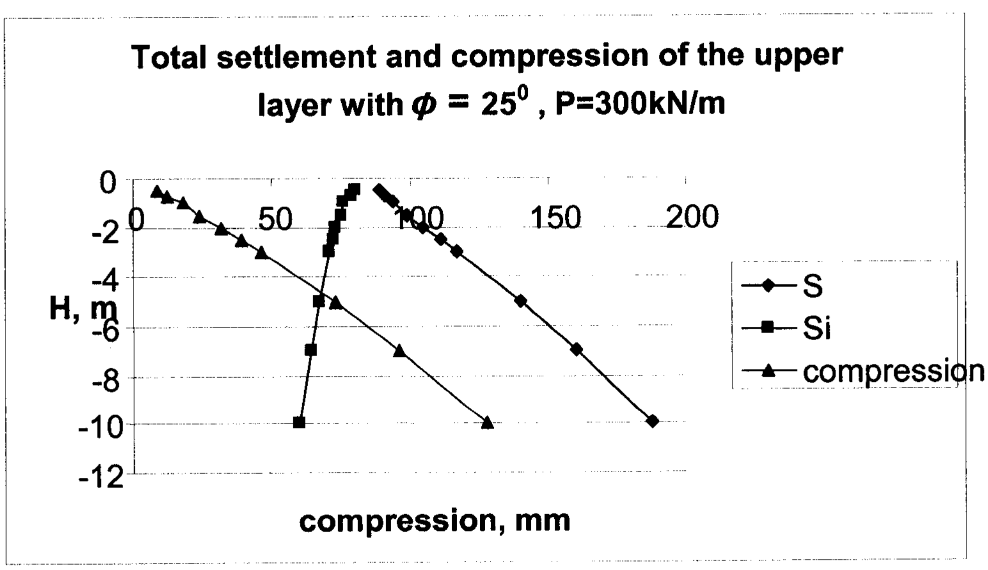

Chart No 12

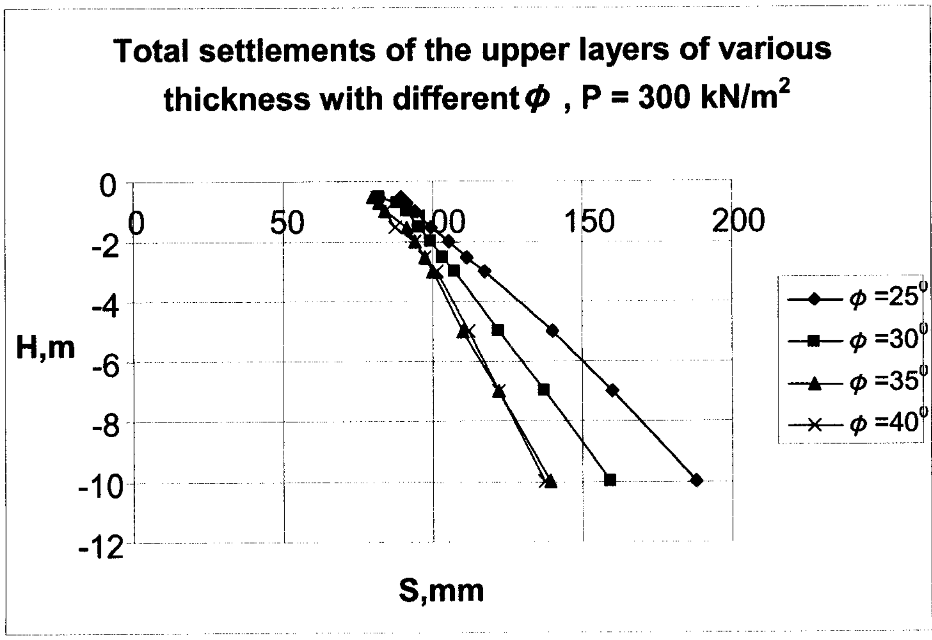

Chart No 13

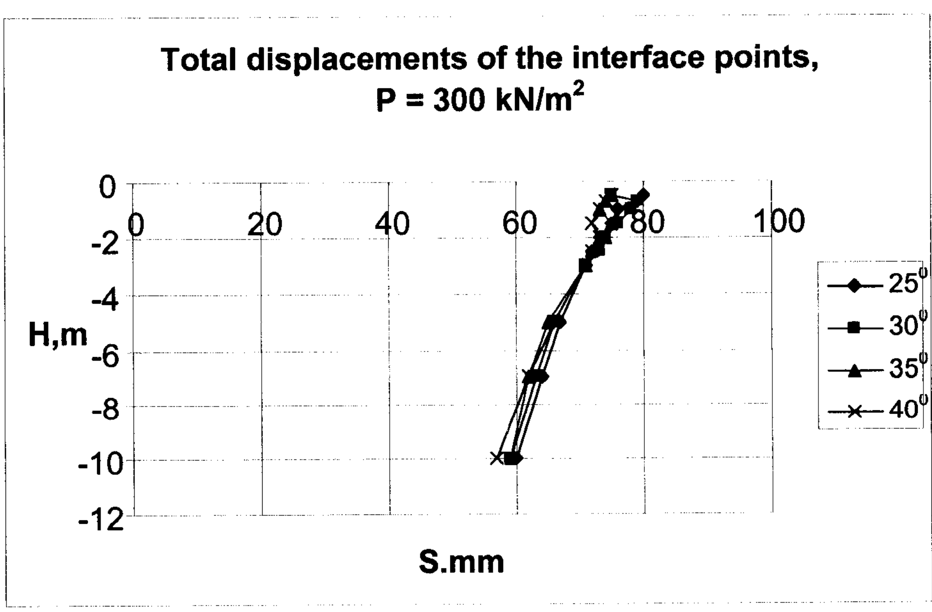

Chart No 14

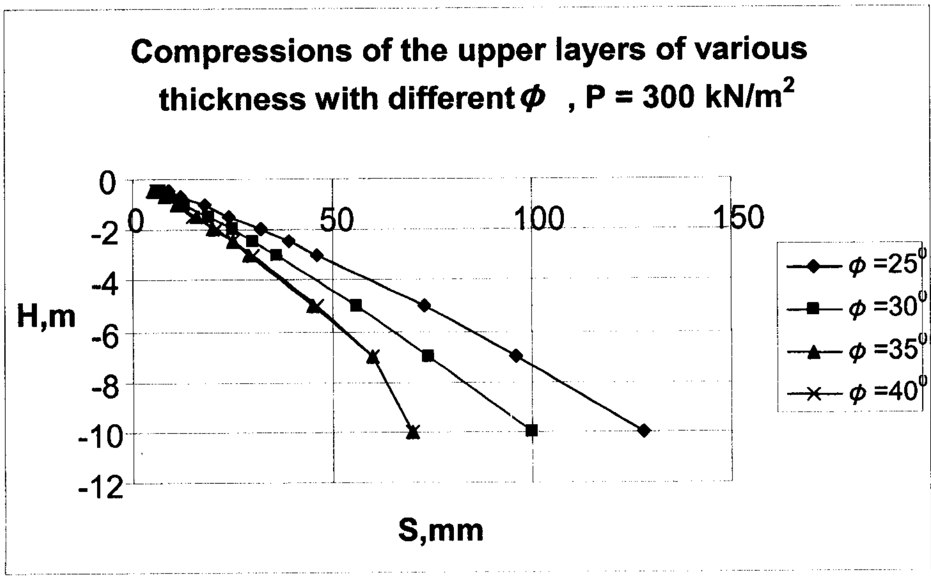

Chart No 15

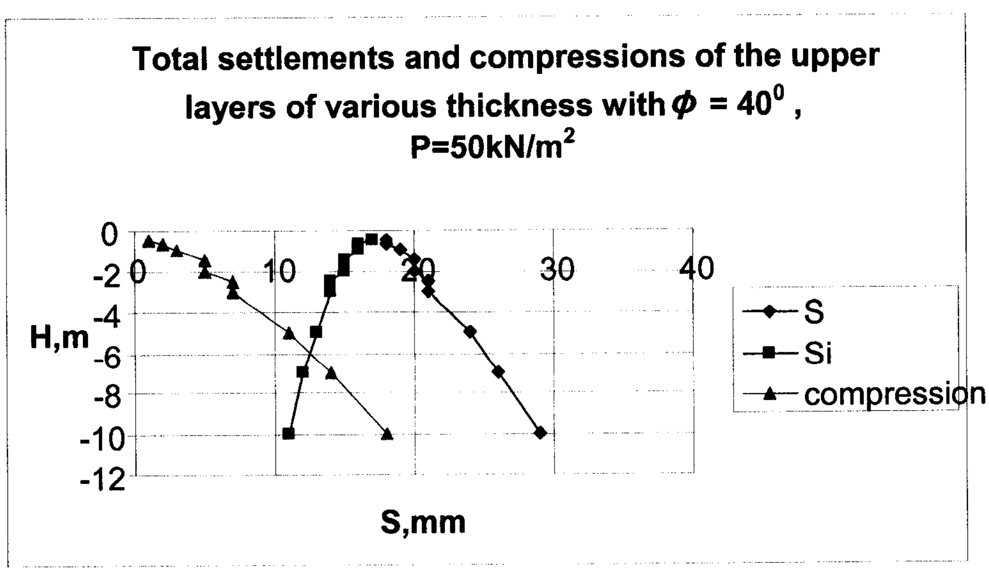

Chart No 16

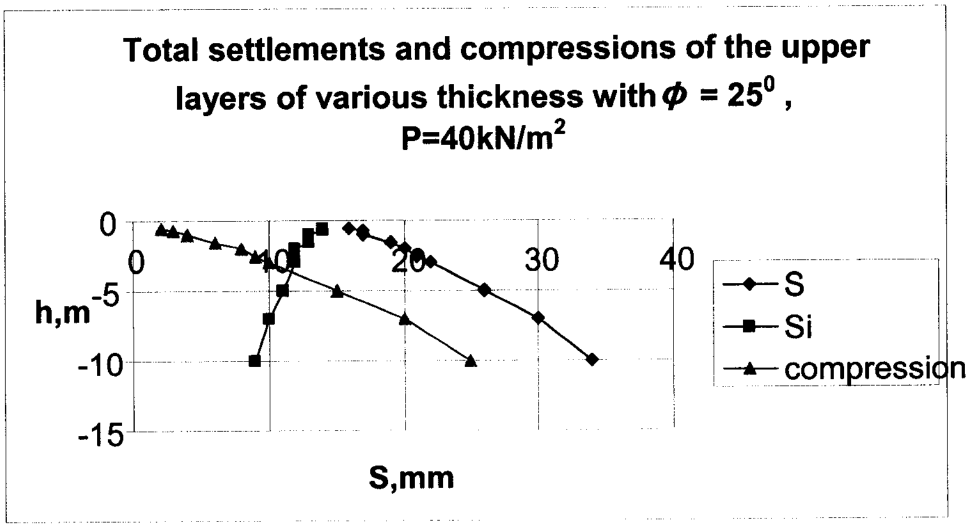

Chart No 17

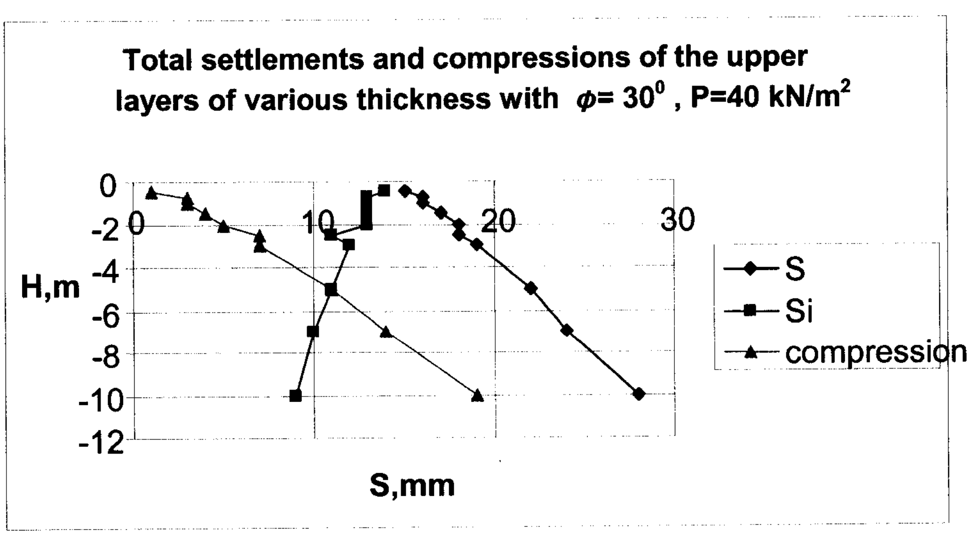

Chart No 18

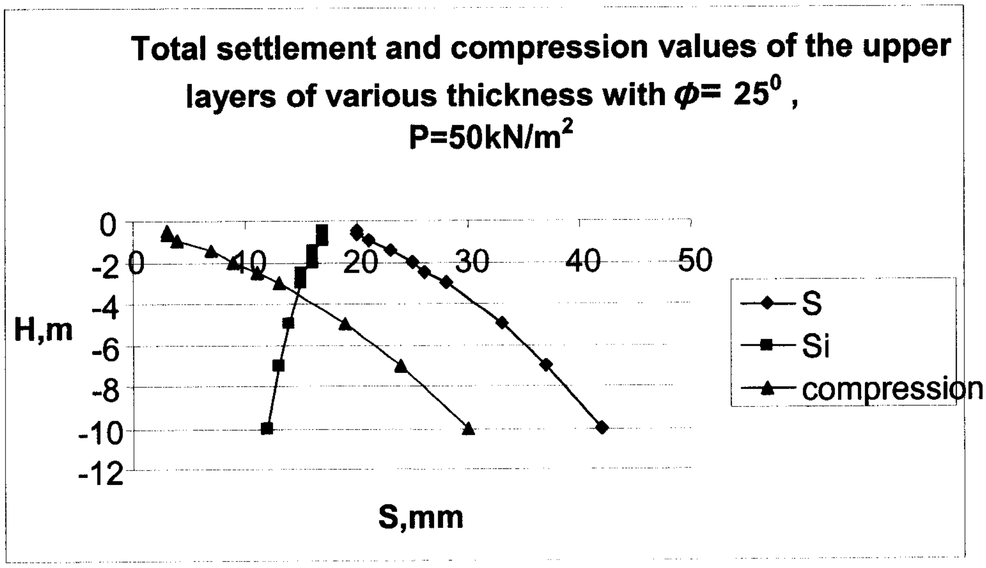

Chart No 19

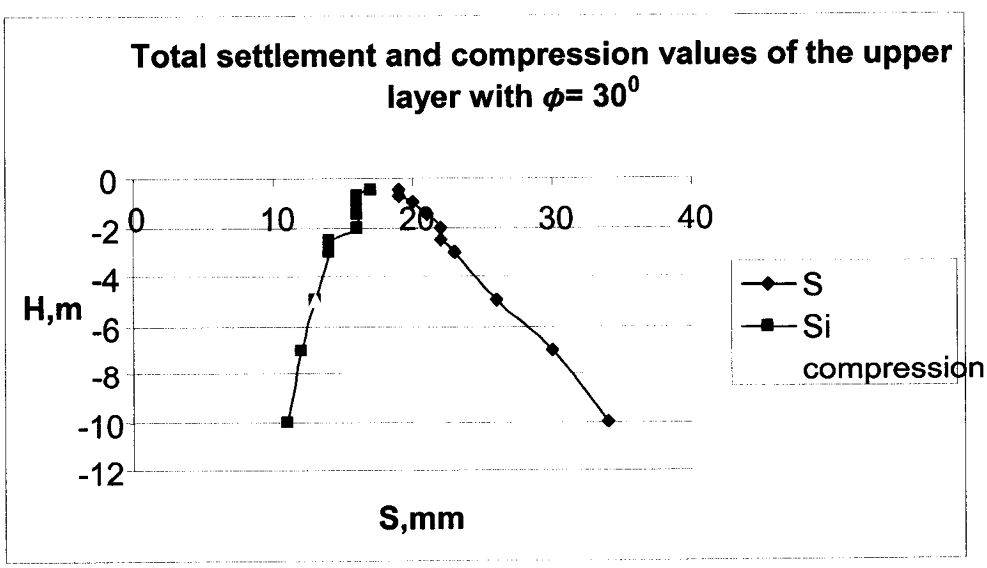

Chart No 20

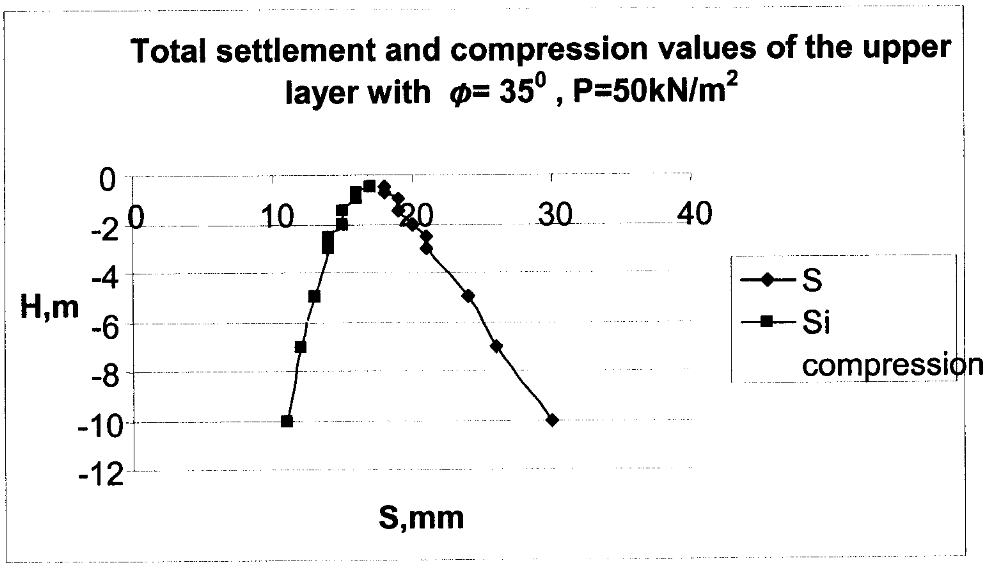

Chart No 21

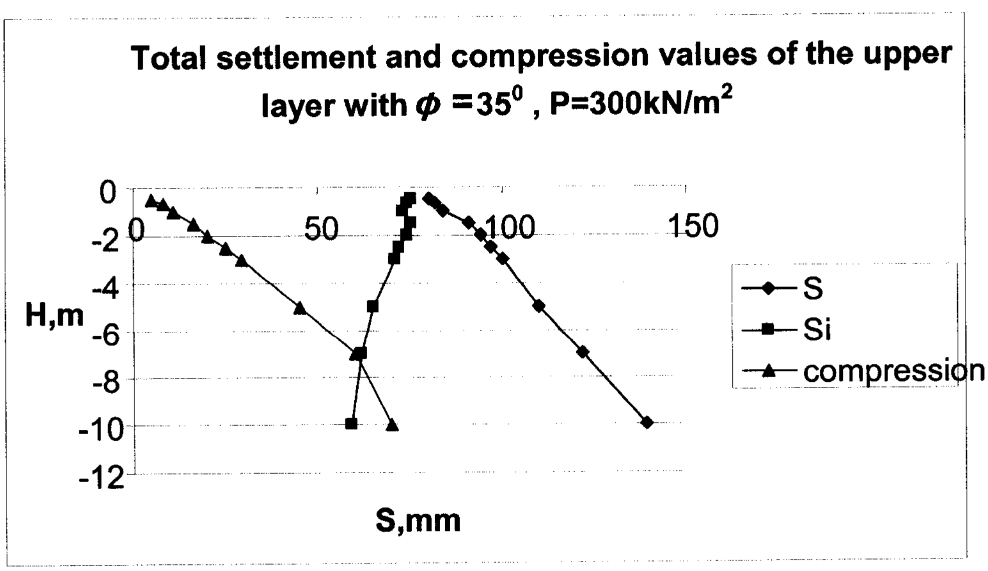

Chart No 22

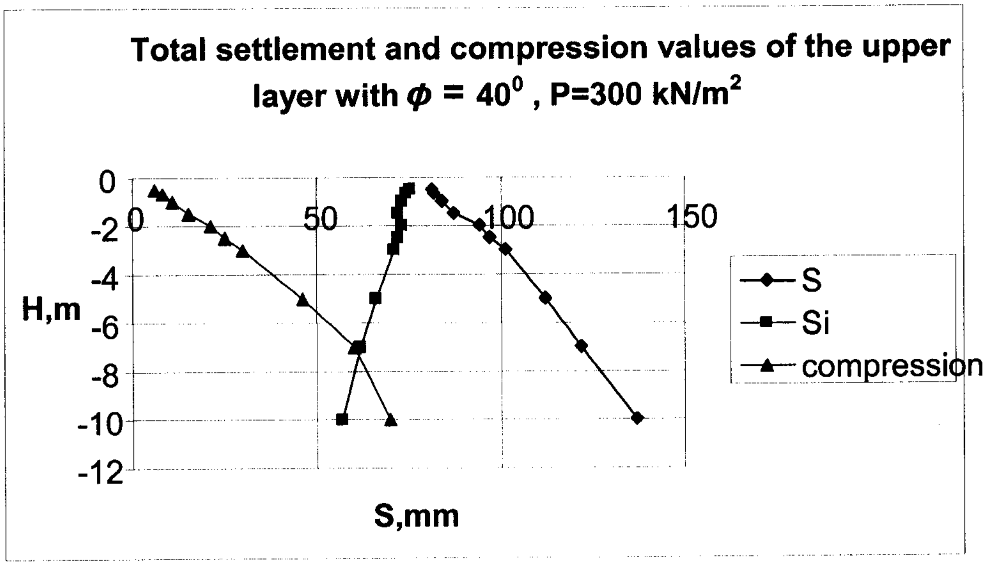

Chart No 23

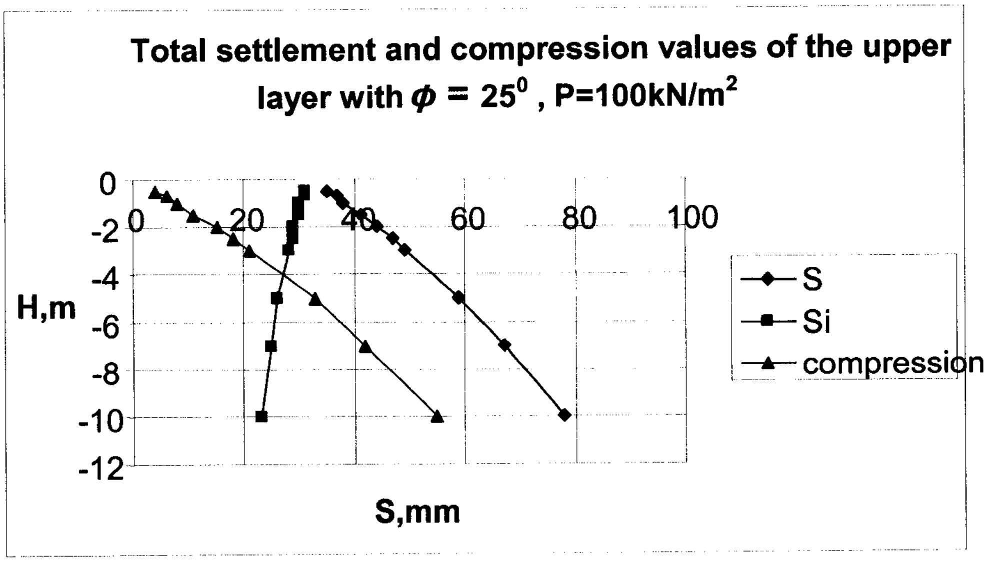

Chart No 24

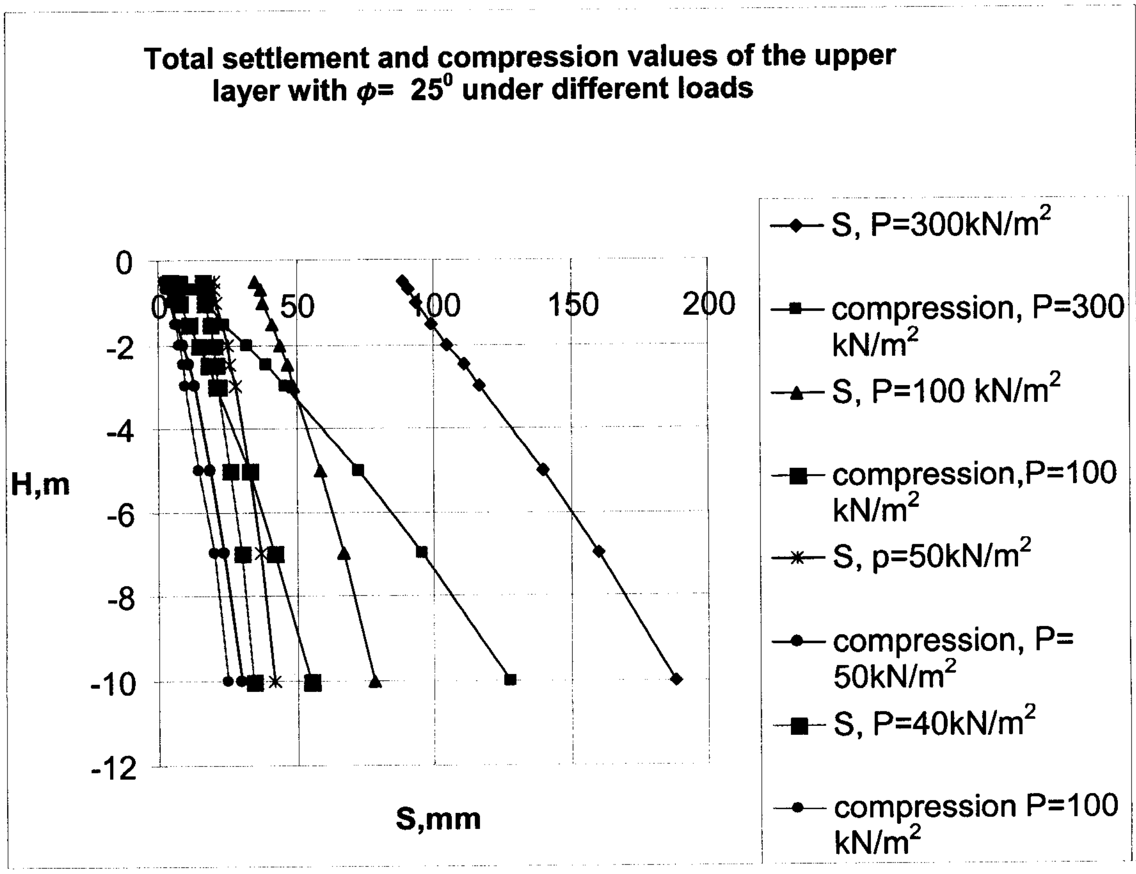

Chart No 25

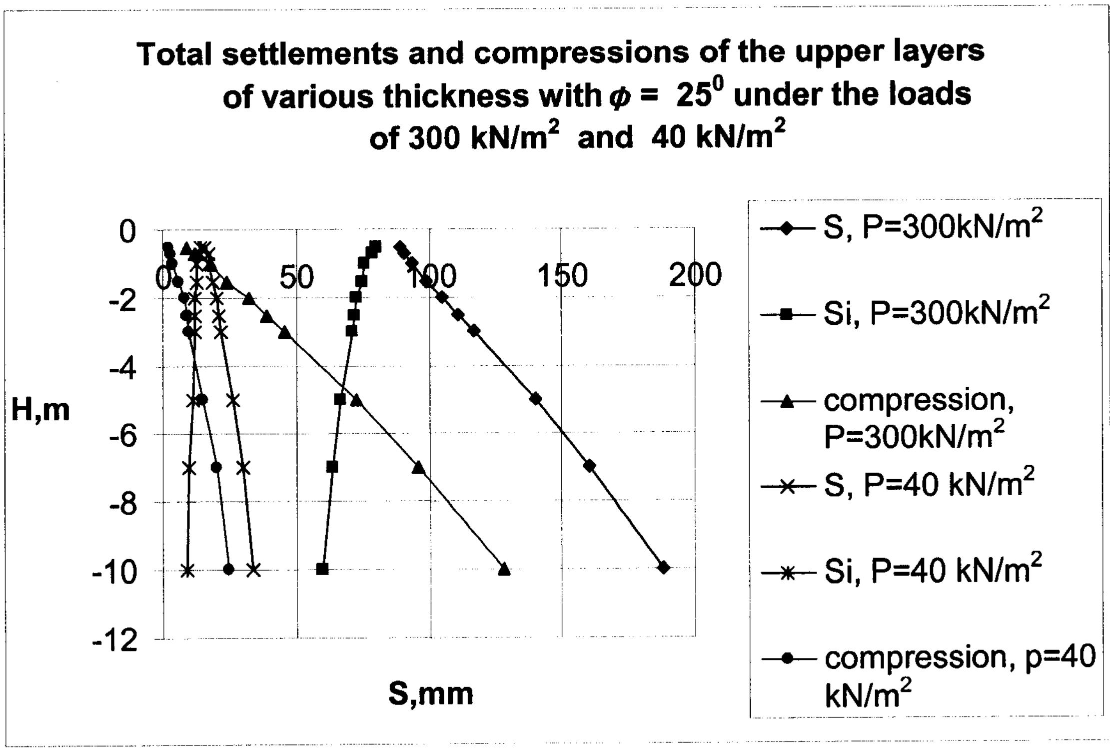

Chart No 26

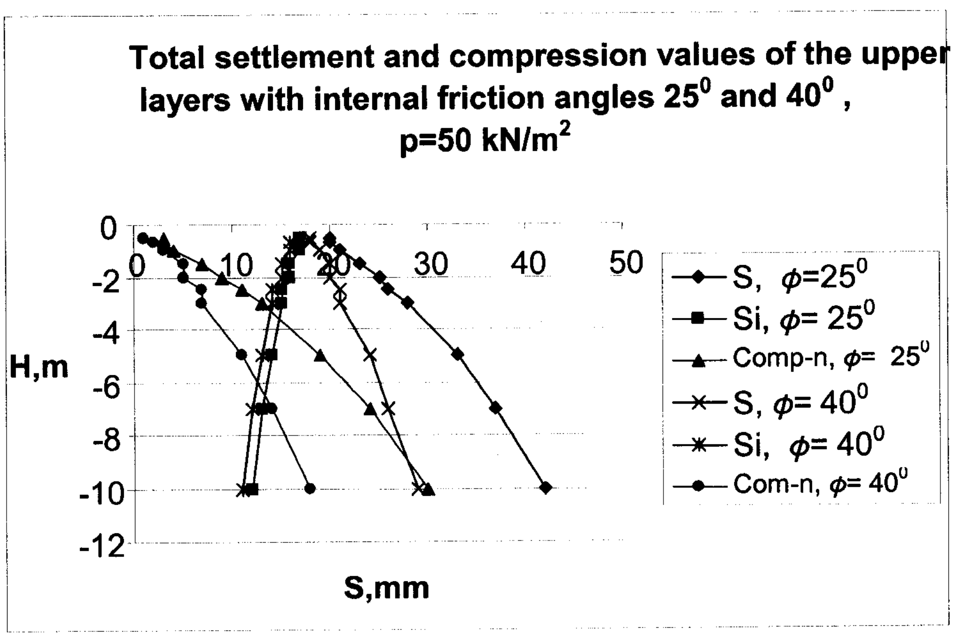

Chart No 27

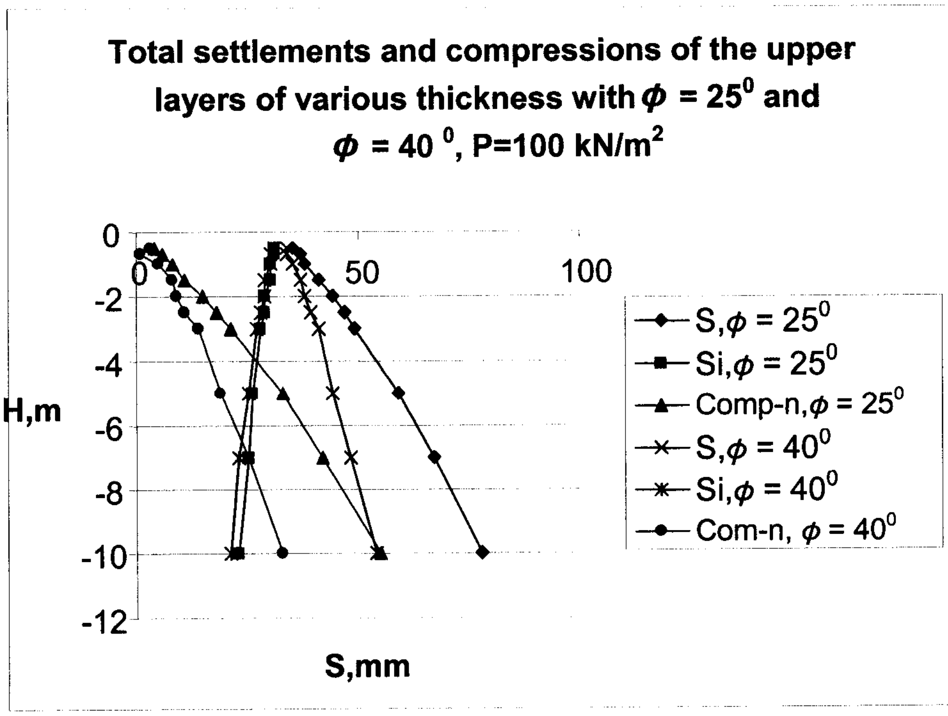

Chart No 28

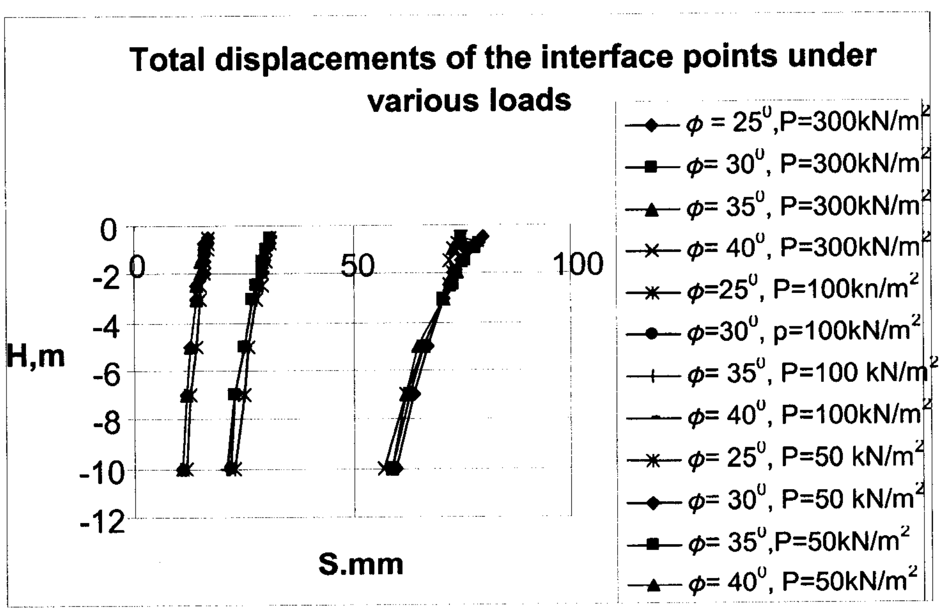

Chart No 29

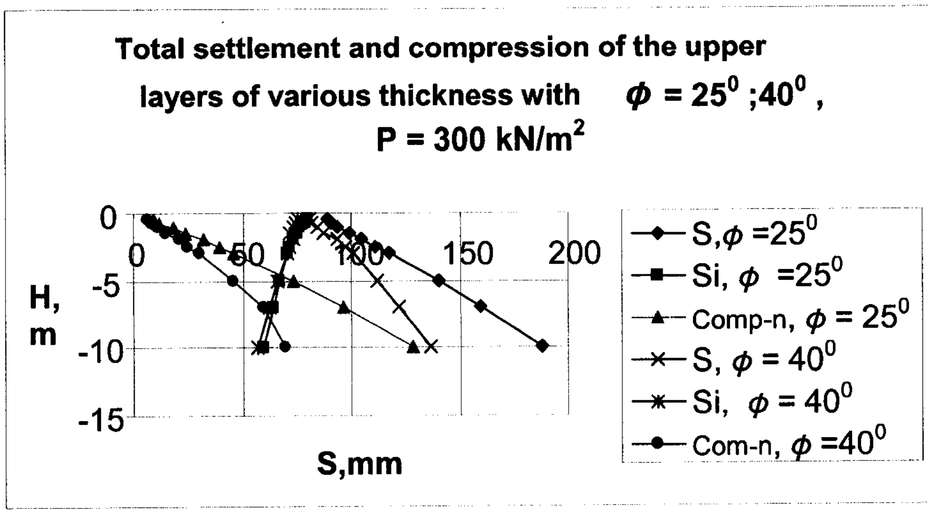

Chart No 30

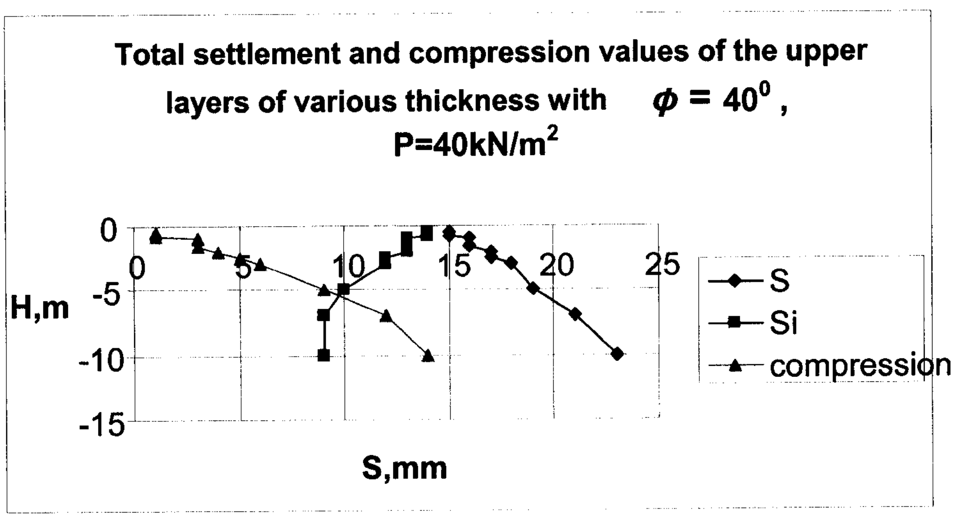

Chart No 31

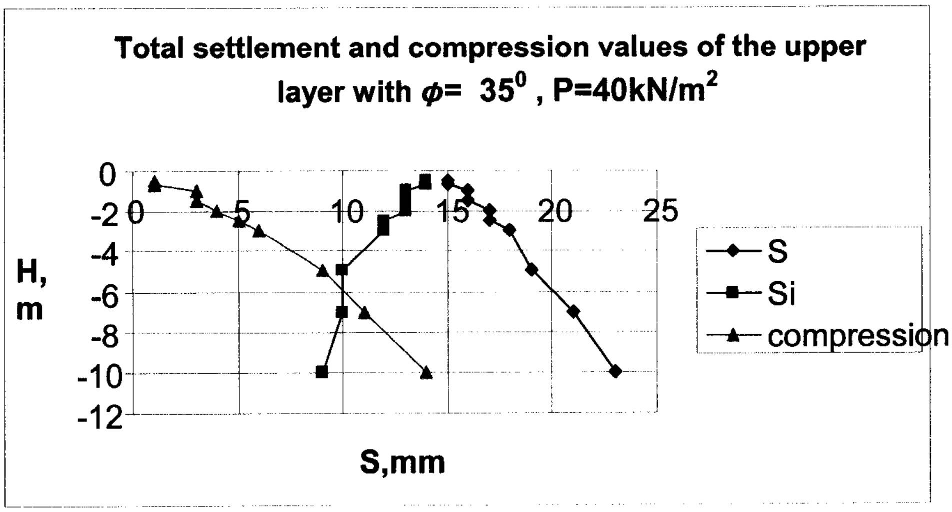

Chart No 32

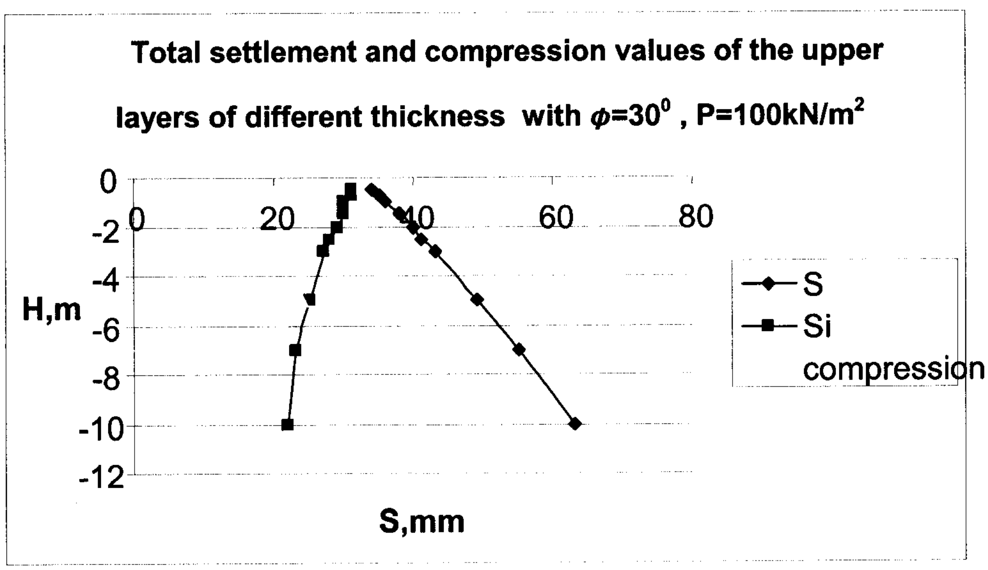

Chart No 33

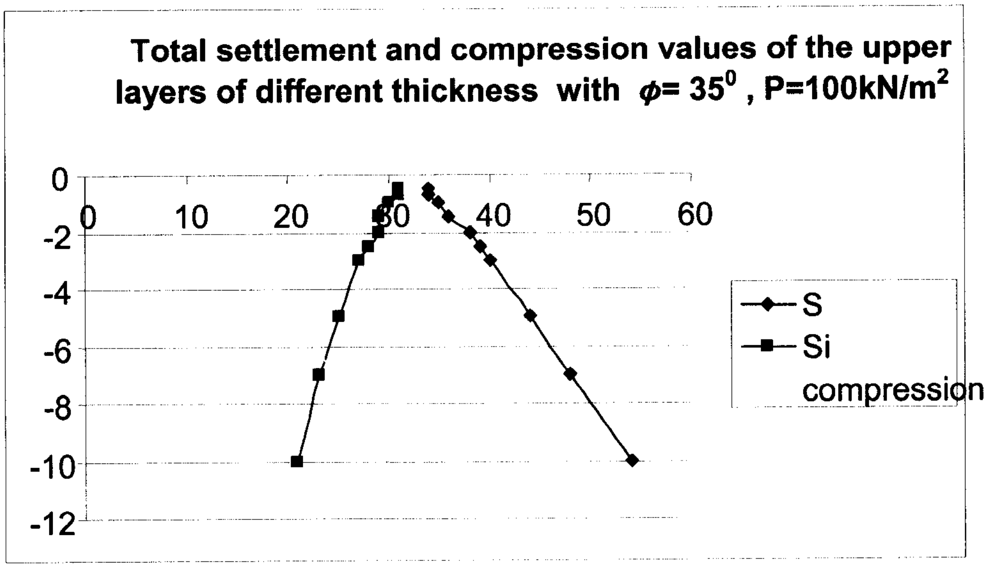
Total settlement and compression values of the upper layers of different thickness with ϕ= 35^0 , P=100kN/m^2
0
-2
-4
-6
-8
-10
-12
0
10
20
30
40
50
60
S
Si
compression

Chart No 34

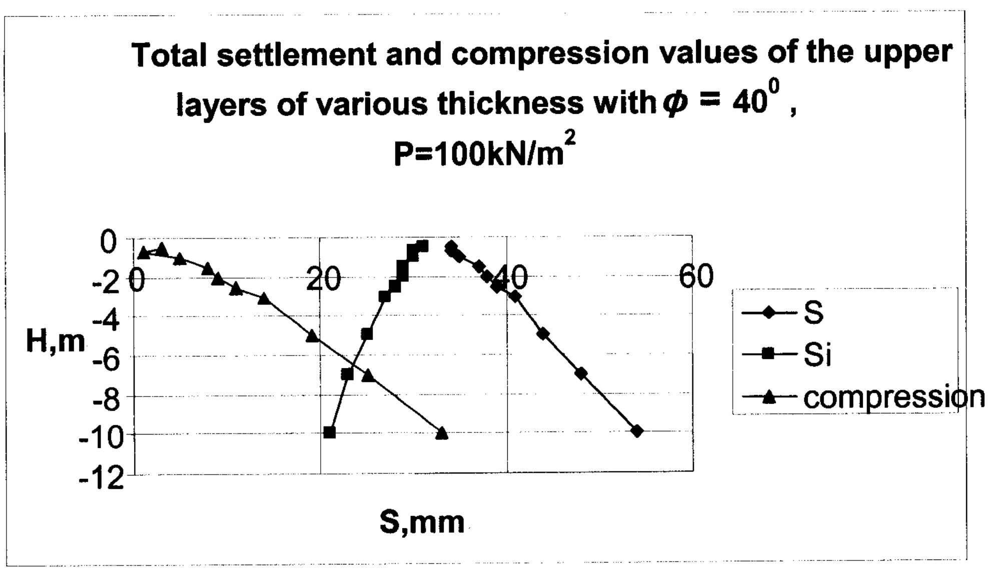
Total settlement and compression values of the upper layers of various thickness with ϕ = 40^0 , P=100kN/m^2
H,m
0
-2
-4
-6
-8
-10
-12
0
20
40
60
S,mm
S
Si
compression